# Genetic Control of Pyramidal Neuron Differentiation and Survival by Neuronal bHLH Transcription Factors Neurod1, Neurod2 and Neurod6

**Inaugural-Dissertation**
**to obtain the academic degree**
**Doctor rerum naturalium (Dr. rer. nat.)**

submitted to the Department of Biology, Chemistry, Pharmacy
of Freie Universität Berlin

by
**OLGA BORMUTH**

2022

Gefertigt in der Zeit von 10/2013 bis 03/2022
unter der Leitung von Prof. Dr. Victor Tarabykin
am Institut für Zell- und Neurobiologie
der Charité – Universitätsmedizin Berlin

| | |
|---|---|
| 1st reviewer: | Prof. Dr. Victor Tarabykin |
| 2nd reviewer: | Prof. Dr. Stephan Sigrist |
| Date of defense: | July 6th, 2022 |

# Acknowledgments

First of all, I would like to thank Victor Tarabykin for giving me the opportunity to come to Berlin and work under his supervision, for trusting my ideas and ambitious during the last years. I would like to express my gratitude to Ingo Bormuth for handing over the project, lots of help with bureaucracy, experimental design, statistical analysis, comments and corrections of the manuscript and language; to Kuo Yan for productive discussions, scientific advice, hundreds of in situ probes and expression plasmids; to Theres Schaub for sharing ideas, cell lines and cloning constructs; to Frederick Rehfeld for his modified version of the pSuper shRNA vector; to Marta Rosario for scientific suggestions and important deep questions; to Olaf Ninnemann for always being ready to advise on cloning; to Roman Wunderlich, Ulrike Günther, Rike Dannenberg und Denis Lajko for technical help with reagents, equipment, in situ hybridization and genotyping; to Jutta Schüler for assistance with the imaging equipment; to Marni Pollrich for all her help with administrative issues. Thank you Eva, Andrew, Magda, Srini, Swathi, Ethi, Duong, Katya E., Katya B., Valya, Sasha, Svetlana for creating a warm, cordial, supportive atmosphere at work and outside.

Neurod1/2/6-deficient mice were generated at the *Department of Neurogenetics* of Prof. Klaus Armin Nave at the *Max-Planck-Institute of Experimental Medicine* in Göttingen. Neurod2-Null mice were generated by Tomoko Yonemasu. Neurod1-Flox and Neurod6-Cre mice were generated by Sandra Göbbels. The mice used in this study were bred at the central animal facilities of *Forschungseinrichtungen für Experimentelle* Medizin (FEM) at Charité.

Deep sequencing was performed by Mirjam Feldkamp at the *Scientific Genomics Platform* (AG Wei Chen) at the *Max-Delbrück-Center for Molekulare Medicine* in Berlin. Preanalytic RNA quality control was done by Ute Ungethüm at the *Labor für Funktionale Genomforschung* at Charité (LFGC).

Hierdurch versichere ich, dass ich meine Dissertation selbständig verfasst und keine anderen als die von mir angegebenen Quellen und Hilfsmittel verwendet habe. Geistiges Eigentum anderer Autoren wurde als entsprechend gekennzeichnet. Ebenso versichere ich, dass ich an keiner anderen Stelle ein Prüfungsverfahren beantragt bzw. die Dissertation in dieser oder anderer Form an keiner anderen Fakultät als Dissertation vorgelegt habe.

# Contents

# Summary

The neuronal bHLH transcription factors Neurod2 and Neurod6 are predominantly expressed in postmitotic pyramidal neurons of the developing neocortex and have previously been shown to promote pyramidal neuron survival, differentiation, migration, and cortical connectivity. The closely related factor Neurod1 is normally only transiently expressed by intermediate precursor cells of the subventricular zone. In Neurod2/6 *double*-deficient mice, however, Neurod1-expression is ectopically maintained in postmitotic pyramidal neurons of the cortical plate, thereby partially compensating for the loss of Neurod2/6. In conditional Neurod1/2/6 *triple*-deficient mice selectively lacking the ectopic up-regulation of Neurod1, neuronal survival, differentiation, migration, and connectivity are significantly stronger disturbed. I aimed to further understand the functions of NeuroD-family bHLH proteins in cortex development, with a mechanistic focus on the maintenance of pyramidal neuron survival and the establishment of different pyramidal neuron identities during earlier cortex development.

In Neurod1/2/6-deficient mice, I identified an unprecedentedly strong wave of apoptotic cell death that was restricted temporarily to E14/15 and spatially to the dorsomedial cortex. Probably as a consequence, Sox5-positive pyramidal neurons of the neocortical layer 6 are lost, and the Tbr2-positive progenitor pool in the subventricular and intermediate zones is expanded. Remaining pyramidal neurons show immature molecular identities and mostly miss axonal connectivity at birth. Artificial expression of Neurod2 or Neurod6 in a subset of postmitotic pyramidal neurons was sufficient to overcome those structural defects, showing that the underlying mechanisms are of cell-intrinsic nature. Initially following a candidate-based approach, I investigated known inhibitors of apoptosis, neurotrophin signaling, and cell cycle control, but I could not identify a mechanism explaining the strong phenotype in Neurod1/2/6-deficient mice.

To gain further mechanistic insight, I performed an unbiased comparable transcriptome analysis of the central neocortex at E13, just before the manifestation of obvious structural abnormalities in Neurod1/2/6-deficient mice. The most interesting finding was a nearly 4-fold up-regulation of Harakiri (Hrk), a small BH3-only pro-apoptotic protein of the Bcl2-family. In-situ hybridization confirmed robustly increased Hrk-expression at E13–E16. In-utero electroporation of Hrk into the developing cortex of wild-type mice was sufficient to kill cortical neurons. Electroporation of Hrk-shRNA into Neurod1/2/6-deficient mice prevented apoptosis of electroporated cells.

As NeuroD-proteins are transcriptional activators, I postulated a transcriptional repressor downstream of Neurod1/2/6 to normally prevent Hrk-triggered apoptosis. The strongest down-regulated genes in Neurod1/2/6-deficient mice were Bhlhb5 and Prdm8, which are known to interact and form a repressors complex in cortical neurons. Electroporation of Bhlhb5 and Prdm8 into the cerebral cortex of Neurod1/2/6-deficient mice could rescue apoptosis, confirming their role in the control of cell death downstream of Neurod1/2/6.

# Zusammenfassung[1]

Die neuronalen bHLH-Transkriptionsfaktoren Neurod2 und Neurod6 werden vorwiegend in postmitotischen pyramidalen Neuronen des sich entwickelnden Neokortex exprimiert und haben bereits gezeigt, dass sie das Überleben, die Differenzierung, die Migration und die kortikale Konnektivität pyramidaler Neuronen fördern. Der eng verwandte Faktor Neurod1 wird normalerweise nur vorübergehend von intermediären Vorläuferzellen in der subventrikulären Zone exprimiert. In Neurod2/6-doppeldeffizienten Mäusen wird die Neurod1-Expression jedoch ektopisch in postmitotischen Pyramidenneuronen der kortikalen Platte aufrechterhalten, wodurch der Verlust von Neurod2/6 teilweise ausgeglichen wird. In konditionalen Neurod1/2/6-Dreifachmäusen, denen selektiv die ektopische Hochregulierung von Neurod1 fehlt, sind das neuronale Überleben, die Differenzierung, die Migration und die Konnektivität deutlich stärker gestört. Mein Ziel war es, die Funktionen der bHLH-Proteine der NeuroD-Familie in der Kortexentwicklung zu verstehen, wobei ich mich mechanistisch auf die Aufrechterhaltung des Überlebens von Pyramidenneuronen und die Etablierung verschiedener Identitäten von Pyramidenneuronen während der frühen Kortexentwicklung konzentrierte.

Bei Neurod1/2/6-defizienten Mäusen konnte ich eine beispiellos starke Welle des apoptotischen Zelltods feststellen, die zeitlich auf E14/15 und räumlich auf den dorsomedialen Kortex beschränkt war. Wahrscheinlich als Folge davon gehen Sox5-positive Pyramidenneuronen der neokortikalen Schicht 6 verloren, und der Tbr2-positive Vorläuferpool in den subventrikulären und intermediären Zonen ist vermehrt. Die molekulare Identität der verbleibenden Pyramidenneuronen ist unreif und ihnen fehlt bei der Geburt meist die axonale Konnektivität. Die künstliche Expression von Neurod2 oder Neurod6 in einer Untergruppe postmitotischer Pyramidenneuronen reichte aus, um diese strukturellen Defekte zu beheben, was zeigt, dass die zugrunde liegenden Mechanismen zelleigener Natur sind. Zunächst untersuchte ich im Rahmen eines kandidatenbasierten Ansatzes bekannte Inhibitoren der Apoptose, der Neurotrophin-Signalübertragung und der Zellzykluskontrolle, konnte aber keinen Mechanismus identifizieren, der den starken Phänotyp in Neurod1/2/6-defizienten Mäusen erklärt.

Um weitere Einblicke in die Mechanismen zu gewinnen, führte ich eine unvoreingenommene, vergleichbare Transkriptomanalyse des zentralen Neokortex bei E13 durch, also kurz vor dem Auftreten offensichtlicher struktureller Anomalien bei

[1] Sinngemäße Übersetzung der englischsprachigen Zusammenfassung von Seite 8

Neurod1/2/6-defizienten Mäusen. Der interessanteste Befund war eine fast 4-fache Hochregulierung von Harakiri (Hrk), einem kleinen, nur BH3 enthaltenden pro-apoptotischen Protein der Bcl2-Familie. Die In-situ-Hybridisierung bestätigte eine stark erhöhte Hrk-Expression bei E13-E16. Die inutero-Elektroporation von Hrk in den sich entwickelnden Kortex von Wildtyp-Mäusen war ausreichend, um kortikale Neuronen abzutöten. Die Elektroporation von Hrk-shRNA in Neurod1/2/6-defizienten Mäusen verhinderte die Apoptose der elektroporierten Zellen.

Da NeuroD-Proteine Transkriptionsaktivatoren sind, postulierte ich einen Transkriptionsrepressor stromabwärts von Neurod1/2/6, der normalerweise die durch Hrk ausgelöste Apoptose verhindert. Die am stärksten herunterregulierten Gene in Neurod1/2/6-defizienten Mäusen waren Bhlhb5 und Prdm8, von denen bekannt ist, dass sie interagieren und einen Repressor-Komplex in kortikalen Neuronen bilden. Die Elektroporation von Bhlhb5 und Prdm8 in die Großhirnrinde von Neurod1/2/6-defizienten Mäusen konnte die Apoptose retten, was ihre Rolle bei der Kontrolle des Zelltods stromabwärts von Neurod1/2/6 bestätigt.

# 1 Introduction

The cerebral cortex is the largest, most flexible, and phylogenetically youngest part of our brain. It produces conscious sensory perception & motor control, attention, learning & memory, emotion, cognition, and language processing (Kandel et al., 2000). The unprecedented structural complexity of the cortex and its modulatory influence on older, simpler, more deterministic, subcortical parts of the brain can be considered as the origin of our self (Schore, 1994).

## 1.1 Anatomy of the Cerebral Cortex

The cerebral cortex is the dorsal aspect of the telencephalon. It is also referred to as the pallium (coat) as it covers most of the remaining brain. The cortex is further divided into three phylogenetically, morphologically, and functionally distinct parts: The paleocortex, the archicortex (together referred to as allocortex), and the neocortex.

### 1.1.1 Allocortex

The allocortex consists of the paleocortex (olfactory cortex or rhinencephalon) and the archicortex (the hippocampal formation). The paleocortex is said to be the phylogenetically oldest part of the cerebral cortex. Due to its unique ability to generate and integrate new neurons throughout life, it gained lots of scientific attention during the last decades. However, paleocortical structures are not the subject of this work.

The archicortex is structurally the most basic part of the cortex. It consists of a single layer of excitatory projection neurons and two adjacent layers that comprise dendrites and inhibitory interneurons (Rolls, 2013). The most prominent archicortical structure is the hippocampus, which is situated at the most medial aspect of the temporal lobe. It contains two regions: the cornu ammonis (CA) and the dentate gyrus (DG). The dominant cell type of the CA is that of hippocampal pyramidal neurons. Those are morphologically similar to neocortical pyramidal neurons (sect 1.2) with whom they share a common initial differentiation program (Slomianka et al., 2011). The DG

consists mostly of hippocampus-specific granule neurons, which transfer neocortical input to the CA (Bull, 2011). The hippocampus is essential for the formation of new episodic and declarative memories (Squire, 1992), it supports flexible cognition that allows for complex social behaviors (Rubin et al., 2014), and it contributes to spatial memory and navigation (Schiller et al., 2015). The hippocampus is probably the most studied structure of the brain.

### 1.1.2 Neocortex

The youngest and largest part of the cerebral cortex is the neocortex (isocortex). The neocortex is a universal processing device that can dynamically acquire complex functionality throughout life. Structurally, it is built as a grid of highly interconnected neurons. Approximately 80 % of these are excitatory projection neurons, large pyramid-shaped cells that define the anatomy of the neocortex (sect 1.2). The remaining 20 % are smaller inhibitory interneurons that scatter between the more prominent pyramidal neurons (Rakic, 2009).

The neocortex is organized in six functionally distinct layers, five of which contain different subtypes of pyramidal neurons. Those in the deeper layers 5 and 6 project away from the cortex, mostly towards the spinal cord and thalamus, respectively (Lam & Sherman, 2010). Pyramidal neurons in the upper layers 2 and 3 connect to other parts of the neocortex. Layer 4 receives sensory information from the thalamus and distributes it to the other cortical layers (Jones, 1998). The most superficial layer 1 is devoid of pyramidal neurons, it contains interneurons and the endings of apical dendrites originating from the other layers (Kandel et al., 2000; Creutzfeldt, 1983).

### 1.1.3 Cell Types

The cerebral cortex consists mostly of excitatory projection neurons, inhibitory interneurons, and supportive glial cells. The principle anatomy and connectivity of the cortex are determined by large pyramid-shaped projections neurons that grow very long axons connecting to distant targets, e. g. in the case of layer 5 to motoneurons in the spinal cord. The general biology and the different subsets of cortical pyramidal neurons are introduced in sect 1.2. To my knowledge, all cortical pyramidal neurons do at least temporarily express Neurod1, Neurod2, and Neurod6 (sect 1.4.2), while interneurons are generally negative for the three factors. This study focuses on the functions of Neurod1/2/6 in the generation, differentiation, and migration of cortical pyramidal neurons (sect 1.5).

A very diverse set of relatively small inhibitory interneurons is scattered within the dense network of cortical projection neurons. Interneurons protect the network from over-activation, and they are the basis for the cortex's enormous computational

capability and flexibility. In contrast to pyramidal neurons, which are born within the cortex (dorsal telencephalon), interneurons are generated in the ventral telencephalon and migrate tangentially into the cerebral cortex (Marín, 2013). Glial cells (astrocytes and oligodendrocytes) are essential for neuronal communication as they nourish, protect, support, and electrically isolate the neurons. Interneurons and glial cells invade the cortex late during development when many basic structures and remote connectivity have already been determined. They do never express Neurod1/2/6 and are thus of the scope of this study.

### 1.1.4 Development

During early embryonic development, the entire central nervous system (CNS) is formed from an area of specialized ectoderm. This neural plate is located at the dorsomedial surface of the embryo. A longitudinal groove is gradually formed in the center of the neural plate. In a process called neurulation, this neural groove deepens until the ridges (the neural folds) meet and fuse to form a closed tube at the back of the embryo, the neural tube (Kandel et al., 2000). The caudal portion of the neural tube gives rise to the spinal cord. The rostral neural tube forms five protrusions (the encephalic vesicles) that grow to form different parts of the brain. The two most rostral vesicles give rise to the telencephalon and the therein enclosed lateral ventricles. The dorsal aspect of the telencephalon forms the cerebral cortex (Bear et al., 1996).

The inner wall of the developing telencephalon is the ventricular zone (VZ). It contains proliferating neural stem cells that multiply and ultimately give rise to neurons, astrocytes, and oligodendrocytes. The most dominant types of cortical stem cells are called radial glia cells (RGCs) as their processes span the entire developing cortex radially from its inner ventricular wall to the pia mater at its outer surface (Anthony et al., 2004; McConnell, 1995; Noctor et al., 2002). The cell bodies of RGCs reside in the VZ (the most apical layer of the developing CNS) and they are therefore also called apical progenitor cells Apical precursor cells (APCs).

Many cortical neurons are not directly generated from RGCs but from mitotically active descendants called intermediate precursor cells (IPCs). The latter reside predominantly in the subventricular zone (SVZ), a temporal cell layer just above the VZ (Noctor et al., 2004; Fishell & Kriegstein, 2003). IPCs are also called Basal precursor cells (BPCs) as the SVZ is located basally in relation to the more apical VZ.

New-born neurons migrate radially along the basal[1] processes of RGCs to reach their final positions within the cerebral cortex (Malatesta et al., 2000). As neurons are generally born in relative proximity to the ventricle (deep inside the developing cortex) and migrate radially to settle in proximity to the outer surface, the cortex is said to develop in an inside-out manner.

## 1.2 Cortical Pyramidal Neurons

PYRAMIDAL NEURONS are the dominant cell population of the hippocampus (sect 1.1.1) and neocortex (sect 1.1.2). Structurally, they are characterized by a big pyramid-shaped cell body, a thick apical dendrite[2] that reaches towards the outer surface of the brain, multiple basal dendrites[3] that connect to surrounding neurons, and a very long axon that projects to distant areas of the CNS. All pyramidal neurons are glutamatergic excitatory projection neurons. They can be further divided into multiple subpopulations that express specific sets of important transcription factors (sect 1.2.4), are located in different cortical layers (sect 1.2.3), connect to different areas of the CNS (sect 1.2), and ultimately serve different functions in the mature brain (Fishell & Hanashima, 2008). Neuronal subtype specification and development of the cerebral cortex are regulated by mutually dependent cell-intrinsic and cell-extrinsic processes (Fishell & Hanashima, 2008). Differentiating pyramidal neurons undergo extreme morphological changes while migrating from the ventricular neuroepithelium to the cortical plate (Cooper, 2014).

### 1.2.1 Neurogenesis

In mice, cortical pyramidal neurons are produced between embryonic day (E) 11.5 and E17.5 in the VZ and SVZ (Caviness & Takahashi, 1995). The principal neurogenic stem cells are the RGCs in the VZ. They divide symmetrically to increase the stem cell pool or asymmetrically to produce neuronal IPCs and neurons that migrate radially along the basal processes of RGCs to leave the VZ. Pyramidal neurons that are born during early cortex development (E 11.5–13.5) mostly give rise to the deeper layers 5 and 6 of the CP; they are generated in the VZ by apical radial glia cells (aRGCs), subapical radial glia cells (saRGCs), or apical intermediate precursor cells (aIPCs). Pyramidal neurons that are born later (E 14.5–17.5) mostly give rise to the upper

[1] The basal process reaches toward the outer (basal) surface of the brain; the inner ventricular surface is considered apical.

[2] The apical dendrite emerges from the *apex* (tip) of the pyramidal cell. The name has *no* relation to the apical/basal (inner/outer) orientation of the cortex (compare *basal process of RGCs* in sect 1.2.1). Most apical dendrites project basally within the cortex.

[3] Basal dendrites emerge from the basis (bottom) of the pyramidal cell.

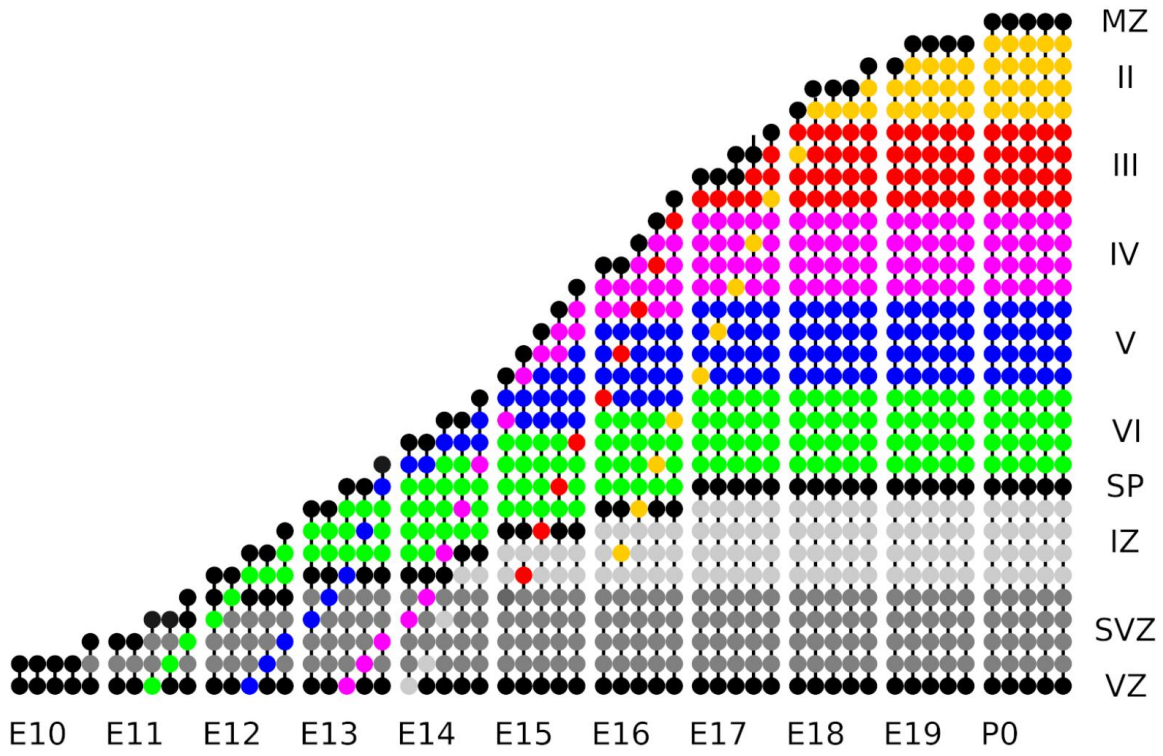


**Figure 1: Radial migration in the developing cerebral cortex**

**Abbreviations** on page 119.

layers 2 and 3 of the CP; they are mostly generated in the SVZ by basal radial glia cells (bRGCs) or basal intermediate precursor cells (bIPCs). The three types of RGCs are characterized by robust expression of the transcription factor paired box gene 6 (Pax6). Both types of IPCs do robustly express the transcription factor T-box brain 2 (Tbr2), also called Eomesodermin (Eomes). Tbr2 is thought to repress Pax6 resulting in mutually exclusive expression of the two factors (De Juan Romero & Borrell, 2015). Pax6 and Tbr2 are considered molecular markers for RGCs and IPCs, respectively (sect 1.2.4).

### 1.2.2 Radial Migration

New pyramidal neurons are born close to the inner surface of the cerebral hemispheres, in the VZ or SVZ. Shortly after their last mitotic division, those cells are determined to the pyramidal neuron fate. However, lacking axons, dendrites, and synapses they do not yet qualify as functional neurons. Over the course of a few days, the cells undergo several stages of neuronal differentiation and maturation. At the same time, they migrate radially from the VZ or SVZ into the intermediate zone (IZ) and ultimately through the cortical plate (CP) towards the outer surface of the brain (fig 1).

Radial migration is not a continuous process. Immature neurons stop e. g. in the IZ where they change morphology before migrating further into the CP. At this stage, cells move in random directions and have multipolar morphology (Noctor et al., 2004; Shoukimas & Hinds, 1978). To become mature functional pyramidal cells and to enter the CP, neurons go through a transition from the multipolar to a bipolar stage. It was shown that Tbr1, Tbr2, Pax6, and Neurod1 are essential for this transition (Englund et al., 2005; Seo et al., 2007; Sessa et al., 2008; Inoue et al., 2014). The main regulator of morphological transition and migration into the CP by controlling the length of the multipolar stage is thought to be Prdm8 (Iwai et al., 2018).

For the normal functioning of the brain, it is necessary that neurons with similar gene expression patterns are organized in layers (Franco et al., 2011). Specific laminarization of the cortex is the result of the radial migration performed by newly born neurons. As described above, RGCs extend their processes to the marginal zone creating a path for the migrating pyramidal neurons into the CP (Rakic, 1972). One of the well-known molecules required for normal radial migration is reelin (Ogawa et al., 1995). Mouse models with impaired reelin pathway exhibit severe cortical abnormalities, including impaired laminarization (Rice & Curran, 2001). Depending on the stage of migration reelin can act as an attractant (Gilmore & Herrup, 2000) or repellent (Schiffmann et al., 1997) for the migrating neurons. Both RGCs and neurons express reelin receptors Vldlr and Apoer2 (Hiesberger et al., 1999). Reelin binding to its receptors promotes phosphorylation of the cytoplasmatic adaptor protein Dab1 (Howell et al., 1999). Activated Dab1 interacts with several molecules, including Lis1 (Assadi et al., 2003). Dab1 and Lis1 regulate in turn multiple molecular targets, affecting actin filaments and microtubule dynamics during radial migration of the neuron (Zhang et al., 2007).

### 1.2.3 Layering

The first cortical neurons are Cajal-Retzius cells. They are born at around E 10.5 and form the so-called preplate (PP), the precursor of the CP. The PP later splits to form a marginal layer of the cortex with the major cell population Cajal-Retzius cells and a subplate. Between the subplate (SP) and the marginal zone (MZ) begins the formation of the six-layered CP (Bayer et al., 1991). The earliest produced pyramidal neurons settle down in layer VI (the deepest layer). Later-born neurons migrate past those earlier-born deeper-layer neurons and form layer V–II (the more superficial layers). Thus, the six-layered structure is built in an inside-first outside-last manner (Molyneaux et al., 2007; Desai & McConnell, 2000; Frantz & McConnell, 1996; Tarabykin et al., 2001).

### 1.2.4 Molecular Markers

| Gene | Dominant in layer | Notes |
|---|---|---|
| Reln | 1 | In Cajal-Retzius cells |
| Cux2 | 2/3 | Also in immature neurons of the SVZ |
| Brn2 | 2/3 | Also in immature and migrating neurons |
| Satb2 | 2/3 | Callosally projecting pyramidal neurons (also in layer 5) |
| Rorb | 4 | Subset of pyramidal neurons in layer 4 |
| Ctip2 | 5 | Also in layer 6 and in interneurons (weaker) |
| Foxp2 | 6 | Subset of pyramidal neurons in layer 6 |
| Sox5 | 6 | Also in immature neurons in SVZ/IZ (weaker) |
| Map2 | CP | In all terminally differentiated neurons |
| Dab1 | CP | Reelin signaling within cortical pyramidal neurons |
| Prdm8 | IZ | In late multipolar neurons |
| Unc5d | IZ | In early multipolar neurons |
| Tbr2 | SVZ | In IPCs |
| Neurod1 | SVZ | In IPCs; postnatally in 2/3 |
| Pax6 | VZ | In RGCs |
| Sox2 | VZ | In RGCs and aIPCs |

**Table 1: Molecular markers in neocortical layering**

**Gene:** Gene symbol; **Layer:** Dominant expression domain; **Notes:** Secondary expression domains and other comments.

Pyramidal neurons in the six layers of the neocortex are characterized by robust expression of unique genes, which can be used as molecular markers to identify previously characterized neuronal subtypes (tab 1). Pyramidal neurons in layer 6 are born at around E12.5 (E11.5–E13.5) and typically express Sox5 (Lai et al., 2008) or Tbr1 (Bulfone et al., 1995; Hevner et al., 2001; Englund et al., 2005). The large corticofugally projecting pyramidal neurons in the general output layer 5 are produced around E13.5 (E12.5–E14.5) and typically express Ctip2 (Arlotta et al., 2005). The smaller pyramidal neurons in the general input layer 4 are generated around E14 (E13.5–E14.5) and typically express Rorb (Giguère, 1999). Pyramidal neurons in the intracortically projecting upper layers 2 and 3 are produced around E15.5 (E14.5–E16.5) and typically express Brn1/2 (McEvilly et al., 2002), Cux1/2 (Nieto et al., 2004), or Satb2 (Britanova et al., 2008; Alcamo et al., 2008).

The most superficial layer 1, also called the MZ, is virtually devoid of pyramidal neuron cell bodies and consists mostly of apical dendrites originating from the pyramidal neurons residing in the layers below. The predominant cells in the MZ are Cajal-Retzius cells, glutamatergic neurons that are considered the oldest neurons of the developing neocortex. During cortex development, Cajal-Retzius cells secrete Reelin to control the targeted radial migration of the later-born pyramidal neurons (Hirota & Nakajima, 2017).

## 1.3 Programmed Cell Death

PROGRAMMED CELL DEATH (PCD) is an evolutionary highly conserved mechanism of cell death, controlled by intracellular programs. PCD has many important functions in organisms (Golstein, 1998). For example, interdigital cells altruistically die during limb formation. In the immune system, cells that can recognize autoantigens or less pathogen-specific undergo cell death. The number of male germ cells is regulated by PCD in early spermatogenesis. Virus-infected cells undergo PCD to decrease the pathogen spread (Vaux et al., 1994).

Concerning cell morphological alterations, cell death historically is classified into three main forms: apoptosis, autophagy, and necrosis (Schweichel & Merker, 1973).

Apoptosis and autophagy are two main types of programmed cell death (PCD). Both are highly regulated and controlled processes. Many environmental and intrinsic factors can induce apoptosis and autophagy, including mitotic failures, DNA damages, lack of growth factors, overload of reactive oxygen species (ROS) as well as ischemia. Several anti-apoptotic and pro-apoptotic molecules regulate cell survival in transcriptional and post-transcriptional manners (Galluzzi et al., 2018). Recently, another form of PCD was described - programmed necrosis or necroptosis (Yuan & Kroemer, 2010).

In contrast, necrosis is classically seen as non-physiological cell death in response to infection, injury, or other external factors (Clarke, 1990). Other than apoptosis and autophagy, necrosis is characterized by swelling of organelles, increased cellular volume, rupture of the plasma membrane, DNA fragmentation, and immune system activation (Lossi & Merighi, 2003).

### 1.3.1 Apoptosis

Apoptosis - from Ancient Greek ἀπό (apo: of, away from) and πτῶσις (ptosis: to fall) - a widespread form of PCD. Biochemical processes during apoptosis result in specific morphological changes in the dying cell. The first detectable changes are chromatin condensation and segregation followed by cytoplasm condensation with the formation of protuberances, so-called blebbing. Cell organelles stay unaffected. Eventually, membrane-bounded apoptotic bodies, that contain nuclear fragments and organelles, are formed (Kerr et al., 1972). Apoptotic bodies are then quickly cleared out by the neighboring cells or macrophages (Alberts et al., 2002).

### 1.3.2 Autophagy

Autophagy is another regulated mechanism of programmed cell death. Similar to apoptosis, it allows for controlled degradation and recycling of cell components (Mizushima & Komatsu, 2011). During autophagic cell death, characteristic autophagosomes,

double-membrane vesicles containing cytoplasmatic components, are formed. Autosomes fuse with cellular lysosomes and multiple proteases destroy and recycle the content (Lockshin & Zakeri, 2002).

### 1.3.3 Necroptosis

Necroptosis and apoptosis can be activated by molecules such as first apoptosis signal ligand (Fasl) or tumor necrosis factor α (TNFα). When the apoptotic pathway is blocked, the cells committed to suicide can be eliminated through necroptosis. This can explain the survival and relatively normal development of mutant mice lacking the key molecules of the apoptotic program (caspases, Apaf1, Bax, or Bak) (Chautan et al., 1999; Lindsten & Thompson, 2006). Although described mutants often are characterized by the accumulation of the cells that normally would die apoptotically, most of these cells undergo non-apoptotic cell death at later stages, leading to the normal functioning of the brain (Nonomura et al., 2013; Oppenheim et al., 2008; Yaginuma et al., 2001).

### 1.3.4 Developmental Cell Death

Neurogenesis, differentiation, migration, and axogenesis are accompanied by waves of programmed cell death, that eliminate fractions of the recently generated cells (Blaschke et al., 1996). Developmental cell death underlies processes such as neuronal deletion, sculpting, quality control, and quantitative neuron-target matching (Buss et al., 2006; Fuchs & Steller, 2011; Yeo & Gautier, 2004; Yamaguchi & Miura, 2015). The effective inhibition of apoptosis in terminally differentiated pyramidal neurons is essential for the formation of a stable neuronal network and long-term memory (Iwasaki et al., 2004). Disinhibition of the apoptotic machinery leads to neurodegenerative disorders, such as Alzheimer's disease (Song et al., 2014). A detailed understanding of neuronal cell death control helps to understand the molecular mechanism of brain trauma, ischemia, or neurodegeneration (Lossi & Merighi, 2003)

During the development of the nervous system, PCD can have different functions depending on the cell type and developmental stage (Buss et al., 2006). The rapid expansion of the progenitors in the VZ is balanced by apoptosis in this area. Although PCD has been observed in post-mitotic neurons as well (Tau & Peterson, 2010). It was shown that around 50% of neurons and their processes are naturally eliminated during development (Dekkers et al., 2013). There are many theories to explain cell death in the developing brain. The neurotrophic hypothesis explains apoptosis by errors in the formation of neuronal connections, neuron afferent inputs, and efferent targets (Buss et al., 2006). Another theory suggests that apoptotic cell death is typical for neurons that fail to migrate correctly or send axons that cannot find their targets (Finlay & Pallas, 1989).

Mature neurons had to develop different strategies to avoid cell death, as they need to function throughout the lifetime of the organism. One way to do this is to induce cell death only if at least two apoptotic pathways are activated simultaneously. The other is the expression of anti-apoptotic brakes, which could act upstream or downstream of mitochondria. Every cell population in the mature nervous system has its own set of anti-apoptotic strategies and understanding these can help to develop therapeutic interventions for the treatment of neurodegenerative diseases (Benn & Woolf, 2004).

### 1.3.5 Initiation of Apoptosis

There are two well-understood mechanisms to initiate apoptotic cell death: the intrinsic (mitochondrial) pathway and the extrinsic (death receptor) pathway (Sastry & Rao, 2000). Being an irreversible process, apoptosis activation is tightly controlled (Böhm & Schild, 2003).

#### 1.3.5.1 Death Receptor Pathway

Death receptors belong to the family of tumor necrosis factor receptors (TNFRs). They are located on the plasma membrane and can bind TNFα or Fasl (Chen & Goeddel, 2002; Raoul et al., 2000; Wajant, 2002). The main source of TNFα are activated macrophages. Fas ligand is expressed mainly on the surface of lymphocytes in response to cell death stimuli. Ligand binding leads to the activation of caspase 8 through the intermediate proteins TNF receptor-associated death domain (TRADD) and Fas-associated death domain (FADD). The activated caspase 8 eventually activates the effector caspase 3, which then cleaves numerous cell proteins resulting in cell death (Blatt & Glick, 2001).

#### 1.3.5.2 Mitochondrial Pathway

The integrity of the mitochondrial outer and inner membranes is essential for the metabolism and survival of aerobic cells. Every permeabilization of the mitochondrial membranes results in disruption of the electron transport chain and leads to rapid cell death. This makes mitochondria a target for various pro-apoptotic proteins e. g. Bcl2-associated protein X (Bax), Bcl2-associated agonist of cell death (Bad), and BH3 interacting domain death agonist (Bid) (Zimmermann et al., 2001). Those increase mitochondrial permeability by creating pores in the outer membrane (Sastry & Rao, 2000). The loss of membrane integrity leads to the release of cytochrome c into the cytoplasm. Cytoplasmatic cytochrome c binds apoptotic peptidase activating factor 1 (Apaf1) and catalyzes its oligomerization. Apaf1 oligomers bind and activate initiator caspase 9 (Yuan et al., 2010). The resulting protein complex is called apoptosome (Acehan et al., 2002). The apoptosome, in turn, activates effector caspases e. g. 3, 6, 7.

#### 1.3.5.3 Bcl2 Protein Family

The intrinsic (mitochondrial) apoptosis pathway is regulated by interactions between three structurally and functionally diverse subgroups of Bcl2-family proteins (Czabotar et al., 2014). All members of the Bcl2-family share one or several Bcl2 homology domains (BH1-BH4). The pro-survival family members like B cell leukemia/lymphoma 2 (Bcl2) itself, BCL2-like 1 (Bcl-XL), BCL2-like 2 (Bcl-W), myeloid cell leukemia sequence 1 (Mcl1), or Bcl2-related protein A1a (Bcl2a1a) as well as the pro-apoptotic effector proteins Bax, Bcl2-antagonist/killer 1 (Bak), and Bcl2-related ovarian killer (Bok) share four BH domains and have similar globular structures (Kvansakul et al., 2008; Muchmore et al., 1996). Pro-apoptotic proteins like Bad, BCL2-like 11 (Bim), Bcl2-interacting killer (Bik), Harakiri (Hrk), Bcl2 modifying factor (Bmf), Bcl2 binding component 3 (Puma), phorbol-12-myristate-13-acetate-induced (Noxa), in contrast, have only one BH3-domain and are shown to be an intrinsically unstructured subgroup of the Bcl2-family (Hinds et al., 2007). BH3-only proteins serve as sensors of cytotoxic stress and as initiators of the intrinsic apoptotic pathway (Tsujimoto & Shimizu, 2000). Their BH3 domain binds pro-survival proteins of the Bcl2 family and inactivates them (Happo et al., 2012). As a result, Bax and Bak (which are normally inhibited by pro-survival Bcl2 proteins) become active and begin to form oligomers that can permeabilize the outer mitochondrial membrane (Willis & Adams, 2005). Some BH3-only proteins like activated Bid and Bim can directly bind and activate Bax or Bak (Gavathiotis et al., 2008; Kuwana et al., 2005). The cell survival thus depends on the balance of pro-apoptotic and anti-apoptotic Bcl2-family proteins (Hutt, 2015).

#### 1.3.5.4 Caspases

Caspases belong to the family of proteolytic enzymes, that play a crucial role in apoptosis and inflammation. The name was inspired by the common structure and function of the proteins — cysteine-dependent aspartate-directed proteases. Cysteine in the active site of the enzyme recognizes and cleaves a target protein always after aspartic acid (Yuan et al., 1993). So far, 13 different caspases have been described in humans. The set of caspases involved in apoptotic cell death is further divided into two classes: initiator caspases (Casp 2, -8, -9, -10) and effector caspases (Casp 3, -6, -7) (Hengartner, 2000; Adams, 2003). Activated initiator caspases trigger a cascade reaction that activates other initiator and effector caspases. This results in the degradation of many cellular proteins and ultimately in cell death (Shalini et al., 2015). Mutations that decrease caspase activity are associated with cancer formation. In contrast, caspase 3 over-activation leads to abundant apoptotic cell death in the brain and can result in neurodegenerative diseases such as Alzheimer's disease (Goodsell, 2000).

#### 1.3.5.5 Neurotrophins

During development, much more neurons are born than are necessary for the normal function of the nervous system (Oppenheim, 1991). There are many theories explaining the programmed cell death of almost half of all cortical neurons during embryonal development (Southwell et al., 2012; Miller, 1995). One of the leading hypotheses explaining neuronal apoptosis during development is the neurotrophic theory. Neurotrophins are secreted growth factors that control neuronal differentiation, growth, and survival of neurons in the nervous system (Hempstead, 2006; Reichardt, 2006; Allen & Dawbarn, 2006). The neurotrophic theory suggests that redundant neurons compete with each other for a restricted amount of neurotrophins secreted by the target cell. Neurons that do not receive enough neurotrophic factors are eliminated by apoptosis (de la Rosa & de Pablo, 2000). The theory was strongly supported by the isolation and description of the first neurotrophic factor — nerve growth factor (Ngf) (Weltman, 1987). Only later it was shown that Ngf indeed promotes differentiation and survival of sympathetic and sensory neurons and that it is expressed mostly in the peripheral nervous system (Bradshaw et al., 1993). Until today three more neurotrophins have been described: brain derived neurotrophic factor (Bdnf), neurotrophin 3 (Ntf3), and Ntf5 (Hofer et al., 1990; Kandel et al., 2000). Receptors that bind neurotrophins fall into two classes: receptor tyrosine kinases (Ntrk1, -2, and -3) and nerve growth factor receptor (Ngfr). Ngfr binds all four neurotrophic factors, whereas Ntrk1 is Ngf-specific, Ntrk2 binds Ntf5 and to a lesser extent Ntf3, and Ntrk3 bind predominantly Ntf3 (Teng et al., 2010; Sanes et al., 2000) while the activation of receptor tyrosine kinases promotes cell survival. The activation of Ngfr promotes apoptotic cell death (Squire et al., 2012; Kandel et al., 2000).

#### 1.3.5.6 Transcriptional Control

Neurons constitutively express both, pro-apoptotic and pro-survival members of the apoptotic machinery. Cell death is regulated by subtle alterations in the balance between these members (Kumar & Cakouros, 2004). BH3-only proteins play a crucial role in the activation of apoptosis, as they inactivate pro-survival Bcl2-family proteins (Adams, 2003). The BH3-only proteins, apart from being controlled by post-translational modification, can be transcriptionally regulated (Puthalakath & Strasser, 2002).

Transcriptional control of developmental cell death is well studied in Caenorhabditis elegans and Drosophila melanogaster. In these models, BH3-only proteins are often transcriptionally regulated (Kumar & Cakouros, 2004). Programmed cell death activator (egl-1) is the single analog of mammalian BH3-only proteins in C. elegans. The promoter of the egl-1 gene contains a binding site for the bHLH transcription factors hlh-2 and hlh-3. These factors are shown to transcriptionally activate egl-1

(Thellmann et al., 2003). Cell death specification (ces-1), a snail-family zinc-finger transcription factor, competes with bHLH proteins to bind the egl-1 promoter. This directly represses the transcription of egl-1 and promotes cell survival (Metzstein & Horvitz, 1999; Thellmann et al., 2003). Another zinc-finger transcription factor, pag-3 can determine the fate of neuroblasts by regulating both differentiation and programmed cell death (Cameron et al., 2002).

In mammals, at least four out of 10 described BH3-only genes are regulated at the transcriptional level (Huang & Strasser, 2000). Among them are Hrk, Noxa, Puma and Bim. Noxa and Puma are both regulated by transformation related protein 53 (Trp53), a very important tumor suppressor (Oda et al., 2000; Nakano & Vousden, 2001). The regulation of Bim expression requires Jun-kinase in neurons (Whitfield et al., 2001) and the forkhead transcription factor FKHR-L1 in hematopoietic cells (Dijkers et al., 2000). Hrk expression is neuron-specific, and it is up-regulated by amyloid ß protein treatment, by the removal of Ngf (Imaizumi et al., 1997), or by Jun-kinase (Harris & Johnson, 2001; Bozyczko-Coyne et al., 2001)

## 1.4 Neuronal bHLH Proteins

Basic helix-loop-helix (bHLH) proteins form a large and diverse family of transcription factors. More than 130 evolutionary conserved bHLH genes are known in humans (Skinner et al., 2010). The bHLH domain consists of two conserved α-helices connected by a short variable sequence, the loop. BHLH proteins usually do homo- or heterodimerize to form functional DNA-binding protein complexes. The targets of bHLH protein dimers are short DNA motives called enhancer boxes (E-boxes) with the palindromic recognition sequence CANNTG (Longo et al., 2008). The spatiotemporal expression of one dimerization partner is often strictly controlled while the other partner is constitutively expressed. Examples of ubiquitously expressed bHLH transcription factors are Tcf3 (E12/E47) or Tcf4 (E2.2), which form dimers with other bHLH proteins to act as transcriptional activators (Flora et al., 2007; Ravanpay & Olson, 2008). Certain HLH proteins lack the typical basic domain and therefore form non-functional dimers that cannot bind DNA. Examples include the inhibitors of DNA-binding (Id1/2/3/4). They act as competitive antagonists by inactivating other transactivating bHLH family members (Murre et al., 1994).

Some bHLH proteins like Myc and HIF-1 are linked to cancer, as they are involved in the control of cell growth and oncogenesis (Hsieh & Dang, 2016). Many tissue-specifically expressed bHLH proteins are known to regulate cell-intrinsic differentiation programs (Saba et al., 2005; Lee & Pfaff, 2003). Brain specifically expressed bHLH transcription factors include, for example, the oligodendrocyte transcription factors (Olig1/2/3), the Neurogenins (Neurog1/2/3), the nescient helix-loop-helix proteins (Nhlh1/2), and the members of the NeuroD-family (Neurod1/2/4/6).

### 1.4.1 Determination and Differentiation Factors

BHLH proteins play important roles in early and late brain development (Pleasure et al., 2000). Proneural determination factors are typically expressed by multipotent progenitor cells and commit those to the neuronal fate (Bertrand et al., 2002). Proneural genes include eg Neurog1/2 (Ma et al., 1996) or Neurod1/4 (Roztocil et al., 1997; Lee et al., 1995). Neuronal progenitor cells then start to express certain postmitotic differentiation factors to establish the neuronal subtype. Differentiation factors include eg Bhlhb5 (Joshi et al., 2008) or Neurod1/2/6 (Schwab et al., 2000).

### 1.4.2 NeuroD-Family bHLH Genes

The NeuroD-family of neuronal bHLH transcription factors comprises the four closely related genes Neurod1, Neurod2, Neurod4, and Neurod6 (Neurod1/2/4/6). In the mouse cerebral cortex, Neurod1, Neurod2, and Neurod6 start to be expressed around E12, when the first pyramidal neuron precursor cells undergo terminal neuronal differentiation and leave the VZ (fig 2a, e, i). These proteins have long been speculated to be important for neuron survival and differentiation (Franklin et al., 2001; Kume et al., 1996; Yasunami et al., 1996).

In comparison with Neurod1/2/6, expression of Neurod4 (Math3) is very low in the developing mouse cerebral cortex (sect 4.10.5, footnote). Neurod4 expression was reported in the dorsal VZ and Neurod4 was discussed as a co-factor of Neurod2 (Mattar et al., 2008). Not expecting any significant role in murine cortex development, I focussed on Neurod1/2/6 and excluded Neurod4 in the following remarks.

#### 1.4.2.1 Neurod1

Overexpression of Neurod1 was shown to convert Xenopus ectodermal cells into neurons (Lee et al., 1995) and to induce neurite outgrowth in vitro (Noma et al., 1999). Neurod1 is expressed not only in the CNS but also in the pancreas and intestine (Naya et al., 1995). Genetic inactivation of Neurod1 (Beta2) in mice leads to apoptotic elimination of insulin-secreting beta cells, which results in severe hyperglycemia and ketonuria (Naya et al., 1997).

In the brain, Neurod1 is robustly expressed by pyramidal neurons in the hippocampus and neocortex, and by granule neurons in the hippocampal dentate gyrus and cerebellum. Genetic inactivation of Neurod1 does not result in obvious defects or reduction of pyramidal neurons. However, the number of cerebellar granule neurons is dramatically reduced, and hippocampal granule cells undergo apoptosis, resulting in mutant mice missing the dentate gyrus (Miyata et al., 1999). Kim and colleagues showed that granule cell apoptosis can be prevented by additional inactivation of Bax, a pro-apoptotic member of the Bcl2 family (Kim, 2012).

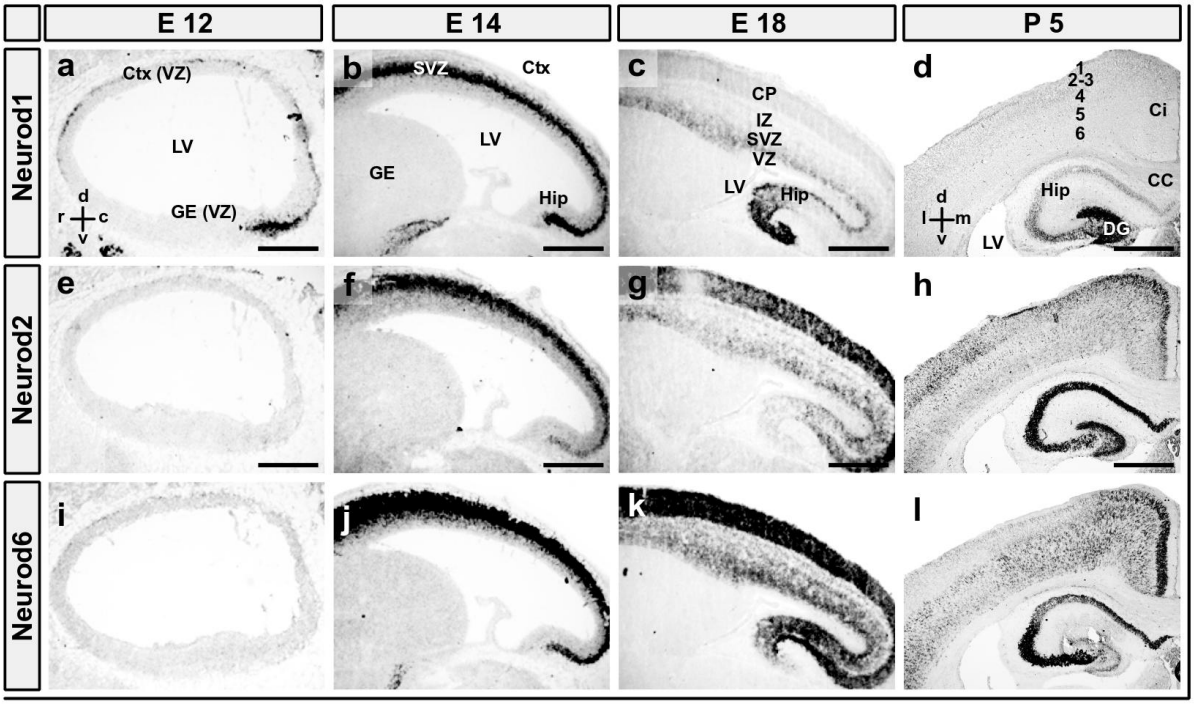


**Figure 2: Expression patterns of Neurod1/2/6 in the developing cerebral cortex**
ISH for Neurod1 **(a-d)**, Neurod2 **(e-h)**, and Neurod6 **(i-l)** in sections of the cerebral cortex at E12, E14, E18, and P5. Adapted from Bormuth (2016). **Abbreviations** on page 119.

### 1.4.2.2 Neurod2

Neurod2 is exclusively expressed in the CNS including the cerebral cortex, amygdala, cerebellum, hippocampus, pontine nucleus, hypothalamus, and the olfactory bulb (Lin et al., 2004; Olson et al., 2001). The strongest expression level is detected shortly after birth, and expression is maintained throughout adulthood (Schwab et al., 1998). Neurod2 was shown to have numerous functions in neurogenesis, differentiation, connectivity formation, and synaptic maturation (Konishi et al., 2000; Bormuth et al., 2013; Ince-Dunn et al., 2006). Neurod2 was identified as a secondary response gene for neuronal apoptosis in cerebellar granule neurons in vivo (Maino et al., 2014). Neuronal survival in the amygdala depends on Neurod2 expression (Lin et al., 2005).

### 1.4.2.3 Neurod6

Expression patterns of Neurod6 are similar to Neurod2. Both genes are expressed by postmitotic pyramidal neurons during embryogenesis. In the adult brain, Neurod6 is predominantly expressed by pyramidal neurons of the deeper neocortical layers (Gummert, 2003; Goebbels, 2002). In vitro studies in PC12 cells implicated Neurod6 in the control of apoptosis (Uittenbogaard & Chiaramello, 2005; Uittenbogaard et al., 2010) However these findings have never been applied to brain development, which is not disturbed in Neurod6-deficient mice (Schwab et al., 1998, 2000; Goebbels

et al., 2006) A recent study identified Neurod6 and its direct target gene phospholipid phosphatase related 4 (Lppr4) (Yamada et al., 2008) as possible biomarkers for Alzheimer's disease (Satoh et al., 2014).

#### 1.4.2.4 Functional Redundancy

Overlapping expression pattern of NeuroD-family transcription factors during embryonic development and high sequence similarity within the bHLH domain suggests functional redundancy of Neurod1, Neurod2, and Neurod6 (fig 2). Pyramidal neuron differentiation and survival do not essentially depend on any single of the three genes (Schwab et al., 2000; Bormuth, 2016), supporting the assumption of functional redundancy. Simultaneous inactivation of Neurod2 and Neurod6 leads to a mild loss of pyramidal neurons and reduced cortical connectivity in the absence of the corpus callosum (Bormuth et al., 2013; Yan, 2016). Neurod2/6 *double*-deficient animals show compensatory upregulation of Neurod1 in the hippocampus and CP. Additional inactivation of Neurod1 results in the loss of most hippocampal pyramidal neurons and microtelencephaly at postnatal day (P) 1 (Bormuth, 2016).

#### 1.4.2.5 Neurod1/2/6 Deficient Mice

Based on the assumption that Neurod1, Neurod2, and Neurod6 regulate pyramidal neuron differentiation and survival in a critical but highly redundant manner, I started to further analyze Neurod1/2/6 *triple*-deficient mice with a focus on pyramidal neuron survival and generation of the pyramidal neuron identity during embryonic cortex development.

The Neurod1/2/6 *triple*-deficient mouse model is partly conditional and based on the following transgenic mouse lines: In Neurod6-Cre (Nex-Cre) mice (Goebbels et al., 2006), the entire open reading frame (ORF) of Neurod6 was replaced by Cre-recombinase (fig 3c), which allows visualizing putatively Neurod6-expressing cells using immunohistochemistry (IHC) for Cre and to drive genetic recombination in the Neurod6-lineage of cells. In Neurod2-Null (NDRF-Null) mice (Bormuth et al., 2013), the entire ORF of Neurod2 was replaced by a neomycin resistance cassette (fig 3b). In Neurod1-Flox mice (Goebbels et al., 2005), the entire ORF of Neurod1 was flanked by LoxP sites (fig 3a), which does not inactivate Neurod1 per se but allows for conditional inactivation of Neurod1 in Cre-expressing cells. Crossing Neurod1-Flox and Neurod6-Cre mice results in permanent inactivation of Neurod1 specifically in the Neurod6-lineage of cells (mostly postmitotic pyramidal neurons of the cerebral cortex and granule cells of the dentate gyrus).

Neurod1/2/6 *triple*-deficient embryos were generated by breeding male and female mice with the genotype Neurod1$^{\text{flox/flox}}$ × Neurod2$^{wt/null}$ × Neurod6$^{\text{cre/cre}}$(Neurod1/6 double-deficient and heterozygous for Neurod2). The ratio of *triple*-deficient offspring

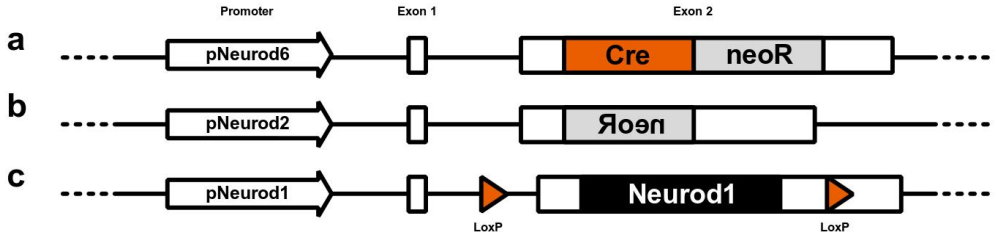


**Figure 3: Targeting constructs for the inactivation of Neurod1/2/6**

**(a)** Classical inactivation of Neurod6 by replacing the ORF with Cre-recombinase, which is expressed under the control of the Neurod6-promoter. **(b)** Classical inactivation of Neurod2 by removing the ORF. **(c)** Conditional inactivation of Neurod1 by flanking the ORF with LoxP recognition sequences. The neomycin resistance cassettes include bacterial promoters, not shown. Adapted from Bormuth (2016).

was 25%. Due to breathing abnormalities, newborn *triple*-deficient pups would die shortly after birth. Thus, only embryonic tissue was used in this study. As previously described, the brains of Neurod1/2/6 *triple*-deficient mice were approximately 25% smaller than those of control animals at E19 (Bormuth, 2016). Volume reduction could be explained by decreased white and gray matter. Neurod1/2/6 *triple*-deficient embryos did lack most hippocampal and intracortical fiber tracts, especially the caudomedial cerebral cortex reduced in volume, and hippocampal pyramidal neurons were almost completely missing.

## 1.5 Aims of this Study

BASIC HELIX-LOOP-HELIX transcriptional factors are key regulators of cellular determination and differentiation processes (Arnold & Winter, 1998). Neuronal bHLH proteins of the NeuroD-family are important for neuronal survival in-vitro (Uittenbogaard & Chiaramello, 2005; Uittenbogaard et al., 2009) and in-vivo in the dentate gyrus (Liu et al., 2000; Schwab et al., 2000), cerebellum (Olson et al., 2001), amygdala (Lin et al., 2005), spinal cord (Bröhl et al., 2008), retina (Cherry et al., 2011), and cerebral cortex (Bormuth, 2016). Neurod1/2/6 are essential for the connectivity of pyramidal neurons in the cerebral neocortex (Ince-Dunn et al., 2006; Bormuth et al., 2013) Detailed molecular mechanisms for these findings have not been proposed.

This dissertation project aims to identify and understand new functions of Neurod1/2/6 in pyramidal neuron differentiation and cerebral cortex development. Building upon initial observations of neuronal misdifferentiation and developmental cell death in the absence of those factors (Miyata et al., 1999; Schwab et al., 2000; Olson et al., 2001; Bormuth, 2016; Yan, 2016), I focus on the transcriptional control of pyramidal neuron identity and apoptosis during early cortex development. Specific questions are:

- The volume of the cerebral cortex is strongly reduced in newborn Neurod1/2/6 *triple*-deficient mice (Bormuth, 2016). — Is this due to decreased production and/or increased loss of pyramidal neurons?
- The inactivation of different NeuroD-family transcription factors results in apoptotic loss of defined sets of cortical neurons while others (that also do normally express the deleted genes) are not affected (Schwab et al., 2000; Lin et al., 2005; Bormuth, 2016). — Which molecular mechanisms trigger and execute apoptosis in the vulnerable cells? Do these mechanisms rely on other factors that are specifically active in certain subpopulations of Neurod1/2/6-positive neurons? Is the apoptotic loss of pyramidal neurons normally prevented by purely cell-intrinsic mechanisms or are cell-extrinsic signals involved?
- The simultaneous inactivation of Neurod2/6 results in compensatory upregulation of Neurod1-expression (Bormuth, 2016) and an abnormal increase of mitotically active Neurod1/Tbr2-positive cells (putatively bIPCs) in the SVZ (Yan, 2016; Li, 2017). — Does the additional inactivation of Neurod1 result in a decrease or a further increase of these abnormal bIPCs? Is the increase of Neurod1-expression in the SVZ a cause or an effect of the bRGC accumulation?
- At birth, different subsets of pyramidal neurons appear to have migrated abnormally in Neurod1/2/6 *triple*-deficient mice (Bormuth, 2016). — Can these migration defects be directly visualized at embryonic stages? Can migration be rescued by reestablishing the expression of Neurod1/2/6 (or appropriate target genes) in scattered cells of the developing cortex?
- Preliminary data (Yan, 2016) suggests that conditional overexpression of Neurod2/6 in the neocortex of Neurod2/6 *double*-deficient embryos might lead to the loss of Pax6 in the VZ. This suggests a feedback signal from Neurod6-positive neurons in the SVZ/CP towards Pax6-positive RGCs that are located in the VZ and did never express Neurod2/6. — Can the same effect be reproduced in Neurod1/2/6 *triple*-deficient mice?
- What are the most important target genes of Neurod1/2/6 in the developing cerebral cortex? Which of these are known to influence the identity or survival of pyramidal neurons?

# 2 Results

To investigate functions of NeuroD-family transcription factors during cerebral cortex development, I analyzed Neurod1/2/6 *triple*-deficient mouse embryos at several time points between the onset of Neurod6-expression at E12 and the end of pregnancy at E20/P0. The following provides a detailed description of the embryonic phenotype focussing on production, identities, radial migration, and premature death of Neurod1/2/6-deficient cortical pyramidal neurons. I used in utero electroporation (IUE) to restore the expression of Neurod2 or Neurod6 and of potential target genes in a subset of differentiating pyramidal neurons of the developing Neurod1/2/6-deficient cerebral cortex. To identify new target genes of Neurod1/2/6, I compared the neocortical transcriptomes of *triple*-deficient and control embryos and followed up on the most promising candidates.

## 2.1 Cell Death in the Developing Cortex

Immunohistochemistry (IHC) for activated caspase 3 is a simple and sensitive method to visualize apoptotic cells in fixed tissue sections (sect 1.3.5.4). Following up on the finding of reduced cortex size and increased cell death in the hippocampus and neocortex of newborn Neurod1/2/6 *triple*-deficient mice (Bormuth, 2016), I systematically studied caspase 3 activity throughout the embryonic phase of cerebral cortex development.

The number of apoptotic cells was increased to varying extents at all examined stages (fig 4). Apoptosis was *particularly* high at E14 and E15 when in some areas of the cortex most cells were apparently in the process of dying (fig 4b', c'). At E16 and E19, apoptosis rates were still significantly increased but orders of magnitude lower than at E14/15 (fig 4d', e').

Strong activation of caspase 3 was confined to the hippocampus and *caudomedial* neocortex but absent from the rhinencephalon and *rostrolateral* neocortex (fig 5). The border between *highly* and *hardly* apoptotic areas of the cortex was surprisingly sharp (arrowheads in fig 4 and fig 5). I stained consecutive coronal paraffin sections and generated three-dimensional reconstructions of entire brains. The cerebral cortex was clearly divided into a *dorsal* portion with very high caspase 3 activity, and a *ventral*

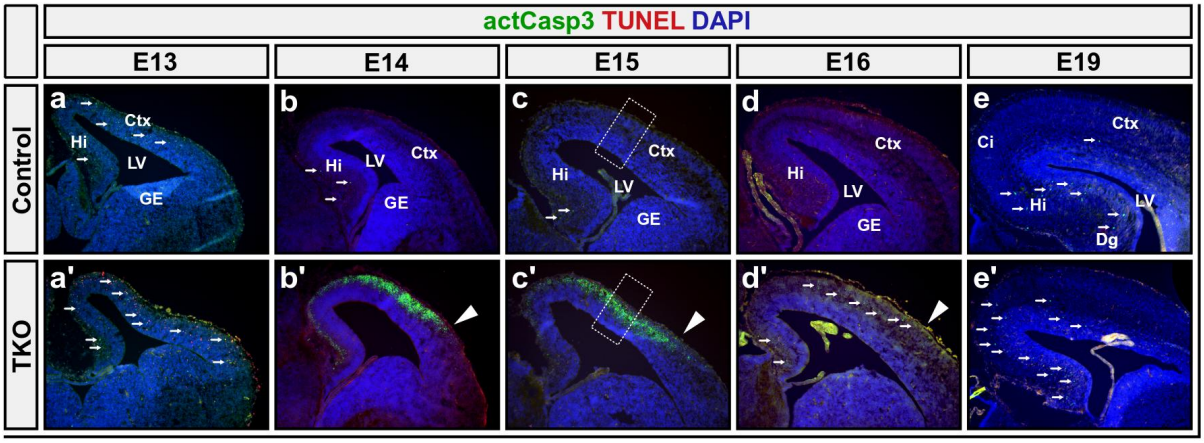


**Figure 4: Temporal restriction of cortical apoptosis**

IHC for activated caspase 3 (green), TUNEL labeling (red), and DAPI counterstaining (blue) in coronal brain sections of Neurod1/2/6 *triple*-deficient embryos (TKO) and Neurod1/6 *double*-deficient littermate controls during cerebral cortex development (E13–E19). **Small arrows** denote cells with strong caspase 3 activity. **Arrowheads** mark the sharp border of strong apoptosis in the central neocortex of Neurod1/2/6 *triple*-deficient mice. Abbreviations on page 119.

portion with low caspase 3 activity. The sharp borderline did approximately follow the horizontal plane at the level of the interventricular foramina of Monro (arrowheads in fig 5b). I am not aware of any genes whose expression patterns would follow this pattern. Notably, the caspase 3 gene itself (procaspase 3) is uniformly expressed in the postmitotic compartment of the entire embryonic telencephalon (eg. CP, CA, OB).[1]

### 2.1.1 Hippocampus

The hippocampus of newborn Neurod1/2/6-deficient mice is severely hypoplastic and virtually devoid of differentiated pyramidal neurons. Neuronal precursor cells are generated in the VZ of the CA, but they presumably undergo apoptosis shortly after the putative onset of Neurod6 expression (Bormuth, 2016).

I used IHC for caspase 3 with DAPI counterstaining at E15 and E17 to confirm apoptotic cells in the postmitotic compartment (but not in the VZ and lower SVZ) of the hippocampal CA1–3 and the adjacent cingulate cortex (fig 6c). The total number of dying cells was much higher at embryonic stages than what had previously been reported for newborn mice (Bormuth, 2016). This suggests that the biggest part of the hippocampal pyramidal neuron progenitor pool is already lost before birth.

The rate of apoptosis was gene-dosage dependent in the hippocampus, but not in the neocortex. Strong activation of caspase 3 in the caudomedial neocortex was only observed in Neurod1/2/6-deficient embryos (fig 6c, e), but not in control littermates that expressed at least a single copy of Neurod2 (fig 6b, d) at E15 and E17. In the

[1] In situ hybridization for caspase 3 at E13, E15, E18 and P4: http://developingmouse.brain-map.org/gene/show/12152

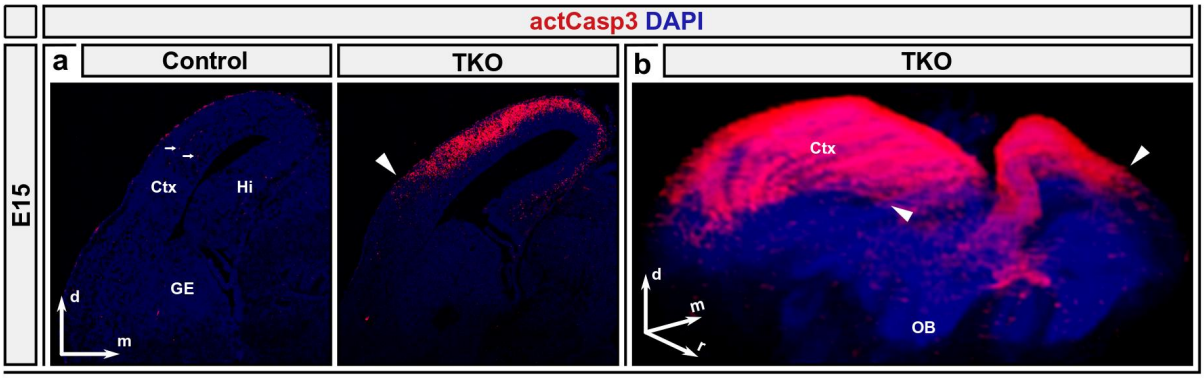


**Figure 5: Spatial restriction of cortical apoptosis**

IHC for activated caspase 3 (red) and DAPI counterstaining (blue) in coronal brain sections of Neurod1/2/6 *triple*-deficient mice (TKO) and Neurod1/6 *double*-deficient littermate controls at E15. **(a)** Example section at the level of the interventricular foramen. **(b)** 3-dimensional reconstruction of an entire Neurod1/2/6 *triple*-deficient brain using 75 consecutive coronal brain sections. **Arrowheads** mark the sharp border of strong apoptosis in the central neocortex of Neurod1/2/6 *triple*-deficient mice. **Labeled axes** visualize the spatial orientation (d: dorsal; m: medial; r: rostral). **Abbreviations** on page 119.

hippocampal CA, two functional alleles of Neurod2 reliably prevented significant apoptosis (fig 6a) while a single allele (Neurod2 gene-dosage reduction) was *not* sufficient (fig 6b, d).

As expected from the largely postmitotic expression patterns of Neurod-family transcription factors (sect 1.4.2), mitotic activity of the hippocampal neuroepithelium was comparable in controls and Neurod1/2/6-deficient mouse embryos: Hippocampal pyramidal neurons are normally born between E12 and birth, with the peak of neurogenesis occurring approximately at E15/E16 (Hayashi et al., 2015). IHC for the RGC-specifically expressed transcription factor Pax6 at E16 demonstrated normal thickness of the sharply delineated VZ in Neurod1/2/6-deficient mice (fig 7a).

IHC for Ki67, a nuclear protein that is present during all phases of the active cell cycle ($G_1$, S, $G_2$, M) but absent from quiescent cells ($G_0$), showed comparable numbers of mitotic cells in the hippocampal neuroepithelium at E15 (red in fig 7b). The latter was confirmed by intraperitoneally injecting 4 mg of the tyrosine-analog bromodeoxyuridine (BrdU) to pregnant mice at E14 and co-staining embryonic tissue that had been fixed 24 h later (at E15) using a BrdU antibody (green in fig 7b). BrdU can readily penetrate the blood-placental barrier before it is quickly eliminated from the maternal and embryonic bodies. During a time window of approximately 20 minutes (min), BrdU is incorporated into the newly synthesized DNA strand of cells that are currently in S-phase. This permanently labels a defined subset of all currently dividing cells and their direct progeny[1] (Martynoga et al., 2005). The compartment of BrdU-positive cells was larger than that of actively cycling Ki67-positive cells (green vs red in fig 7b). This demonstrates that the cell cycle length in the developing hippocampus

[1] Consecutive cell divisions result in a gradual dilution of the BrdU signal because the labeled chromosomes are divided between the daughter cells.

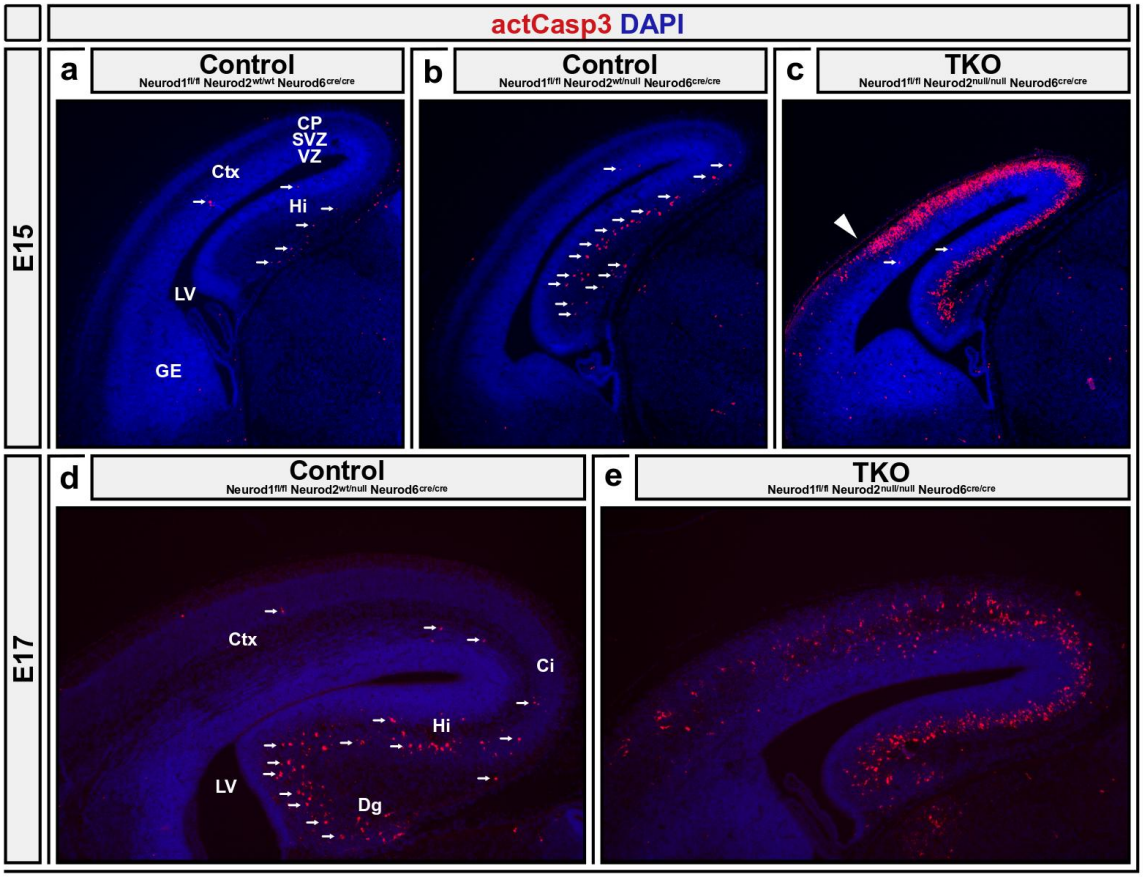


**Figure 6: Dosage dependency of hippocampal apoptosis**

IHC for activated caspase 3 (red) and DAPI counterstaining (blue) in coronal brain sections of Neurod1/2/6 *triple*-deficient embryos (TKO) and Neurod1/6 *double*-deficient littermate controls at E15 **(a–c)** and E17 **(d–e)**. In the neocortex, significant numbers of apoptotic cells were only observed in Neurod1/2/6 *triple*-deficient embryos **(c, e)** but not in control littermates that expressed a single copy of Neurod2 **(b, d)**. In the hippocampus, apoptosis was significantly increased in control embryos that expressed a single copy of Neurod2 **(b, d)** but only mildly increased in control littermates that expressed two copies of Neurod2 **(a)**. **Small arrows** denote cells with strong caspase 3 activity. **Arrowheads** mark the sharp border of strong apoptosis in the central neocortex of Neurod1/2/6 *triple*-deficient mice. Abbreviations on page 119.

is substantially shorter than 24 hours and that postmitotic neurons migrate radially away from the neurogenic VZ and SVZ into the IZ. The numbers and the spatial distribution of BrdU-positive and at the same time Ki67-negative cells were comparable in Neurod1/2/6-deficient and control embryos (only green fig 7b). This suggests that early postmitotic pyramidal neuron differentiation to the transient multipolar stage of the IZ is independent of Neurod1/2/6.

In-situ hybridization (ISH) for the IPC-specifically expressed transcription factor Tbr2 at E16 suggests a moderately increased thickness of the SVZ (fig 7c). Tbr2 is known to be important in activating the projection neuron-specific genes such as Tbr1, and in repressing the neuronal progenitor genes like Pax6(Hevner, 2019). ISH for vesicular glutamate transporter 1 (Vglut1) vesicular glutamate transporter type 1, at E16 confirmed the absence of terminally differentiated glutamatergic pyramidal neurons from the hippocampus of Neurod1/2/6-deficient mouse embryos (fig 7d).

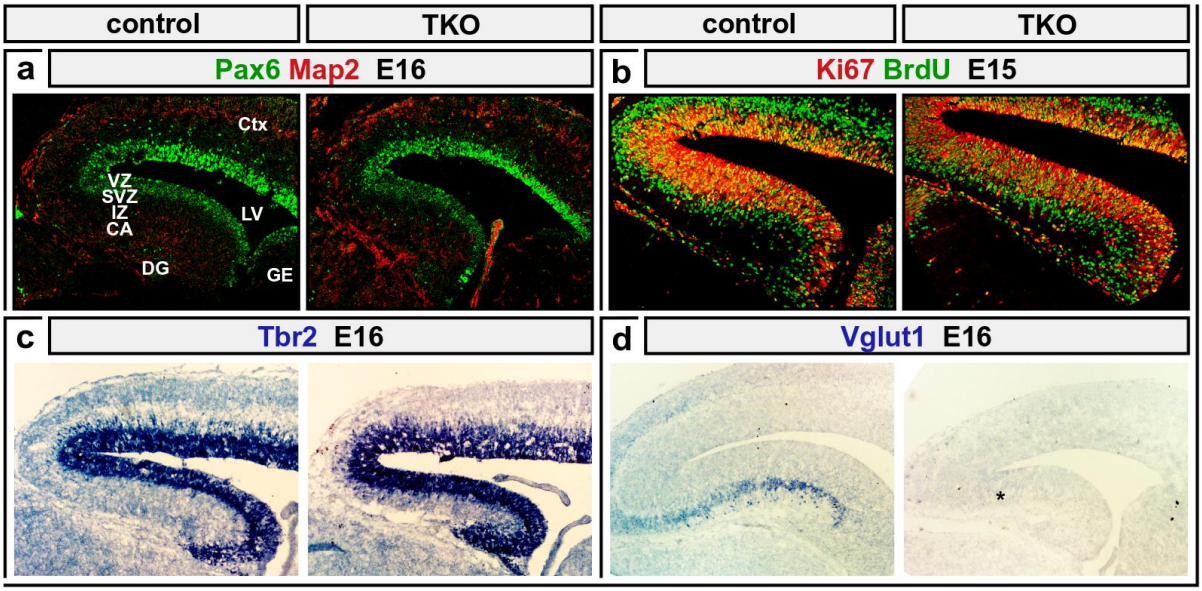


**Figure 7: Differentiation of hippocampal pyramidal neurons**

**(a)** IHC for Pax6 (green) at E16 shows the VZ not to be reduced in thickness or density. **(b)** Following intraperitoneal injection of BrdU at E14, double IHC for Ki67 (red) and BrdU (green) at E15 confirm comparable numbers of currently and recently born cells in the hippocampal VZ and SVZ. **(c)** ISH for Tbr2 (blue) at E16 reveals the number of IPCs not to be decreased but rather increased in the hippocampus of Neurod1/2/6-deficient mice. **(d)** ISH for Vglut1 at E16 confirms the absence of functional pyramidal neurons in the hippocampus and medial neocortex of Neurod1/2/6-deficient mouse embryos. **Asterisks** denote strongly reduced expression in the cortex of Neurod1/2/6-deficient mice. **Abbreviations** on page 119.

### 2.1.2 Neocortex

Cell death rates in the neocortex of Neurod1/2/6-deficient mice were very dynamic over time (fig 8). The relative number of apoptotic cells increased quickly after E13 and reached its maximum between E14 and E15, the time when deep layer neurons normally migrate into the CP. During that time window, the majority of cells in the emerging CP were positive for activated caspase 3 or fragmented DNA as visualized by terminal deoxynucleotidyl transferase dUTP nick end labeling (TUNEL) (fig 8b, c). At later stages, when typically upper layer neurons and glial cells invade the CP, apoptosis was still increased but orders of magnitude weaker than before (fig 8d, e).

Naturally occurring cell death at these stages is mostly confined to precursor cells in the proliferative zones (VZ/SVZ). Apoptosis of these cells is thought to be important to select neuronal precursors before they fully differentiate into pyramidal neurons (Blaschke et al., 1996). In contrast to this mechanism, most apoptotic cells of Neurod1/2/6-deficient embryos were located in the CP.

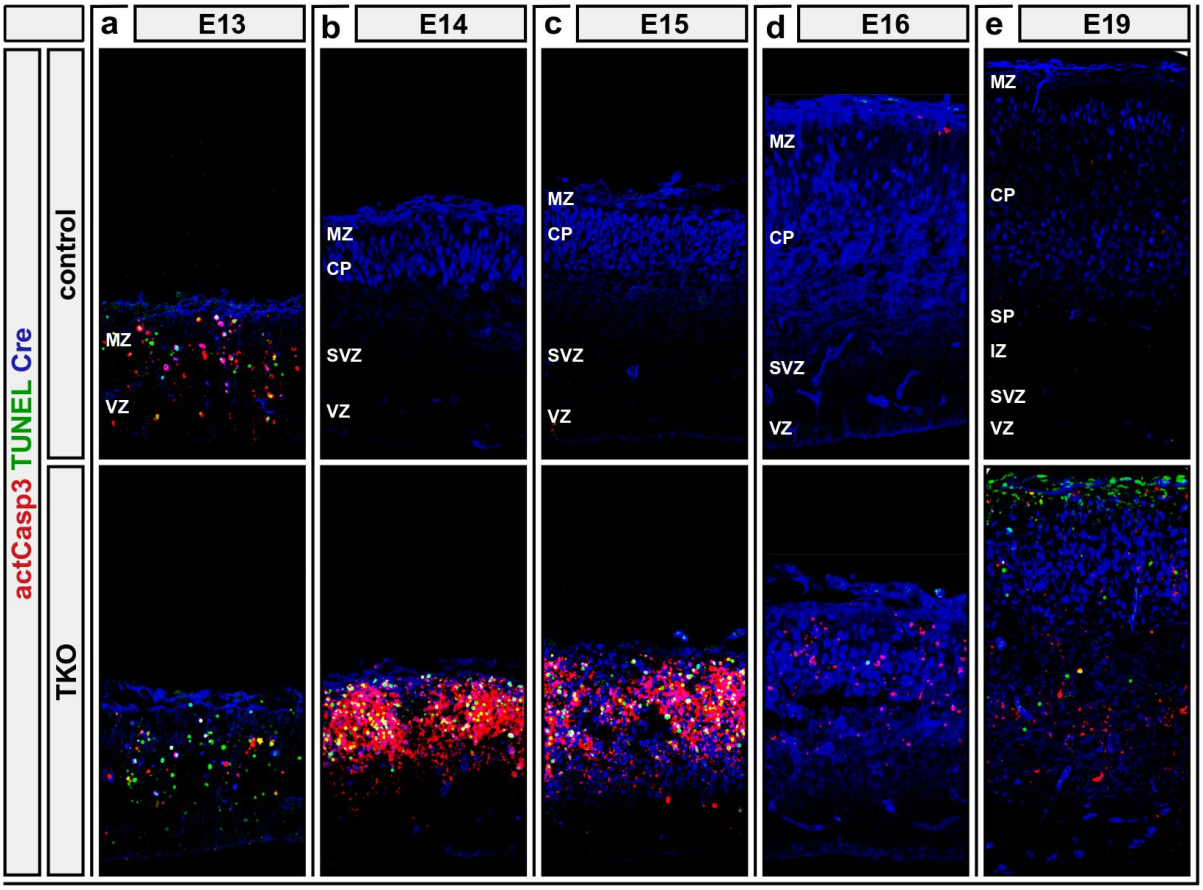


**Figure 8: Apoptosis during development of the CP**

Simultaneous visualization of caspase 3 activation (red), DNA fragmentation (TUNEL in green), and double-stranded DNA (DAPI counterstaining in blue). The images in c approximately correspond to the boxed areas in fig 4c, c'. **Abbreviations** on page 119.

## 2.2 Pyramidal Neuron Identity

While in Neurod1/2/6-deficient mice hippocampal and early-born neocortical pyramidal neurons mostly undergo apoptosis at an immature stage (sect 2.1), later-born neurons of the neocortex usually survive and differentiate to varying degrees. At birth, most surviving pyramidal neurons fail to express typical markers of layer-specific identity or terminal differentiation, and their axons do not reach their putative targets. However, a small subset of spinal projection neurons can grow axons that reach down to the spinal cord (Bormuth, 2016). To further investigate functions of Neurod1/2/6 that drive pyramidal neuron differentiation and influence the establishment of certain pyramidal subtype identities, I stained brain sections at several developmental stages for typical marker proteins.

Expression levels of Pax6 and the numbers of Pax6-positive cells appeared unchanged in Neurod1/2/6-deficient mice at E13 (red in fig 9a), E16 (green in fig 7a), and E19 (not shown). This had been expected, as the neuroepithelium (and specifically Pax6-

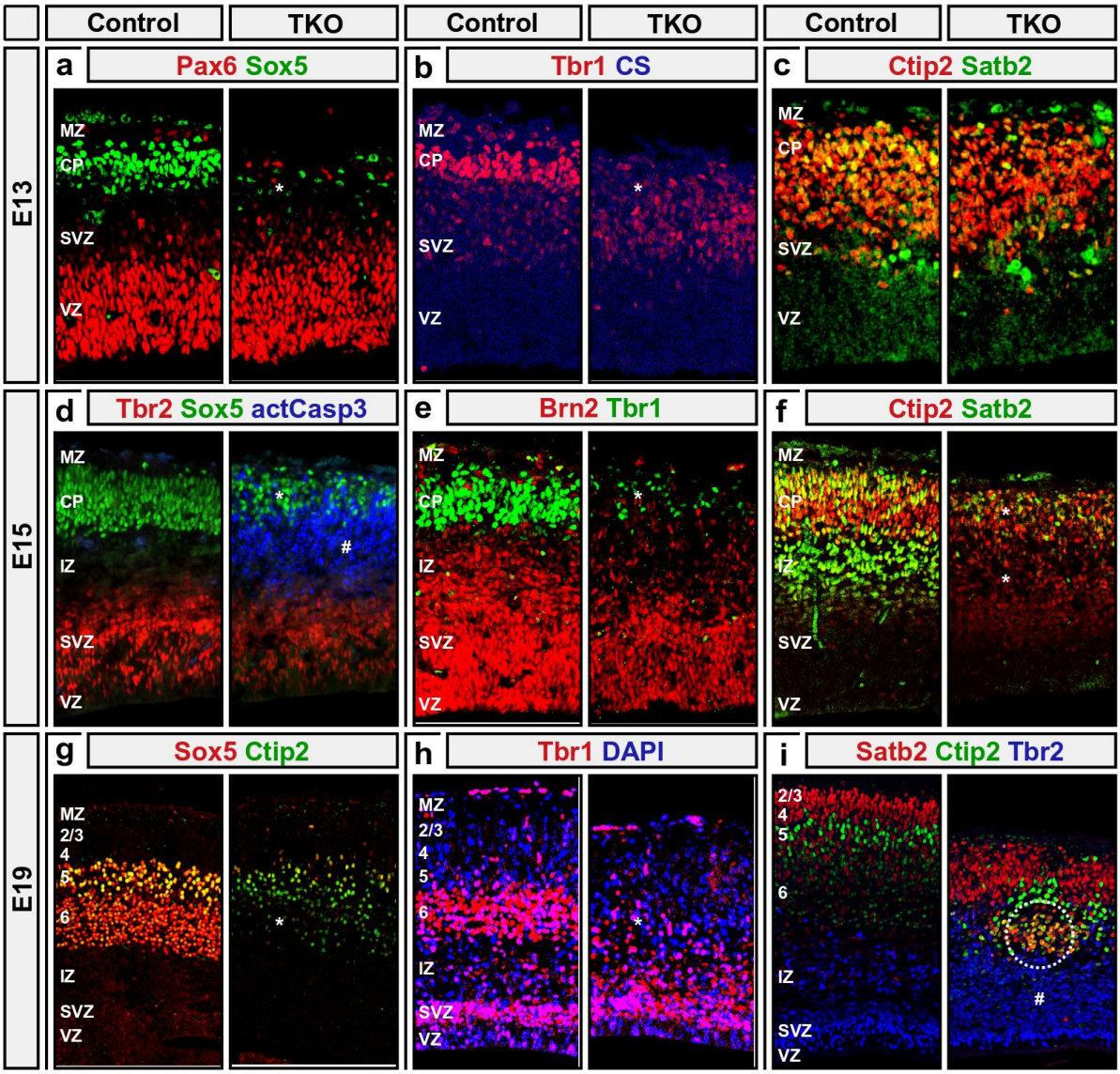


**Figure 9: Acquisition of pyramidal neuron identity during neocortex development**

**(a)** IHC for Pax6 (red, RGCs in the VZ) and Sox5 (green, corticofugal neurons in layer 6), **(b)** for Tbr1 (red, strong in layer 6, weaker in SVZ) with DAPI counterstaining (blue), **(c)** for Ctip2 (red, corticospinal neurons) and Satb2 (green, callosal neurons) at E13. **(d)** IHC for Tbr2 (red, BPCs in the SVZ), Sox5 (green) and activated caspase 3 (blue, apoptotic cells), **(e)** for Tbr1 (green) and Brn2 (red, radially migrating upper layer neurons), **(f)** for Ctip2 (red) and Satb2 (green) at E15. **(g)** IHC for Sox5 (red) and Ctip2 (green), **(h)** for Tbr1 (red) with DAPI counterstaining (blue), **(i)** for Satb2 (red), Ctip2 (green) and Tbr2 (blue) at E19. The **dotted circle** marks a local accumulation of Satb2/Ctip2 double-positive cells in the lower CP. **Asterisks** and **number signs** denote strong changes in the number of cells that were clearly positive for the stained marker protein (decrease and increase in Neurod1/2/6-deficient mice, respectively). **Abbreviations** on page 119.

positive RGCs in the cortical VZ) are generally negative for Neurod1/2/6 (Schwab et al., 1998; Goebbels et al., 2006; Bormuth, 2016). Genetic inactivation of the three NeuroD-factors has thus no direct effect on these cells. The possibility of mild indirect effects, e.g. a diffusible feedback signal from the CP to the VZ, were investigated by quantitative means (sect 2.4, compare Yan 2016, 5.10).

The number of cortical cells expressing SRY-box 5 (Sox5) was strongly reduced in Neurod1/2/6-deficient mice at E13 (green in fig 9a), E15 (green in fig 9d), and E19 (red in fig 9g). During normal cortex development, Sox5 is robustly expressed by corticofugal pyramidal neurons in layer 6, weaker expressed by corticospinal neurons in layer 5, and mostly absent from upper layers (Lai et al., 2008). Immunostaining for Sox5 thus labels the first wave of terminally differentiated pyramidal neurons that invade the CP at E12/13; these cells were mostly lost in Neurod1/2/6-deficient mice (compare sect 2.1.2).

T-box brain 1 (Tbr1) is a transcription factor acting upstream of Sox5, driving the molecular identity of layer 6 and inhibiting that of layer 5 (Bedogni et al., 2010). The number of *strongly* Tbr1-expressing cells was reduced in the CP of Neurod1/2/6-deficient mice at E13 (red in fig 9b), E15 (green in fig 9e), and E19 (red in fig 9h). However, the number of *weakly* Tbr1-expressing cells in the SVZ and IZ was not reduced but rather increased (fig 9h).

COUP-TF interacting 2 (Ctip2) is a well-established marker of corticospinal projection neurons in layer 5, where its expression level is particularly high. While immature pyramidal neurons of other layers do transiently express Ctip2 at lower levels, robust expression is inhibited by other identity-generating transcription factors such as Satb2 in callosal projection neurons (Srinivasan et al., 2012) or Tbr1 (indirectly via Fezf2) in layer 6 (Han et al., 2011). Ctip2 expression levels and the number of Ctip2-positive cells were only mildly reduced in the neocortex of Neurod1/2/6-deficient mice at E13 (red in fig 9c), a time-point when normally most corticospinal projection neurons have been born but are still migrating into the CP. Two days later, at E15, the number of *strongly* Ctip2-positive cells in the CP was reduced while the number of weakly Ctip2-positive cells in the SVZ/IZ was increased (red in fig 9f). This could be explained by a combination of cell death and temporal delay of pyramidal neuron differentiation in the absence of Neurod1/2/6. At E19, when deeper layer neurons have normally settled at their final position in the CP, the number of Ctip2-positive cells was reduced in Neurod1/2/6-deficient mice (fig 9g, i). The number and distribution of the remaining Ctip2-positive cells varied substantially in different areas of the cerebral cortex (fig 10a).

Special AT-rich sequence binding protein 2 (Satb2) promotes the fate of callosally projecting pyramidal neurons in layers 2, 3, and 5 by repressing other factors that promote alternative fates, e.g. Ctip2 (Britanova et al., 2008; Baranek et al., 2012), Lmo4, Foxp2, Sox5, or Tle4 (Whitton et al., 2018). At E13, migrating pyramidal neurons in the SVZ and early CP do normally express Satb2 at moderate levels. Satb2-protein was detectable in the SVZ and CP of Neurod1/2/6-deficient embryos, but the level of expression was clearly decreased in comparison to control littermates (green in fig 9c; confirmed in tab 4). At E15, Satb2 is normally robustly expressed by pyramidal neurons that migrate radially in the IZ or that recently settled in the CP. This was not the case in Neurod1/2/6-deficient mice where only few cells in the CP were clearly Satb2-positive and where Satb2 was not detectable in the IZ (green

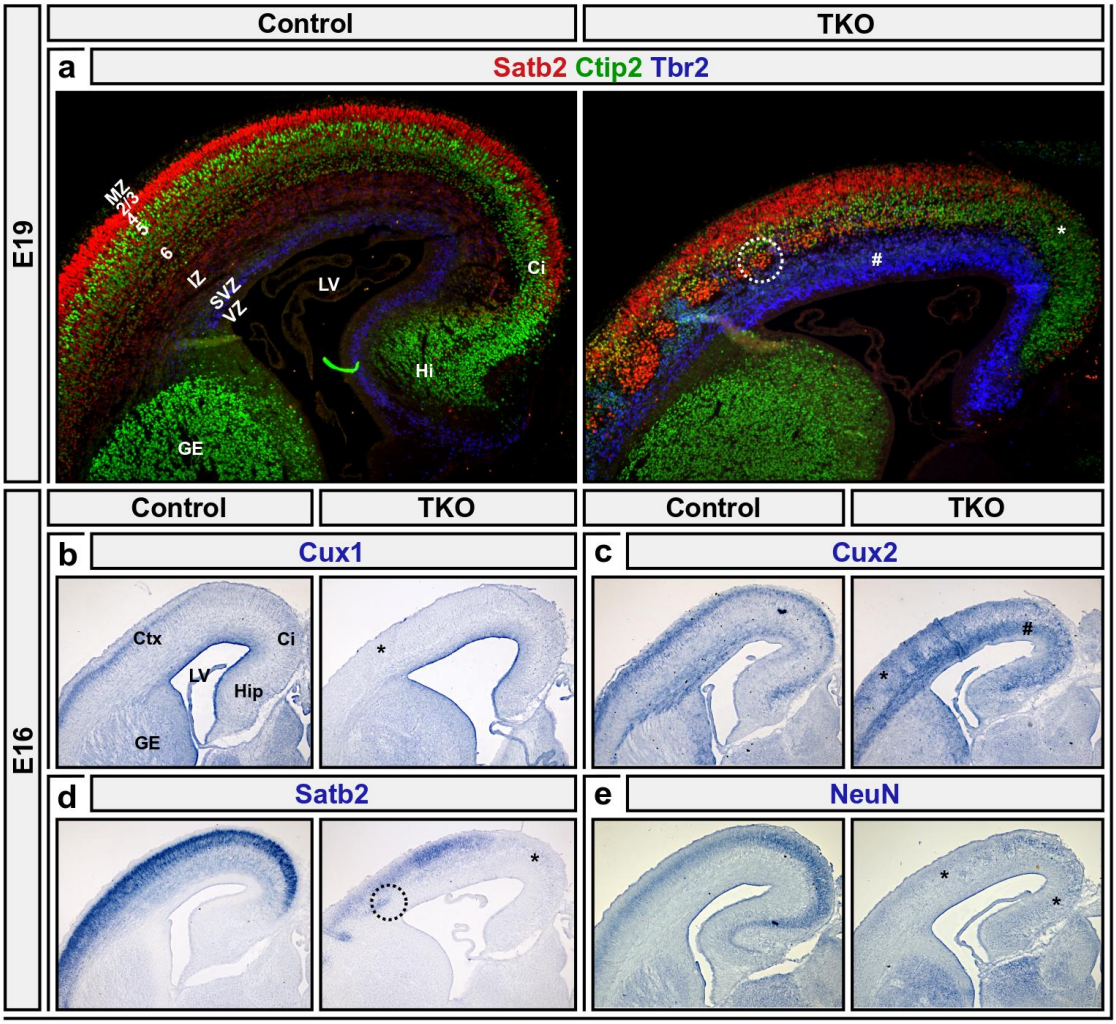


**Figure 10: Regional differences of pyramidal neuron identity**

**(a)** IHC for Satb2 (red), Ctip2 (green) and Tbr2 (blue) at E19. **(b-e)** ISH for **(b)** Cux1, **(c)** Cux2, **(d)** Satb2, and **(e)** NeuN at E16. **Dotted circles** mark local accumulations of Satb2/Ctip2 double-positive cells in the lower CP. **Asterisks** and **number signs** denote strong changes in the number of cells that were clearly positive for the stained marker protein (decrease and increase in Neurod1/2/6-deficient mice, respectively). **Abbreviations** on page 119.

in fig 9f; E16 in fig 10d). Interestingly, this loss of Satb2 was only transient: At E19, Satb2-expression is normally particularly strong in pyramidal neurons that have already settled in layer 2/3 and weaker in those that still migrate radially in the CP or IZ. This principle pattern was maintained in Neurod1/2/6-deficient mice, although the CP was significantly thinner and its strict layering was significantly disturbed (red in fig 9i; fig 10a). Most Satb2-positive/Ctip2-negative cells (putative upper layer neurons) had migrated into the upper CP and were situated above a population of Satb2-negative/Ctip2-positive cells (putative deeper layer neurons). However, an abnormal population of Satb2/Ctip2 double-positive cells clustered below the CP and above the enlarged SVZ (dotted circles in fig 9i and fig 10a).

Tbr2 is normally expressed in IPCs that are located in the SVZ of the developing cortex (sect 1.2.1). As already shown for the hippocampus (sect 2.1.1), the number of Tbr2-positive cells was strongly increased in the SVZ/IZ of the Neurod1/2/6-deficient neocortex at E19 (blue in fig 9i).

The layer-specific expression of Satb2, Ctip2, and Tbr2 is normally relatively homogeneous across the neocortical surface but showed regional alterations in Neurod1/2/6-deficient mice at E19 (fig 10a). Patched accumulations of Ctip2/Satb2 double-positive or double-negative cells in the lower CP were mostly defined to the lateral neocortex (dotted circles in fig 10a, d) while the medial neocortex showed a loss of Satb2 and an expansion of Ctip2 expression (asterisks fig 10a, d).

Cut-like homeobox 1 (Cux1) is normally exclusively expressed in pyramidal neurons of the upper neocortical layers (Nieto et al., 2004). In Neurod1/2/6-deficient mice, Cux1 expression was not detectable by ISH at E16 (fig 10b). Cut-like homeobox 2 (Cux2) is normally expressed by IPCs in the SVZ and pyramidal neurons of the upper cortical layers (Nieto et al., 2004). In Neurod1/2/6-deficient mice, the Cux2 expression domain in the SVZ was similarly expanded as that of Tbr2; Cux2 expression in the CP was reduced but still detectable by ISH at E16 (fig 10c). The expression of the pan-neuronal RNA-binding protein neuronal nuclear antigen (NeuN) was reduced as shown by ISH at E16 (fig 10e).

## 2.3 Radial Migration

HAVING OBSERVED the abnormally clustered rather than a layered distribution of Satb2/Ctip2-positive neurons in Neurod1/2/6-deficient animals at E19 (fig 9i; fig 10a), I set out to examine pyramidal neuron migration more mechanistically and at earlier developmental stages.

Timed injections of thymidine analogs followed by co-staining with molecular markers allow correlating the molecular identity of migrated neurons with the cell's time-of-birth, which in turn reflects the onset of radial migration in the cortical VZ/SVZ. To cover the relevant phases of neocortex development (sect 1.2.1) and to allow labeled cells to terminate radial migration before analysis at E19, I serially injected idoxuridine (IdU) at E12 (to label layer 6), BrdU at E13 (to label layer 5), and ethynyl desoxyuridine (EdU) at E14 (to label layer 4 and early upper layers).

In control animals, co-staining with Ctip2 or Satb2 confirmed that early-born (IdU/BrdU-positive) neurons settled in the deeper neocortical layers 5/6 (co-localization with strong/weak expression of Ctip2 in fig 11a, respectively) while later-born (EdU-positive) neurons settled in upper layers (co-localization with Satb2 in fig 11b). The pattern of radial migration, however, was severely disturbed in Neurod1/2/6-deficient mice. Especially later-born (EdU-positive) cells had failed

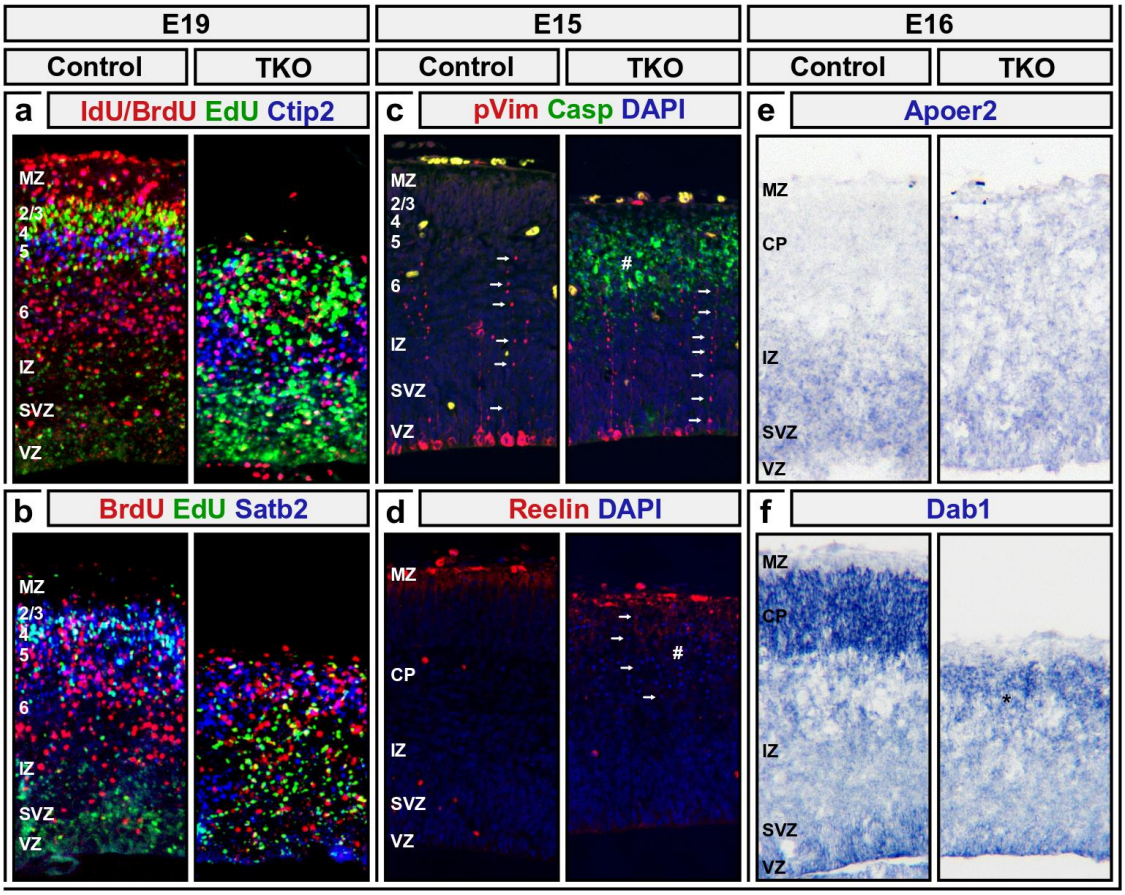


**Figure 11: Radial Migration at Birth**

**(a, b)** Birthdating of cortical pyramidal neurons by serial injections of IdU at E12, BrdU at E13, and EdU at E14; brains were fixed at E19. **(a)** IHC for EdU (green), IdU/BrdU (red), and Ctip2 (blue). **(b)** IHC for EdU (green), IdU (red) and Satb2 (blue). **(c)** IHC for pVimentin (red), activated Caspase (green), and DAPI counterstaining (blue) at E15; arrows point to pVimentin-positive basal processes of RGCs. **(d)** IHC for Reelin (red) and nuclear counterstaining using DAPI (blue) at E15; arrows point to pyknotic cells. **(e)** ISH for Apoer2 (blue) at E16. **(f)** ISH for Dab1 (blue) at E16. **Asterisks** and **number signs** denote strong changes in the number of cells that were clearly positive for the stained marker protein (decrease and increase in Neurod1/2/6-deficient mice, respectively). **Abbreviations** on page 119.

to migrate into the CP by E19. Those cells were stuck in the putative SVZ below (apically of) the Ctip2-positive expression domain (fig 11a), where I had previously observed accumulations of Tbr2- and Cux2-positive IPCs (sect 2.2). The migratory pattern of early-born cells was less obvious in Neurod1/2/6-deficient mice with IdU/BrdU-positive cells spreading the entire cortex, partially co-localizing with Satb2 (fig 11b).

Radial migration in the cerebral cortex is guided along the radially orientated basal processes of RGCs (sect 1.2.2). IHC for phosphorylated Vimentin at E15 did label RGCs with their cell bodies located in the VZ and their basal processes radially spanning the entire cortical anlage to reach the MZ equally in controls and Neurod1/2/6-deficient mice (red signal and arrows in fig 11c).

For proper radial migration, young pyramidal neurons need to correctly interact with the radially oriented basal processes of RGCs. Attachment and detachment are thought to be mediated by reelin-signaling from Cajal-Retzius cells in the MZ (sect 1.2.2). IHC for reelin at E15 confirmed the presence of reelin-secreting Cajal-Retzius cells in the MZ in Neurod1/2/6-deficient mice (red in fig 11d).

Expression of the reelin receptors apolipoprotein receptor related 8 (Apoer2) and very low density lipoprotein receptor (Vldlr) did not show significant differences by ISH at E16 (fig 11e; not shown) and by RNA deep sequencing (RNA-Seq) at E13 (tab 4) in control versus Neurod1/2/6-deficient mice.

Intracellularly, reelin-signaling is mediated by the cytoplasmatic adaptor protein disabled homolog 1 (Dab1) and its target lissencephaly 1 (Lis1). Genetic inactivation of Dab1 has previously been shown to result in the inability of radially migrating neurons to enter the CP and in the accumulation of multipolar neurons in the SVZ/IZ (Franco et al., 2011). In Neurod1/2/6-deficient mice, neocortical expression of Dab1 and Lis1 is substantially reduced, as shown by ISH at E16 (fig 11f; not shown) and by RNA-Seq at E13 (tab 4). Disturbed intracellular reelin signaling might partially explain failed radial migration into the CP and cellular accumulation in the SVZ/IZ of Neurod1/2/6-deficient mice.

I used in utero electroporation (IUE) of green fluorescent protein (GFP) at E14.5 to selectively label a subset of later-born neurons in the developing neocortex. In control mice, co-staining of GFP with Ctip2 and Satb2 at E19 visualized individual radially oriented pyramidal neurons that had mostly migrated into the Satb2-positive upper layers of the CP (arrows in fig 12a); apical dendrites had reached the MZ above the Satb2-positive expression domain; and basal axons had grown tangentially below the IZ to form the coronal radiation (CR), the principal axonal output tract of the neocortex (fig 12a). In Neurod1-2-6-deficient animals, however, the number of surviving GFP-positive neurons in the CP was substantially reduced (fig 12b); remaining neurons mostly were of multipolar rather than pyramidal morphology (arrowheads in fig 12b); only few GFP-positive apical processes had reached the thin MZ; and bundled axon outgrowth or formation of the typical CR were not visible (fig 12b).

To test whether the inability of most Neurod1/2/6-deficient pyramidal neurons to migrate radially into the CP is caused by cell-intrinsic defects or rather by cell-extrinsic effects from the surrounding tissue environment, I used early IUE at E13 to rescue the expression of Neurod2/6 in a small subset of neurons within the otherwise Neurod1/2/6-deficient developing neocortex. The brains were fixed and stained at E15; this time-point was chosen as a compromise: late enough to allow for at least two days of radial migration, but early enough to reduce secondary effects from massive cortical apoptosis (sect 2.1.2). Neurod2 or Neurod6 were bicistronically expressed from the synthetic chicken beta actin based (CAG) promoter followed by an IRES and GFP for visualization (sect 4.8.1).

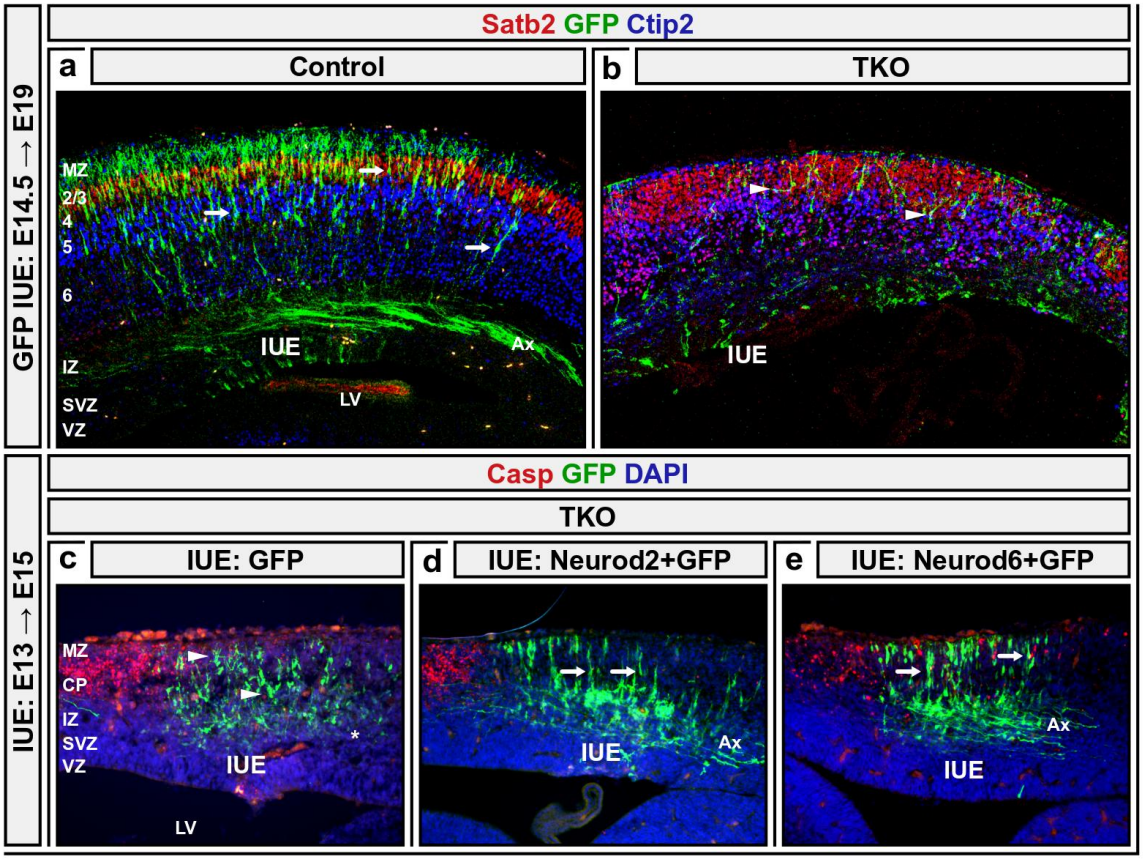


**Figure 12: Radial Migration**

**(a, b)** IUE of GFP at E14 followed by IHC for GFP (green), Satb2 (red), and Ctip2 (blue) at E19. **(c-e)** Bicicstronic IUE of **(c)** only GFP (control), **(d)** Neurod2 and GFP, **(e)** Neurod6 and GFP into the neocortex of Neurod1/2/6-deficient mouse embryos at E13 followed by IHC for GFP (green), activated caspase 3 (red), and DAPI counterstaining (blue) at E15. **Arrows** and **arrowheads** mark clearly radially and not radially oriented cells, respectively. **Abbreviations** on page 119.

Following the electroporation of only GFP into the Neurod1/2/6-deficient neocortex at E13 (no rescue), labeled pyramidal neurons had migrated radially by E15 (fig 12c). The number of GFP-positive cells was not as strongly reduced as at E19 (fig 12c vs b). Most GFP-positive cells were of multipolar rather than pyramidal morphology (arrowheads in fig 12c). Apical dendrites have not reached the MZ and an axonal output tract was not visible below the CP (asterisk in fig 12c). Following the electroporation of either Neurod2 or Neurod6 (rescue), however, GFP-positive cells within the Neurod1/2/6-deficient neocortex showed the morphology of typical pyramidal neurons (arrows in fig 12d, e). Apical dendrites mostly reached the MZ and GFP-positive axons accumulated below the CP (Ax in fig 12d, e).

These cellular rescue experiments showed that the cell morphological and migrational defects in neocortical pyramidal neurons of Neurod1/2/6 *triple*-deficient mice are mostly cell-intrinsic.

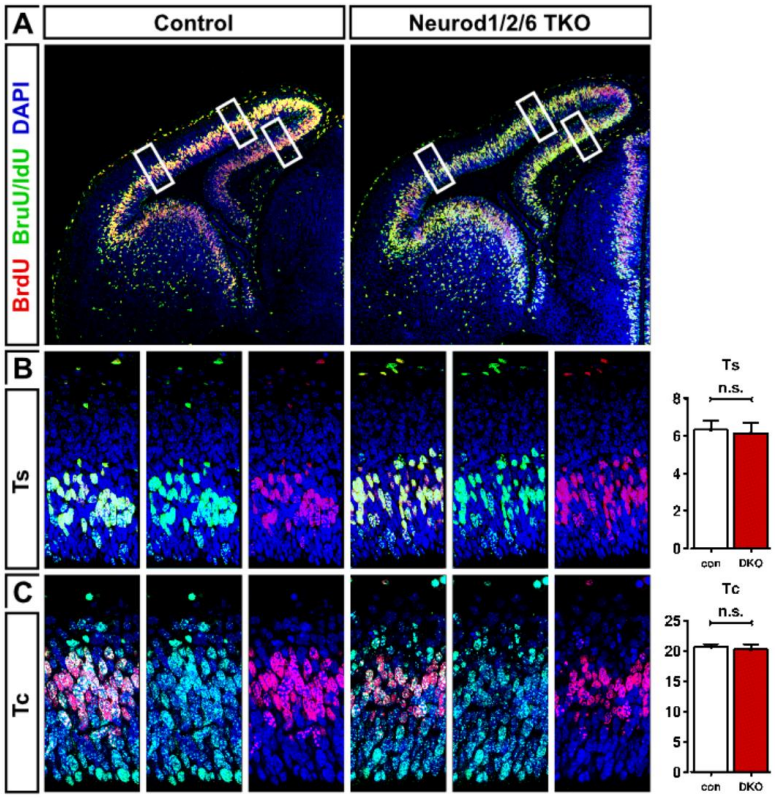


**Figure 13: Cell cycle parameters in the developing cerebral cortex**

IdU and BrdU were sequentially injected at E13 with an interval of 90 min. Coronal brain sections from rostral and caudal levels were co-stained for BrdU (BrdU-specific antibody; red), BrdU/IdU (antibody recognizing both BrdU and IdU; green in *a* and *b*) or Ki67 (green in *c*), and double-stranded DNA (DAPI, blue). **(a)** Overview sections at the caudal level. **(b)** The time of S-phase in hours was calculated by $T_S$ = 1.5 h × (BrdU/IdU-positive cells / only IdU-positive cells) = 1.5 h × yellow cells / green cells. **(c)** The time of cell cycle in hours was calculated by $T_C$ = $T_S$ × Ki67-positive cells / BrdU- or IdU-positive cells = $T_S$ × green cells / red cells. **Abbreviations** on page 119.

## 2.4 Cell Cycle Parameters

HAVING OBSERVED increased numbers of Tbr2-positive mitotic cells in the SVZ of Neurod1/2/6 *triple*-deficient (fig 9i; fig 10a) and Neurod2/6 *double*-deficient (Yan, 2016) mouse embryos, I hypothesized a compensatory increase of the periventricular progenitor pool. It had previously been shown that Neurod6 can stimulate cyclin-dependent kinase (CDK) inhibitors to promote cell cycle arrest (Uittenbogaard & Chiaramello, 2004), and that loss of NeuroD-family transcription factors might lead to increased cell proliferation.

As described in Martynoga et al. (2005), I sequentially injected timed pregnant females with the thymidine analogs IdU and BrdU at an interval of 90 min to quantify s-phase length ($T_S$) and cell cycle legth ($T_C$) in the cerebral cortex of Neurod1/2/6 *triple*-deficient and control mice at E13 and E15. The tissue was fixed 30 min after the second injection, and brain sections from the rostral and caudal cortex were stained for IdU/BrdU (nuclei of cells labeled by either injection), BrdU (nuclei of cells labeled only

by the second injection), Ki67 (nuclei of all mitotic cells) and DNA (DAPI for nuclei of all cells). Fluorescent images were taken from the hippocampus, the medial neocortex, and the lateral neocortex and randomized for double-blinded quantification. Cells that were only stained using the IdU/BrdU-unspecific antibody but not using the BrdU-specific antibody were considered to have left the S-phase during the 90 min interval (L-cells, green in overlays of fig 13b). Cells that were stained using both antibodies were considered to be still in S-phase (S-cells, yellow in overlays of fig 13b). The length of the S-phase was calculated from the proportion of L-cells versus S-cells as $T_S$ = 1,5 h × S-cells / L-cells.

At E13, $T_S$ and $T_C$ were not significantly different in Neurod1/2/6-deficient embryos when compared to littermate controls (fig 13b, c). Quantification of the same cell cycle parameters at E15 gave similar results (not shown). Notably, the variations between the different assessed cortex areas were much higher than the variations between the genotypes (compare Miyama et al., 1997).

## 2.5 Regulation of Apoptosis

Determination and differentiation of cortical pyramidal neurons essentially are relatively robust cell-intrinsic processes controlled by evolutionally well-conserved transcription factors (Gaspard et al., 2008, 2009; Lancaster et al., 2013). Cortical arealization, neuronal subtype specification, and the timing of neuronal production, however, underly a multitude of cell-extrinsic signals from local tissue environments (O'Leary & Sahara, 2008; Seuntjens et al., 2009). It was already shown before that the cell death of neurons independent of environment and apoptosis can be determined by an intrinsic program (Southwell et al., 2012). It is also known that many neurons undergo apoptosis after they establish synaptic contacts, which supports the neurotrophin theory and extrinsic regulation of programmed cell death (Buss et al., 2006).

### 2.5.1 In-Vitro

#### 2.5.1.1 Organotypic Slice Culture

I use a standard organotypic slice culture model to recapitulate in vivo development of the Neurod1/2/6-deficient cortex. The establishment of this technique on the Neurod1/2/6 mutant mouse model allowed me to perform live imaging on the mutant and control tissue to analyze neuronal survival and migration. Organotypic slice cultures prepared from Neurod1/2/6-deficient animals at E16 behave similarly to the in vivo situation. After 6 days in culture, only a small fraction of hippocampal neurons express Cre recombinase (fig 14b).

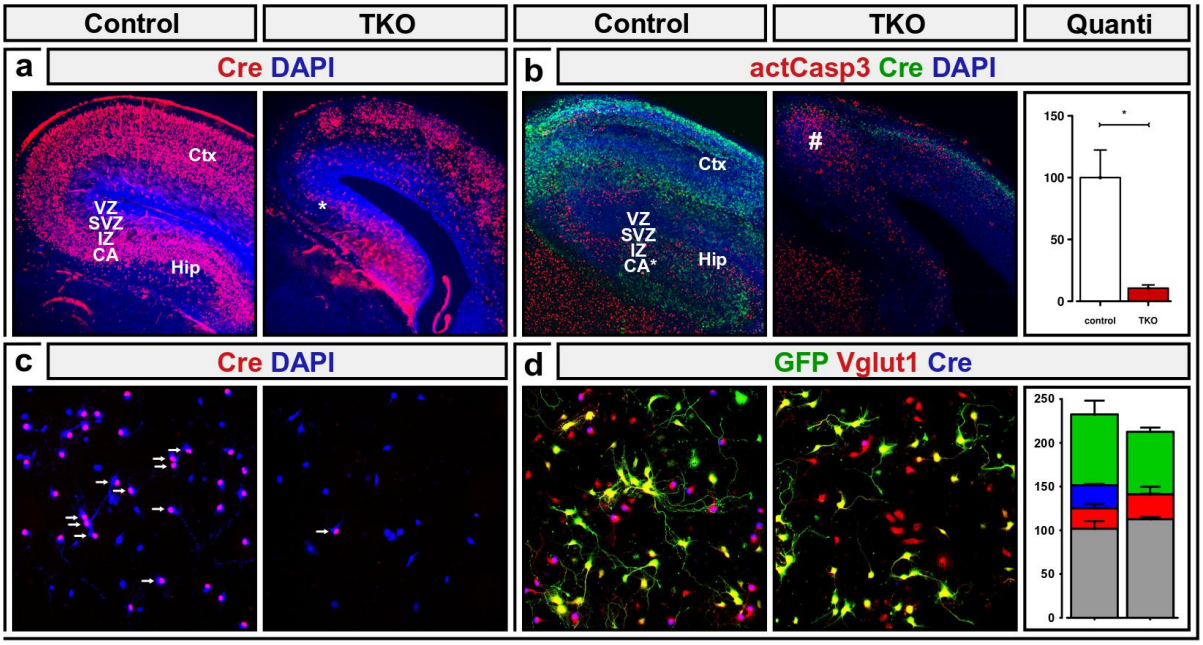


**Figure 14: Loss of hippocampal pyramidal neurons in vitro**

**(a)** IHC for Cre recombinase (red) – marker of endogenous Neurod6-promoter activity – showed loss of pyramidal neurons in the hippocampus Neurod1/2/6-deficient brains. **(b)** IHC performed on organotypic slice culture of control and Neurod1/2/6-deficient mice at E16 after 6 days of incubation. Activated caspase 3 (red) showed an increase of apoptosis in the mutant hippocampus and cingulate cortex. Cre recombinase (green) is almost missing in the hippocampus of mutant animals. Significantly decreased numbers of Cre-positive cells in Neurod1/2/6 mutants are demonstrated in the graphs. **(c)** IHC for Cre recombinase (red) in dissociated cell culture of mutant and control hippocampal tissue prepared at E16 and cultured for 6 days in vitro. **(d)** IHC performed on mixed hippocampal cell cultures of E16 embryos after 3 days in vitro. GFP (green) is specific for all cells from the hippocampus of GFP-positive control mice. Vglut1 (red) – a protein, expressed in glutamatergic pyramidal neurons – is presented in controls as well as in Neurod1/2/6 mutant cultures. Cre recombinase (blue) is strongly reduced in mutant cultures, quantified in the graphs. **Abbreviations** on page 119.

### 2.5.1.2 Dissociated Cell Culture

First I address the question of whether affected cortical and hippocampal pyramidal neurons primarily die due to a cell-intrinsic genetic program or in response to cell-extrinsic signals, e.g. growth factor deprivation. In contrast to the neocortex where many neurons survive the loss of Neurod1/2/6, hippocampal pyramidal neurons undergo apoptosis shortly after activating the Neurod6 promoter. Endogenous Neurod6-promoter activity, which was monitored by immunohistochemistry for Cre-recombinase (Goebbels et al., 2006), was hardly detectable in the hippocampus of Neurod1/2/6-deficient mice (asterisk in fig 14a). I dissociated hippocampal pyramidal neurons to remove possible extrinsic factors that can lead to massive apoptosis in the hippocampus. After 6 days in vitro, only very few Cre-positive neurons in the cultures from Neurod1/2/6-deficient animals were detected (fig 14c).

To exclude neuronal cell death as a result of the lack of some extrinsic factor I prepared mixed dissociated neuron cultures from hippocampal tissue of Neurod1/2/6-deficient and GFP-expressing wild-type mice at E16 (fig 14d). The presence of normally

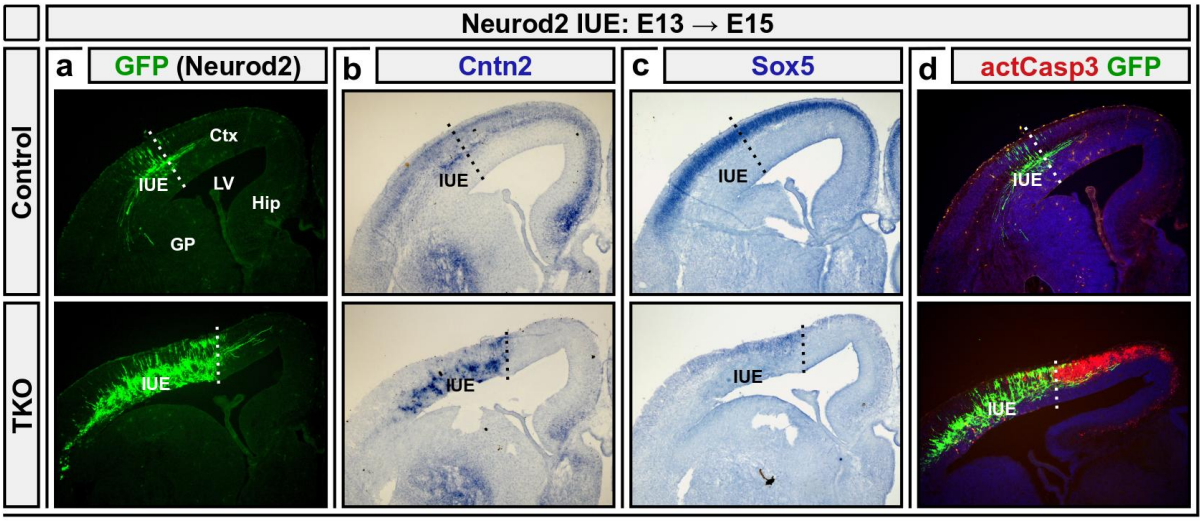


**Figure 15: Restoration of Neurod2-expression prevents neuronal apoptosis**

**(a)** IHC for GFP (green) in the cells, that are in-utero electroporated with pCAG-Neurod2-GFP plasmid at E13 and analyzed at E15. **(b–c)** ISH for Cntn2 (blue) and Sox5 (blue) showed restored expression of these genes in the electroporated area. **(d)** Double-IHC for GFP (green) and activated caspase 3 (red) in the electroporated hemisphere demonstrate a lack of double-positive cells and survival of electroporated neurons. **Abbreviations** on page 119.

differentiating wild-type neurons did not influence the survival of Neurod1/2/6-deficient pyramidal cells. Quantification after 3 days in vitro confirmed increased cell death and the complete loss of Cre-positive neurons in mixed cultures. The results of both experiments argue for the cell-intrinsic mechanism of cell death regulation in Neurod1/2/6-deficient neuron cultures.

### 2.5.2 Genetic Rescue

Concluding that terminal pyramidal neuron differentiation is promoted and neuronal apoptosis is inhibited by Neurod1/2/6 in a cell-intrinsic manner, I over-express Neurod2 (fig 15) in the embryonic neocortex of Neurod1/2/6-deficient mice by in-utero electroporation. I then performed immunostaining and in situ hybridization on the adjacent electroporated brain sections. I observed that electroporated cells expressed Cntn2 – an adhesion molecule from the immunoglobulin-superfamily (fig 15b). Cntn2 expression and callosal axogenesis were shown to be already disturbed in Neurod2/6-deficient brains (Bormuth et al., 2013). Expression of Sox5 – layer 6 specific transcription factor – was at least partially rescued in the electroporated pyramidal neurons that had migrated into the Neurod1/2/6-deficient CP (fig 15c). Activation of caspase 3 did not co-locate with GFP expression (fig 15d). The observed data lead to the conclusion that cells in the cortex, having received Neurod2 transcription factor after in-utero electroporation, could at least partially restore their normal identity and they most probably survive, even in the Neurod1/2/6-deficient surrounding.

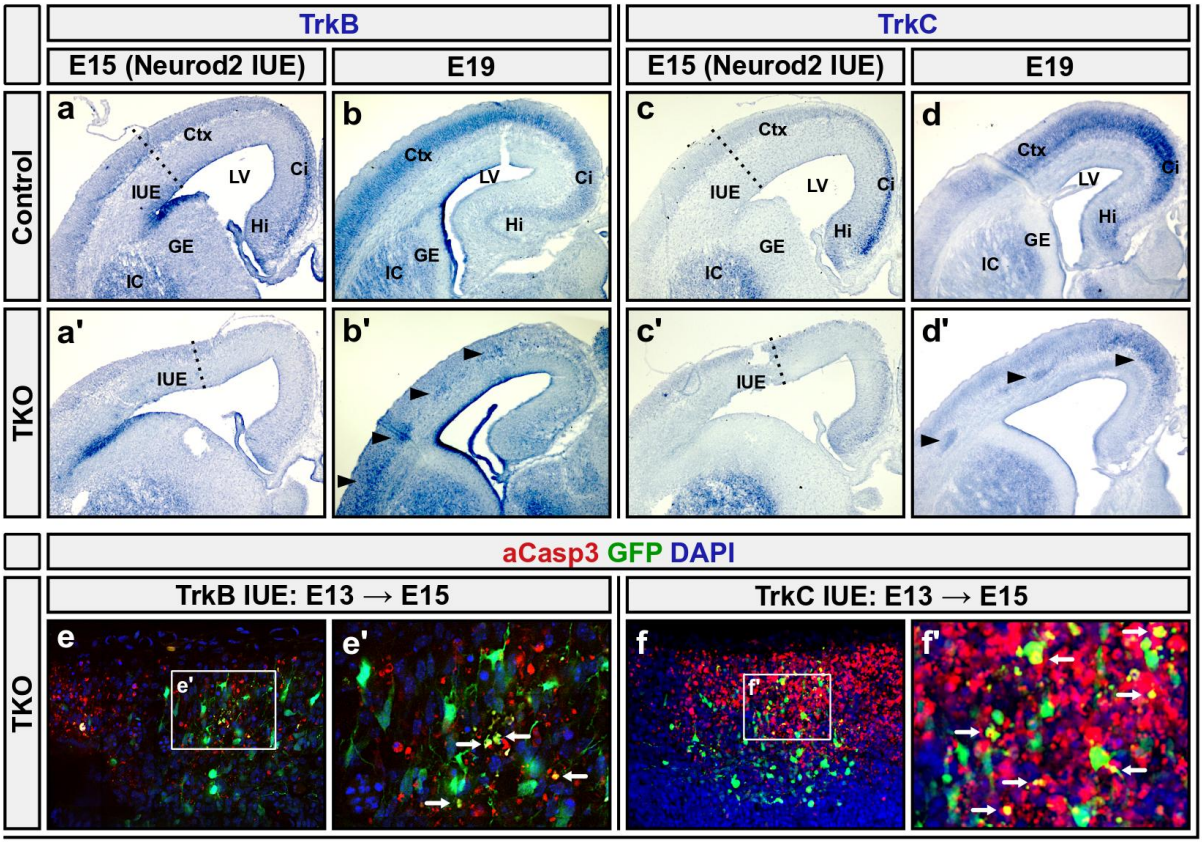


**Figure 16: Neurotrophin signaling does not regulate neuronal survival in Neurod1/2/6-deficient cortex**

**(a, c)** ISH for Ntrk2 (TrkB) and Ntrk3 (TrkC) mRNA (blue) showed the absence of restored expression of these genes after Neurod2 overexpression by in-utero electroporation at E13 and analyzed at E15. **(b, d)** ISH for Ntrk2 (TrkB) and Ntrk3 (TrkC) mRNA represented the expression of these genes in Neurod1/2/6-deficient brains compared to control brains at E19. **(e–f)** IHC for GFP (green) and activated caspase 3 (red) in cortex sections of Neurod1/2/6-deficient mice electroporated with pCAG-Ntrk2-GFP and pCAG-Ntrk3-GFP. **Dotted lines** mark the medial border of the electroporated area. **Arrowheads** point to remaining mRNA expression in the cortex of Neurod1/2/6-deficient mice. **Arrows** point to apoptotic electroporated cells (double-positive for actCasp3 and GFP). **Boxed areas** are also shown in higher magnification. **Abbreviations** on page 119.

### 2.5.3 Neurotrophins

Cell-extrinsic regulation of neuronal survival is classically mediated by neurotrophin signaling (Dekkers & Barde, 2013). Neurotrophins like EGF, NT-3, BDNF, and NT-4/5 are ligands for the neurotrophin receptors Ntrk1 (TrkA), Ntrk2 (TrkB), and Ntrk3 (TrkC) respectively. There are different sources of neurotrophins: paracrine, afferent-derived, blood-born, glia-derived, target-derived (Sanes et al., 2000). Ntrk2/3 are normally expressed in the developing cortex (Puehringer et al., 2013) and are down-regulated in the CP of Neurod1/2/6-deficient animals (fig 16b', d'). In situ hybridization does not suggest differential expression of the neurotrophic ligands BDNF or NT3 in Neurod1/2/6-deficient and control mice (data not shown). Overexpression of Neurod2 by in-utero electroporation of pCAG-Neurod2-GFP plasmid in the Neurod1/2/6-deficient cortex showed a lack of Ntrk2/3 mRNA in the subset of electroporated neurons (fig 16a, c). When I overexpressed Ntrk2 and Ntrk3 in the Neurod1/2/6-

deficient cortex by in-utero electroporation, I could observe, that cells with additional copies of those receptors still activate caspase 3 and undergo apoptosis (fig 16e, f). Taken together these data argue that neurotrophin receptors are probably not directly controlled by NeuroD-family transcription factors. Loss of the Ntrk2/3 expression is the secondary effect of massive cell death in the cortex of Neurod1/2/6-deficient animals. This suggests that programmed cell death might be regulated primarily by a cell-intrinsic developmental program and that extrinsic signals might play a minor role during earlier cortex development in Neurod1/2/6-deficient mice.

### 2.5.4 Bcl2-Family Proteins

There are 6 known members of the Bcl2 family that have a pro-survival effect on the neuron. Bcl2 itself, structurally closely related Bcl2l1 also known as Bcl-XL, Bcl-W (Bcl2l2), MCL-1 (myeloid cell leukemia sequence 1), A1 (BFL1 in humans) keep the mitochondrial integrity and prevent the cytochrome c release, that activate the effector caspases (Adams & Cory, 1998; Zou et al., 1997; Gibson et al., 1996; Czabotar et al., 2014). Using the in situ hybridization technique I could show that Bcl2 and Bcl2l1 mRNAs are down-regulated in Neurod1/2/6-deficient animals (fig 17b'-d'). Expression levels were detectable starting from E14 on.

Overexpression of Neurod2 by in-utero electroporation in the cortex of Neurod1/2/6-deficient mice resulted in at least partial rescue of the Bcl2 expression in the electroporated area (fig 17a'). That can argue for Bcl2 being a direct target of Neurod2.

After creating a Bcl2 (pCAG-Bcl2-GFP) construct and in-utero electroporating this into the cortex of Neurod1/2/6-deficient animals, I did not detect cells that were both positive for GFP (green) and caspase 3 (red) in the electroporated area (fig 17g'). That, in turn, can confirm that Bcl2 is important for cell survival in the Neurod1/2/6-deficient cortex.

To the pro-apoptotic effector proteins belong Bax, Bad and Bok (Bcl2 - related ovarian killer protein) (Hutt, 2015; Harris & Johnson, 2001). ISH for Bax (fig 17e, f), Bad, and Bok (data not shown) revealed lower levels of mRNA expression at E13, E14, E15, and E16, that was similar in control as well as in Neurod1/2/6-deficient brains.

To summarize this set of data: Bcl2 and Bcl-XL are important for cell protection from apoptosis. They are down-regulated in the Neurod1/2/6-deficient cortex. Bcl2 itself might be a direct transcriptional target of Neurod2. The analyzed pro-survival proteins are actively expressed after E14. That could mean, that both Bcl2 and Bcl-XL are important for cell survival in the Neurod1/2/6-deficient brains, but do not trigger massive cell death at E13. Pro-apoptotic proteins do not show significant changes of expression in Neurod1/2/6-deficient and control brains, which excludes their role in the onset of apoptosis.

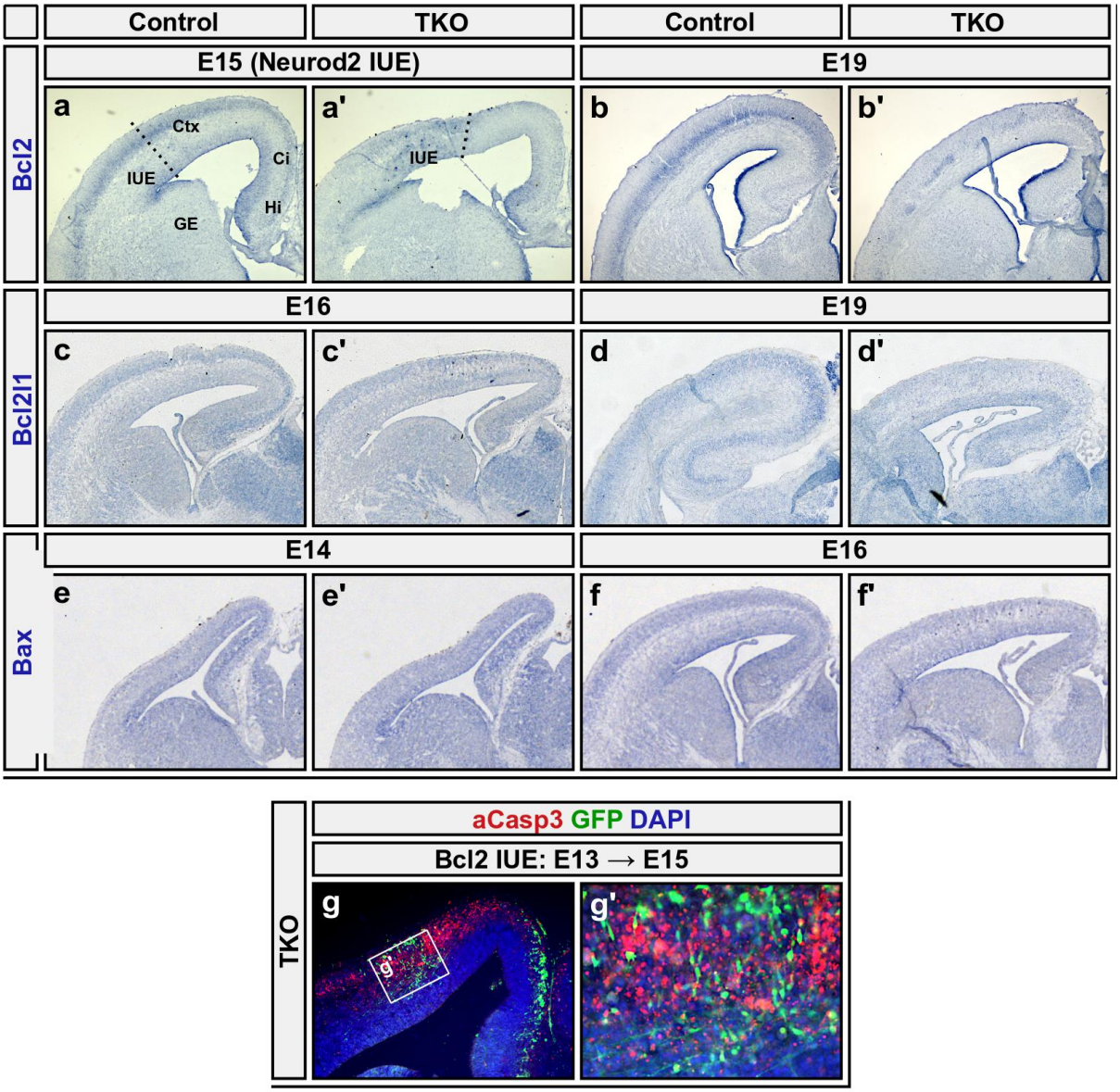


**Figure 17: Expression of Bcl-family genes**

**(a)** ISH for Bcl2 (blue) showed the restored expression of this gene after Neurod2 overexpression by in-utero electroporation at E13 and analyzed at E15. Dotted lines mark the borders of the electroporation areas. **(b, c, d)** ISH for Bcl2 and Bcl2l1 represented the expression of these genes in Neurod1/2/6-deficient brains compared to control brains at E16 and E19. **(e, f)** ISH for the pro-apoptotic protein Bax demonstrated similar expression levels in coronal sections of Neurod1/2/6-deficient brains and control brains at E14 and E16. **(g)** ISH for GFP (green) and activated caspase 3 (red) in cortex sections of Neurod1/2/6-deficient mice electroporated with pCAG-Bcl2-GFP. **Boxed area** is shown in higher magnification. **Abbreviations** on page 119.

## 2.5.5 Neurod6-Controlled Pro-Survival Proteins

Neurod6 was shown to promote differentiation and the survival of cultured neuron-like PC12 cells (Uittenbogaard & Chiaramello, 2002, 2005). In a microarray-based transcriptome analysis, the authors identified a set of heat shock proteins up-regulated in Neurod6-expressing versus native PC12 cells (Uittenbogaard et al., 2010). I matched the dataset of this study with expression data from the Allen Developing Mouse Brain

| **Gene:** | **PC12:** | | | **ISH:** | | | | **Seq:** |
|---|---|---|---|---|---|---|---|---|
| | Ctrl | Nd6+ | FC | E | Area | Ctrl | TKO | Change |
| **Anti-apoptotic Bcl:** | U2005, fig 3 | | | | | | | |
| - BclXl (Bcl2l1) | + | ++++ | | 15 | CP | + | + | 8% ↘ |
| - BclW (Bcl2l2) | – | ++ | | | | | | 3% ↘ |
| **Inhibitors of Apoptosis:** | U2005, fig 4 | | | | | | | |
| - Birc5 (Survivin) | – | +++ | 14.27 ↘ | 14 | VZ | +++ | +++ | 5% ↗ |
| - Xiap (Birc4) | + | ++ | | 14 | VZ | ++ | ++ | 7% ↗ |
| **Heat shock proteins:** | U2010, fig 2, 3 | | | | | | | |
| - Hmox1 (Hsp32, HO-1) | + | ++ | 8.45 ↗ | 14 | Ctx | – | – | 1% ↗ |
| - Hspa1b (Hsp72, Hsp70) | + | ++ | 2.97 ↗ | 14 | VZ, CP | ++ | ++ | 7% ↘ |
| - Hspb1 (Hsp27) | ++ | ++++ | 4.15 ↗ | 14 | Ctx | – | – | – |
| **Other apoptosis related:** | | | | | | | | |
| - Rbp4 | | | 38.91 ↘ | 14 | DG | + | + | – |
| - S100a2 (S100ab) | | | 27.00 ↗ | 14 | Ctx | – | – | – |
| - Lats2 | | | 26.32 ↗ | 14 | Ctx | – | – | 7% ↘ |
| - Uchl1 | | | 25.84 ↘ | 14 | CP, CA | ++ | ++ | 9% ↘ |
| - Trp53 (p53) | | | 1.80 ↘ | 14 | VZ | ++ | ++ | 3% ↘ |
| - Apaf1 | | | | 14 | Ctx | – | – | 3% ↗ |
| **Others (controls):** | | | | | | | | |
| - Gap43 | | | 6.21 ↗ | 16 | CP | ++ | ++ | 44% ↘ |
| - Mafb | | | 2.68 ↗ | 16 | lat. CP | – | + | 44% ↗ |

**Table 2: Neurod6-dependent pro-survival factors**

**Gene:** gene symbols grouped by protein families; **PC12:** in-vitro expression data from Uittenbogaard et al. (*Ctrl:* dot blot of wild type PC12 cells, *Nd6+:* dot blot of constitutively Neurod6-expressing PC12 cells, *FC:* microarray-based expression analysis as fold change in wild type vs. Neurod6-expressing PC12 cells); **ISH:** in situ hybridization (*Region:* area of the cerebral cortex, *E:* embryonic stage, *Ctrl:* control mice, *TKO:* Neurod1/2/6 *triple*-deficient mice); **Seq:** in-vivo expression data from embryonic mouse cortex tissue (*Change:* sex-corrected expresison in relative %, details in sect 2.6); **U2005:** Uittenbogaard & Chiaramello (2005); **U2010:** Uittenbogaard et al. (2010); **–:** not detectable or indistinguishable from background signal; **+:** weak signal **++:** moderate signal; **+++:** strong signal; **++++:** very strong signal. **Abbreviations** on page 119.

Atlas[1] (2008) to identify differentially expressed candidate genes that are normally expressed in the mammalian cortex. Chromogenic ISH in frozen brain sections of Neurod1/2/6-deficient and control mice at E14, however, did not reveal any of these candidates to be robustly differentially expressed in the absence of Neurod1/2/6 (fig 18; tab 2).

There are two well-known members of apoptotic cascades - Apaf1 and Trp53 (Cecconi et al., 1998; Yoshida et al., 1998; Eizenberg et al., 1995). They were as well included in the described gene analysis (tab 2). Nevertheless, I was not able to see any difference in the gene expression of Apaf1 (data not shown) or Trp53 (fig 18i) in the Neurod1/2/6-deficient condition.

[1] http://developingmouse.brain-map.org/

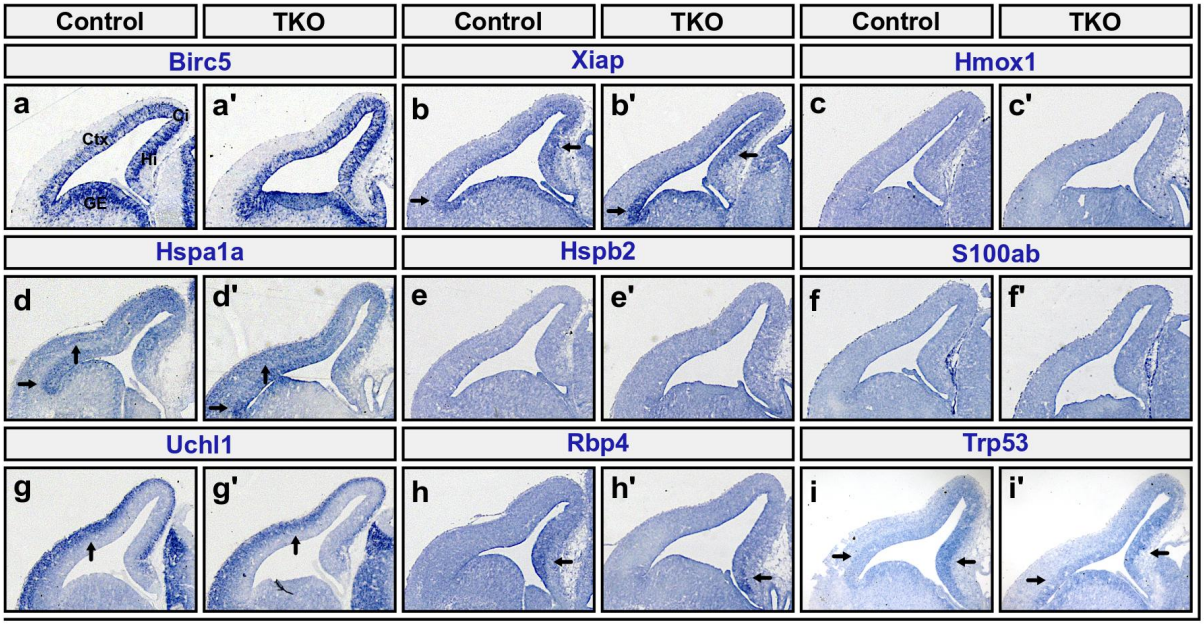


**Figure 18: Pro-survival factors as identified by Uittenbogaard et al.**

IHC in coronal brain sections of Neurod1/2/6-deficient mouse embryos and control littermates at E14. **Arrows** denote expression domains in the cerebral cortex. **Abbreviations** on page 119.

As I could not apply the results of the published in vitro microarray-based gene analysis to the mouse model used in my research, I decided to perform comparative transcriptome analysis myself. And thus evaluate different gene expressions in Neurod1/2/6-deficient brains vs. control brains in vitro.

## 2.6 Comparative Transcriptome Analysis

THE CANDIDATE-BASED APPROACH to identify molecular mechanisms controlling neuronal survival and differentiation downstream of Neurod1/2/6 has so far been not very successful: The restoration of neurotrophin receptors and well-known Bcl2-family cell death regulators was not sufficient to rescue massive apoptosis in Neurod1/2/6 *triple*-deficient brains (sect 2.5.3; sect 2.5.4) and previously identified regulators of neuronal apoptosis were not expressed in the cerebral cortex or were not differentially expressed in Neurod1/2/6-deficient embryos (sect 2.5.5). I decided to perform comparable whole transcriptome analysis using neocortical tissue of Neurod1/2/6 *triple*-deficient and control embryos to identify potential target genes in an unbiased manner.

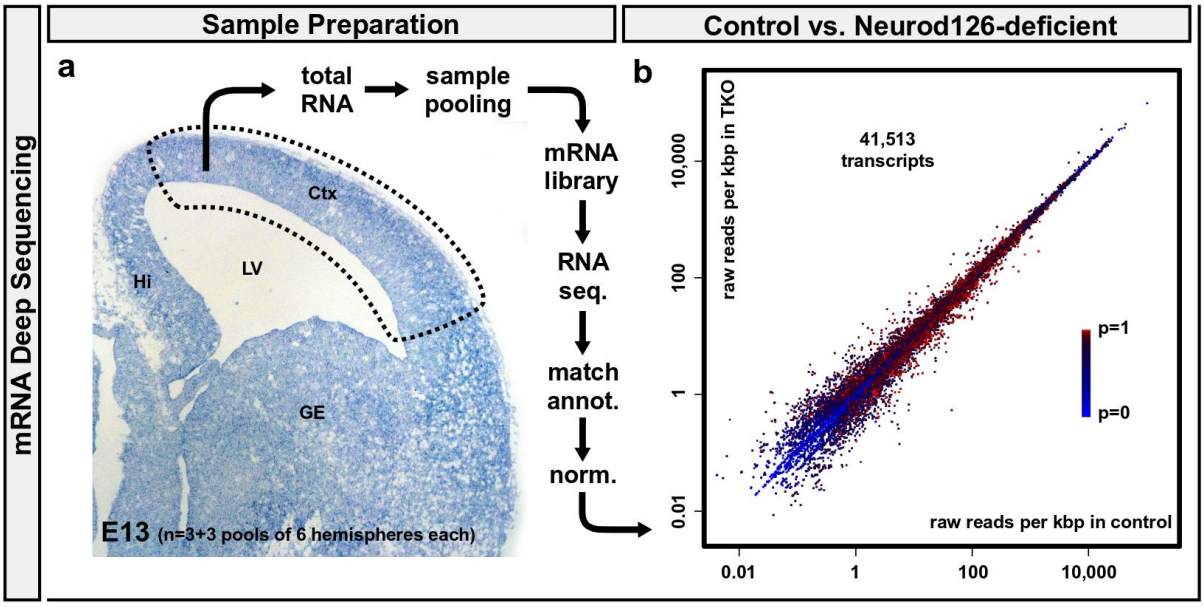


**Figure 19: Overview of transcriptome analysis**

Whole transcriptome analysis using E13 neocortex tissue from Neurod1/2/3 *triple*-deficient vs. control embryos. **(a)** Overview of the methodic procedure (sect 4.10). **(b)** Correlation of total raw reads in Neurod1/2/6 *triple*-deficient vs. control tissue. The color of data points visualizes the p-value of the paired t-test, as given in the legend. **Abbreviations** on page 119.

Similar approaches have already been undertaken but did not identify regulators of developmental cell death and cell identity: Microdissected tissue from the neocortex of Neurod2 single-deficient and control mice at P28 was used for RNA-Seq (unpublished[1]). Cerebellar tissue from young adult mice lacking Neurod1 selectively in cerebellar granule cells was used for microarray-based transcriptome analysis (unpublished[2]). Microdissected tissue from the neocortex of newborn Neurod2/6 *double*-deficient mice was used for RNA amplification and microarray-based transcriptome analysis, however, no developmental regulators could be identified and known target genes such as Gap43, Cntn2, and Robo1 did not appear to be differentially expressed in the dataset (unpublished[3]).

| RNA samples: | | Number of raw reads: | | | Reads per transcript: | | |
|---|---|---|---|---|---|---|---|
| Pool | Genotype | Total | Matched | in % | Raw | Stable | Norm |
| #1 | Control | 32,639,230 | 24,681,225 | 75.6 | 1,423 | 2,039 | 1,315 |
| #2 | Neurod1/2/6-deficient | 28,890,990 | 21,509,066 | 74.5 | 1,230 | 1,778 | 1,304 |
| #3 | Control | 28,177,154 | 21,373,271 | 75.9 | 1,343 | 1,922 | 1,317 |
| #4 | Neurod1/2/6-deficient | 30,605,002 | 23,367,054 | 76.4 | 1,247 | 1,794 | 1,310 |
| #5 | Control | 30,590,011 | 23,443,247 | 76.6 | 1,339 | 1,936 | 1,304 |
| #6 | Neurod1/2/6-deficient | 29,244,676 | 21,943,706 | 75.0 | 1,271 | 1,839 | 1,302 |
| | Average over all pools: | 30,024,511 | 22,719,595 | 75.7 | 1,309 | 1,885 | 1,309 |
| | Variance in % of average: | 4.18 | 4.89 | 0.84 | 4.55 | 4.30 | 0.41 |

**Table 3: RNA-Seq samples, pooling, and normalization**

Paired pools of neocortical RNA preparations were used for RNA-Seq. Every RNA sample from a Neurod1/2/6-deficient embryo was matched with a littermate control in the corresponding pool (#1/2, #3/4, #5/6). Approximately 75 % of all sequenced reads could be directly matched to annotated reference transcripts (last column of middle block). The variation of matched raw reads per transcript was 4.55 % over all pools (2.66 % over three genetically identical control pools #1/3/5; 1.16 % over the three identical Neurod1/2/6-deficient pools #2/4/6; first column in the block). DESeq normalization reduced the variance by more than one order of magnitude to 0.41 % over all pools (0.41 % over the three genetically identical control pools #1/3/5; 0.24 % over the three identical Neurod1/2/6-deficient pools #2/4/6; last column in last block).

### 2.6.1 Experimental Design

I aimed to design an experiment as stringent as possible in order to minimize the number of false-positive results: I collected neocortical tissue from Neurod1/2/6-deficient and control mice at E13 and isolated total RNA-Seq (fig 19a). The early time-point was chosen to prevent the dilution of differential gene expression (primary effect) by alterations in the cellular composition of the neocortex due to apoptosis, misdifferentiation, or mismigration (secondary effects). E13 was considered the earliest possible time point because the normal onset of Neurod6-expression is approximately at E12. (Goebbels et al., 2006). E14 was considered too late as the CP of Neurod1/2/6-deficient mice already contains a large number of apoptotic cells at that stage (sect 2.1.2). The genotypes of Neurod1/2/6-deficient and control embryos differ in only one allele of Neurod2[1] (sect 4.1). The central neocortex was carefully dissected under RNA-stabilizing conditions (sect 4.10) to prevent contaminations with tissue from e. g. the hippocampus, the olfactory cortex, or the ganglionic eminence. Neocortical tissue from both hemispheres was pooled to control for lateralized gene

[1]Unpublished manuscript by Bugeon S, Lafi S, Beurrier C, Sahu S, Runge K et al. (2018). Preprint available at bioRxiv: http://doi.org/10.1101/296889. Title: Morphofunctional deficits in the cerebral cortex of NeuroD2 mutant mice are associated with autism/schizophrenia-like behaviors.

[2]Personal communication. Experiment by Pieper A, Stünkel C, Wiechert S, Rossner M, Goebbels S, et al. (2007). Conditional inactivation of Neurod-Flox (Goebbels et al., 2005) using the GABA(A) receptor alpha6 subunit promoter (Fünfschilling & Reichardt, 2002).

[3]Personal communication. Experiment by Bormuth I, Stünkel C, Wichert S, Rossner M, Schwab M et al. (2010). Secondary changes in the cellular composition of the cerebral cortex and signal saturation during RNA amplification might have masked relevant differences in expression levels.

[1]Neurod1/2/6 *triple*-deficient: Neurod1$^{flox/flox}$ × Neurod2$^{null/null}$ × Neurod6$^{cre/cre}$
Control: Neurod1$^{flox/flox}$ × Neurod2$^{wt/null}$ × Neurod6$^{cre/cre}$

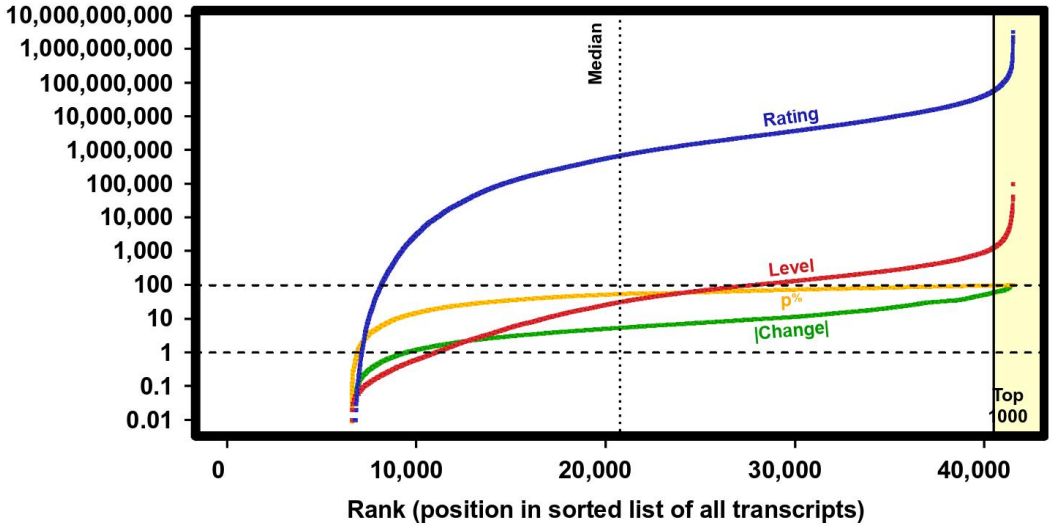


**Figure 20: Ranking of RNA-Seq data**

**Level:** Calculated expression level in normalized reads per kbp; **|Change|:** Relative change of expression level in Neurod1/2/6-deficient mice versus control littermates (plotted as modulo in %); **$p^{\%}$:** P-value of paired student's t-test plotted as $(1 - p) * 100$; **Rating:** Combination of the former three values ($\sqrt{Level} \times Change^2 \times p^2$). **Rank:** Position on the list of all transcripts ascendingly sorted by the combinatorial rating. **Median:** The median value (ranked at 20,757 of 41,513 transcripts); **Top1000:** The 1000 highest-ranked values (yellow area; top 2.4%). The x-axis is independent for each curve as the list of transcripts is ordered by the respective parameter; the y-axis is in logarithmic scale.

expression.[1] RNA preparations from three independent brains were pooled to increase the total amount of total RNA and to minimize the effect of preparation artifacts. RNA pools were paired in a way that each Neurod1/2/6-deficient sample was matched with a control sample that originated from the same litter and was processed in parallel. Three independent biological and technical replicates were prepared for each genotype to allow for statistical evaluation (n=3; three RNA-pools per genotype, each based on paired tissue from three independent embryos). Following mRNA enrichment and multiplex tagging, the samples were sequenced in one lane of an Illumina next-generation sequencing device.

## 2.6.2 Data Analysis

Raw reads were mapped to the latest published reference transcriptome.[2] The calculated expression of any given transcript (in the following simply called *expression*) is given in normalized reads per kilo base pair (kbp). Initial data analysis showed that the global expression profiles of Neurod1/2/6-deficient and control tissues were highly similar (correlation coefficient = 0.9937; scatterplot in fig 19b). The genotype-

[1] The expression of Neurod6 (and its direct target gene Gap43) is significantly higher in the left hemisphere of E17 mice, but not at two months after birth (Grabrucker et al., 2017). Neurod1 is asymmetrically expressed in the cerebral hemispheres of human postmortem brains (Karlebach & Francks, 2015).

[2] NCBI reference sequences (RefSeq): http://www.ncbi.nlm.nih.gov/refseq/about/
Mouse transcriptome: http://ftp.ncbi.nlm.nih.gov/refseq/M_musculus/mRNA_Prot/

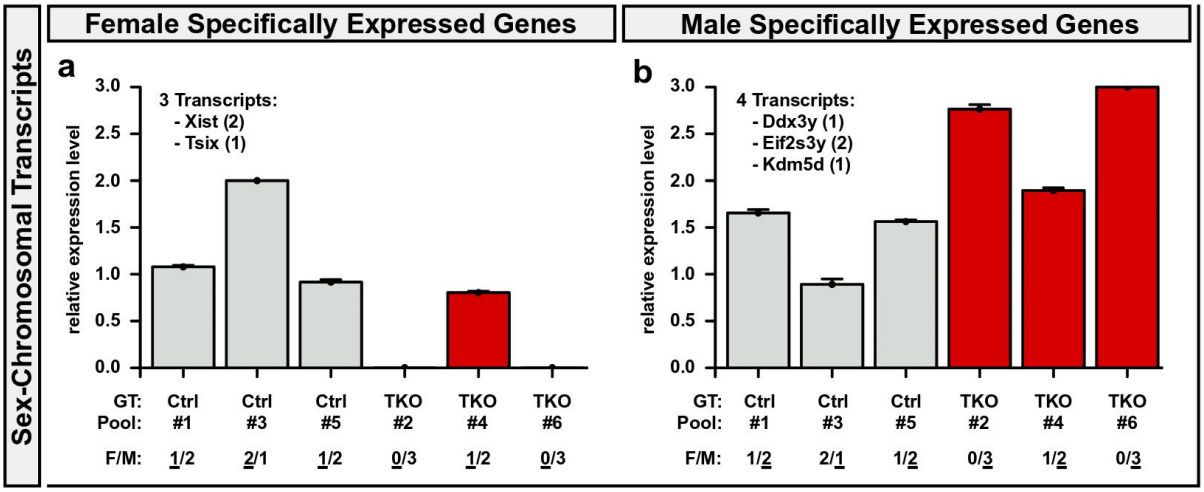


**Figure 21: Sex-specific references genes**

Average relative expression level of known sex-chromosomal and sex-specifically expressed transcripts for every sequenced mRNA pool: **(a)** Female-specific genes Xist and Tsix; **(b)** male-specific genes Ddx3y, Eif2s3y, and Kdm5d. **GT**: Genotype; **Pool**: Number of the mRNA pool; **F/M**: Number of female/male individuals in the pool. **Error bars** represent SEM over the listed number of transcripts (n=3 in *a* and n=4 in *b*).

independent expression level of any transcript (in the following simply called *expression level*) is the expression in Neurod1/2/6-deficient or control tissues, whatever is larger. Changes of expression in Neurod1/2/6-deficient versus control tissue (in the following simply called *change*) are given in the asymptotic form “difference of expression over maximum expression in %” (sect 4.10).

The set of significantly differentially expressed transcripts was relatively small: The following *lax* criteria were met by only 222 of 25,053 genes (297 of 41,513 transcripts): expression *level* $\geq$100 normalized reads per kbp,[1] expression *change* of at least 20 % (1.2-fold; LFC $\mp$0.26), and p-value $\leq$0.2 in two-tailed paired Student t-test over the three independent biological replicates (red colored data points within yellow areas of fig 22a). Only 20 genes (25 transcripts) satisfied the stricter and more commonly used criteria: expression *level* $\geq$100, expression *change* at least 50 % (2-fold; LFC $\mp$1), and p-value $\leq$0.05.

All transcripts/genes were ranked by a combination of expression level, relative change of expression in Neurod1/2/6-deficient versus control tissue, and p-value (Rating in fig 20; tab 4; sect 4.10.5).

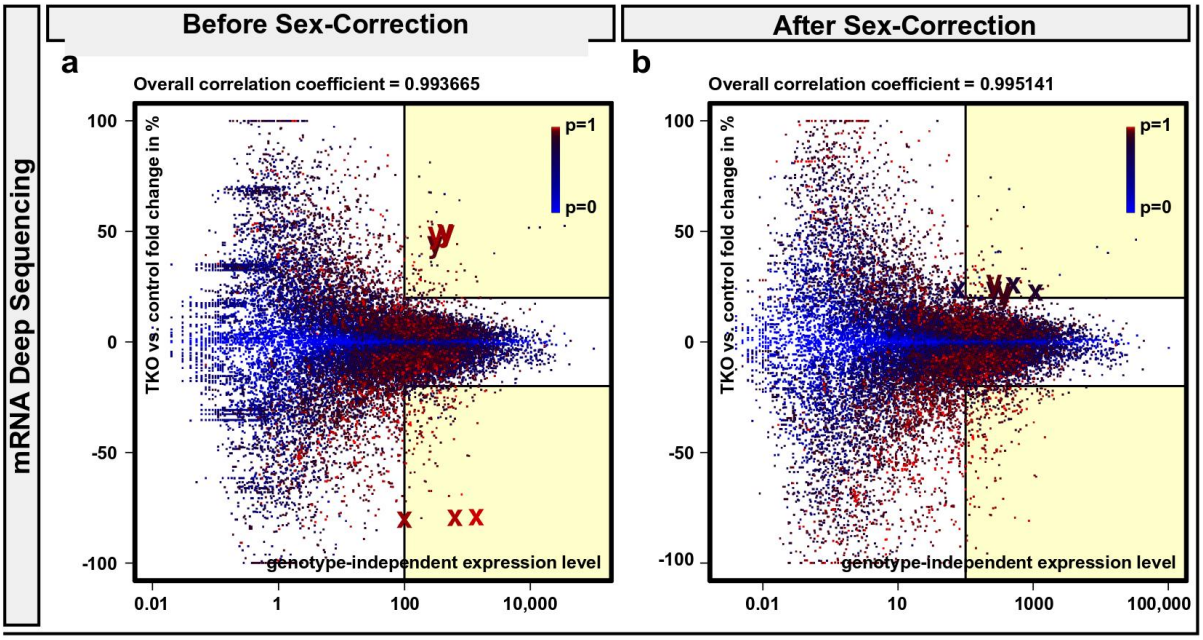


**Figure 22: Sex-correction of RNA-Seq data**

Scatterplots of expression *change* (x-axis) plotted over genotype-independent expression *level* (y-axis) before **(a)** and after **(b)** sex-correction. The **color of a data point** visualizes the p-value of a two-tailed paired t-test over the three (pools) biological replicates (red=high, blue=low significance; see legend). Data points plotted as 'x' or 'y' correspond to the sex-chromosomal transcripts used for sex-correction. **Yellow areas** represent the selection criteria (level ≥100; change ≥20 %).

## 2.6.3 Sex-Correction

Some sex-chromosomal and sex-specifically expressed genes (Armoskus et al., 2014) ranked unexpectedly high (asterisks in tab 4; data points plotted as *x* or *y* in fig 22). For example Xist, which is exclusively expressed from the inactivated X chromosome and is thus considered female-specific, was the highest-ranked gene (stable expression level, 79 % reduction in Neurod1/2/6-deficient tissue, p=0.9962). Eif2s3y, which is located on the Y chromosome and thus male-specifically expressed, was ranked at position 19 of all 41,514 transcripts/genes (stable expression level, 48 % increase in Neurod1/2/6-deficient tissue, p=0.9913).

The simplest explanation for this anomaly was that the embryos that were used for the Neurod1/2/6-deficient RNA-pool were predominantly male and/or the control embryos were predominantly female. The embryonic tissue had unfortunately not been checked or controlled for sex before pooling. Plotting relative expression levels of the strictly sex-specifically expressed genes for each individual pool confirmed that hypothesis (fig 21): Two of the three Neurod1/2/6-deficient mRNA-pools had been

[1]Detection by chromogenic ISH was usually difficult for transcripts that had resulted in less than 200 normalized reads per kbp. The mean value over all transcripts/genes was 300; the median value was 72; Neurod4 (which I could never detect by ISH) resulted in 106; Neurod1 (which is only mildly expressed in the SVZ) resulted in 231, Neurod2 and Neurod6 (which are more robustly expressed in the SVZ and CP) resulted in 2270 and 1659, respectively; Tubb3 (which is robustly expressed by all neuronal cells) resulted in 10329 normalized reads per kbp.

prepared exclusively from male embryos (female/male ratio = 0/3), while one of the three control pools contained predominantly mRNA from female embryos (female/male ratio = 2/1).

Applying a sex-correction algorithm (sect 4.10.6) to the expression data slightly increased the overall correlation coefficient to 0.9951 (+0.0014) and resulted in a significant down-ranking of many genes that had not been expected to be related to the functions of Neurod1/2/6 (e.g. Xist, Sla, Prokr2). Most interesting candidates ranked higher (e.g. Bhlhb5, Gap43, Sox5) or only slightly lower (e.g. Hrk, Prdm8, Cntn2) after sex-correction (last column in tab 4).

The above-mentioned lax criteria ($\geq$100 reads/kbp; change $\geq$20 %; p$\leq$0.2) were now met by 284 genes or 390 transcripts; about one-fifth of those (57 genes or 70 transcripts) showed increased expression in Neurod1/2/6-deficient mice. The stricter criteria ($\geq$100 reads/kbp; change $\geq$50 %; p$\leq$0.05) were met by 33 genes or 41 transcripts; ~10 % of those showed increased expression (3 genes/transcripts).

### 2.6.4 Validation

Several genes (positive controls) that had previously been shown to be differentially expressed in Neurod2/6- or Neurod1/2/6-deficient embryos showed equivalent differential expression in the RNA-Seq data: Sox5 expression, which I have shown to be significantly reduced in the neocortex of Neurod1/2/6-deficient mouse embryos at E13 (sect 2.2; fig 9a, d), was reduced by nearly 50% in this dataset (-42%, p=0.0167 before and -48%, p=0.0119 after sex-correction). The expression of contactin 2 (Cntn2), a cellular adhesion molecule whose expression is virtually lost in Neurod2/6-deficient mouse embryos as E16 and E19 (Bormuth et al., 2013), was reduced by nearly 50% (-46%, p=0.0575 before and -49%, p=0.0483 after sex-correction). Expression of growth associated protein 43 (Gap43), a known direct target gene of Neurod6 (Chiaramello et al., 1996), which is not significantly down-regulated in Neurod2/6-deficient embryos at E16 or P1 (Bormuth et al., 2013), was reduced by more than one-third (-37%, p=0.0058 before and -43%, p=0.0043 after sex-correction). Satb2 expression, which I have shown to be weak in controls and even weaker in Neurod1/2/6-deficient mice at E13 (fig 9c), was reduced by more than one-third (-35%, p=0.0443 before and -45%, p=0.0268 after sex-correction).

Several genes (negative controls) previously shown to not be significantly differentially expressed in Neurod2/6- or Neurod1/2/6-deficient embryos did not show significantly altered expression in the RNA-Seq data: Pax6 expression, which is limited to Neurod1/2/6-negative RGCs in the cortical VZ and not changed in Neurod1/2/6-deficient mice (fig 9a), was mildly increased (+6%, p=0.0326 before and +6%, p=0.0308 after sex-correction); this increase can be explained by the loss of neuronal cells in the CP leading to a relative enlargement of the VZ. Tbr1 expression, which I had shown to

| Gene: | | Not corrected: | | | | Corrected for sex-dependent expression: | | | | |
|---|---|---|---|---|---|---|---|---|---|---|
| Symbol | # | Level | Change | p | Rank | Sex | Level | Change | p | Rank |
| **Bhlhb5** = Bhlhe22 | 1 | **809** | **69% ↘** | **0.0006** | **7** | -23 | **864** | **82% ↘** | **0.0003** | **1** |
| Rn18s R | 1 | **35003** | **52% ↗** | 0.1981 | **1** | -10 | **32652** | 45% ↗ | 0.2694 | **2** |
| **Tiam2** | 4 | **755** | **62% ↘** | 0.0331 | **10** 30, 32 69, 74 | **-27** | **818** | **79% ↘** | 0.0177 | **3** **13, 16** 30, 37 |
| **Sez6** | 2 | **2057** | **52% ↘** | 0.0366 | **8** **13, 14** | -20 | **2150** | **61% ↘** | 0.0240 | **4** **7, 8** |
| Syt4 | 1 | **508** | **70% ↘** | **0.0093** | **9** | -18 | **535** | **80% ↘** | **0.0063** | **5** |
| Ndrg1 | 1 | 185 | **80% ↘** | 0.0556 | **15** | **-30** | **207** | **96% ↘** | 0.0265 | **6** |
| **Nr4a3** = Nor1 | 2 | 160 | **70% ↘** | 0.0200 | 26 48, 153 | **-33** | 180 | **92% ↘** | **0.0088** | **9** **20**, 79 |
| Kcnq3 | 1 | 120 | **66% ↘** | 0.0381 | 52 | **-43** | 140 | **96% ↘** | 0.0133 | **10** |
| Clmp | 1 | **332** | **56% ↘** | 0.0168 | 28 | **-27** | **358** | **72% ↘** | **0.0086** | **11** |
| Camk2b | 3 | 182 | **65% ↘** | 0.0130 | 29 87, 91 106 | **-31** | **200** | **83% ↘** | **0.0065** | **12** 50, 51 62 |
| Sh3gl2 | 1 | **266** | **67% ↘** | 0.0133 | **17** | -14 | **277** | **76% ↘** | **0.0096** | **14** |
| Dact1 | 2 | **512** | **50% ↘** | 0.0186 | 31 72, 73 | **-27** | **547** | **64% ↘** | **0.0098** | **15** 32, 33 |
| **Prdm8** | 1 | **245** | **67% ↘** | 0.0124 | **18** | -14 | **256** | **76% ↘** | **0.0091** | **17** |
| Hpca | 4 | **244** | **64% ↘** | 0.0294 | 24 97, 98 104, 107 | -19 | **257** | **75% ↘** | 0.0195 | **18** 83, 85 93, 94 |
| Mpped1 | 4 | **1043** | 34% ↘ | 0.0302 | 76 274, 289 290, 303 | **-25** | **1119** | **51% ↘** | 0.0120 | **19** 88, 95 97, 98 |
| Shtn1 | 2 | **226** | **50% ↘** | 0.0230 | 81 51, 57 | **-31** | **251** | **72% ↘** | **0.0086** | 21 46, 52 |
| Rn45s R | 1 | **9488** | **52% ↗** | 0.1986 | **5** | -13 | **8662** | 42% ↗ | 0.2989 | 22 |
| Cacna1e | 1 | 74 | **72% ↘** | 0.0303 | 56 | **-33** | 83 | **94% ↘** | 0.0140 | 23 |
| Rn28s1 R | 1 | **14082** | **52% ↗** | 0.1959 | **4** | -15 | **12535** | 39% ↗ | 0.3315 | 24 |
| **Crym** | 1 | 45 | **99% ↘** | 0.0281 | 22 | **-66** | 57 | **100% ↘** | **0.0038** | 25 |
| Ptpro | 4 | 159 | **64% ↘** | **0.0052** | 35 128, 134 177, 204 | -22 | 169 | **76% ↘** | **0.0031** | 26 110, 112 153, 157 |
| **Gap43** | 1 | **1449** | 37% ↘ | **0.0058** | 34 | -16 | **1492** | 44% ↘ | **0.0038** | 27 |
| Rspo3 | 1 | 99 | **79% ↘** | 0.0486 | 27 | -13 | 104 | **88% ↘** | 0.0361 | 28 |
| **Cdh13** | 1 | **296** | 42% ↘ | 0.0397 | 112 | **-34** | **325** | **63% ↘** | 0.0149 | 29 |
| **Hrk** | 1 | **254** | **81% ↗** | 0.0717 | **11** | -12 | **231** | **74% ↗** | 0.1012 | 31 |
| Dscam | 1 | 75 | **72% ↘** | **0.0047** | 51 | **-25** | 81 | **86% ↘** | **0.0027** | 34 |
| Dync1i1 | 5 | 75 | **56% ↘** | 0.0444 | 154 | **-36** | 86 | **85% ↘** | 0.0147 | 35 |
| Mir8091 M | 1 | 35 | **76% ↘** | **0.0081** | 77 | **-49** | 43 | **100% ↘** | **0.0062** | 36 |
| Grik3 | 1 | 101 | **57% ↘** | 0.0788 | 122 | **-34** | 113 | **80% ↘** | 0.0333 | 38 |
| Plk2 | 1 | **254** | 47% ↘ | 0.0280 | 88 | **-27** | **273** | **63% ↘** | 0.0137 | 39 |
| **Sox5** | 4 | **705** | 42% ↘ | 0.0167 | 49 | -15 | **726** | 49% ↘ | 0.0114 | 40 |
| Tac1 | 2 | 41 | **79% ↗** | **0.0034** | 68 92, 197 | **+37** | 50 | **94% ↗** | **0.0015** | 41 70, 122 |
| Slc1a1 | 1 | 106 | **55% ↘** | **0.0012** | 94 | **-36** | 116 | **75% ↘** | **0.0005** | 42 |
| Chl1 | 1 | 182 | 41% ↘ | 0.1343 | 305 | **-34** | **205** | **68% ↘** | 0.0451 | 43 |
| Lmo1 | 3 | **565** | 43% ↘ | 0.0445 | 59 | -16 | **585** | **51% ↘** | 0.0301 | 44 |
| Cnih3 | 3 | 70 | **71% ↘** | 0.0270 | 63 | -20 | 75 | **84% ↘** | 0.0169 | 45 |
| Rs5-8s1 R | 1 | **748** | **64% ↗** | 0.1834 | **16** | -6 | **713** | **60% ↗** | 0.2179 | 47 |
| Rasgef1b | 2 | 557 | 41% ↘ | 0.0035 | 70 120, 125 | -19 | 578 | 49% ↘ | 0.0021 | 48 100, 102 |
| Mc4r | 1 | 36 | **85% ↘** | 0.1996 | 118 | **-46** | 47 | **100% ↘** | 0.0829 | 49 |

**Table 4: Results of RNA-Seq — part 1: top 50**

The 50 highest-ranked transcripts (by sex-corrected rank as shown in last column). Table continues on page 59; legend on page 60.

be decreased in the CP but increased in the SVZ of Neurod1/2/6-deficient mice at E13 (fig 9b), was only mildly decreased in the RNA-Seq data from the entire neocortex (-5%,

| Gene / Transcripts: | | Not corrected: | | | | Corrected for sex-dependent expression: | | | | |
|---|---|---|---|---|---|---|---|---|---|---|
| Symbol | # | Level | Change | p | Rank | Sex | Level | Change | p | Rank |
| Calb2 = Calreinin | 1 | **277** | **53%** ↗ | 0.0598 | 57 | +14 | **295** | **60%** ↗ | 0.0430 | 53 |
| **Sip1** = Zeb2 | 7 | **842** | 37% ↘ | **0.0000** | 65 | -15 | **865** | 43% ↘ | **0.0000** | 55 |
| Syn2 | 3 | **244** | **51%** ↘ | **0.0090** | 60 | -15 | **252** | **58%** ↘ | **0.0064** | 58 |
| Cbln4 | 1 | 54 | **80%** ↗ | **0.0071** | 47 | +11 | 57 | **84%** ↘ | **0.0056** | 60 |
| **Plxna4** | 1 | **610** | 44% ↘ | **0.0061** | 42 | -6 | **616** | 46% ↘ | **0.0054** | 61 |
| Thy1 | 1 | 24 | **84%** ↘ | 0.0557 | 95 | **-40** | 28 | **100%** ↘ | 0.0100 | 64 |
| **Vglut1** = Slc17a7 | 1 | **312** | **55%** ↘ | 0.0544 | 41 | -1 | **313** | **56%** ↘ | 0.0523 | 66 |
| Gpr88 | 1 | 54 | **84%** ↗ | 0.0024 | 33 | -6 | 53 | **82%** ↗ | 0.0027 | 68 |
| Rasgrf1 | 4 | 22 | **97%** ↘ | 0.0525 | 61 | **-25** | 25 | **100%** ↘ | 0.0283 | 73 |
| Snord22 | 1 | **236** | **55%** ↗ | 0.0219 | 53 | +3 | **240** | **56%** ↗ | 0.0202 | 75 |
| **Nhlh2** | 1 | **687** | 44% ↗ | 0.0113 | 36 | -5 | **676** | 42% ↗ | 0.0127 | 80 |
| Bmp3 | 2 | 50 | **56%** ↘ | 0.0166 | 209 | -34 | 55 | **77%** ↘ | **0.0074** | 84 |
| Rtn4rl2 | 1 | **248** | **53%** ↘ | 0.0102 | 54 | +1 | **247** | **53%** ↘ | 0.0103 | 86 |
| **Cntn2** = Tag1 | 1 | **376** | 46% ↘ | 0.0575 | 78 | -8 | **382** | 49% ↘ | 0.0482 | 87 |
| Prokr2 | 1 | 171 | **75%** ↗ | 0.0640 | **20** | -16 | 156 | **65%** ↗ | 0.1000 | 90 |
| Hspa12a | 2 | 81 | **59%** ↘ | 0.0432 | 111 | -13 | 84 | **67%** ↘ | 0.0307 | 108 |
| Wnt7b | 3 | **1317** | 31% ↘ | 0.1271 | 142 | -11 | 1342 | 35% ↘ | 0.0977 | 119 |
| Necab3 | 1 | **203** | **55%** ↘ | 0.0226 | 58 | +6 | 200 | **52%** ↘ | 0.0263 | 123 |
| **Ctip2** = Bcl11b | 3 | **1099** | 23% ↘ | **0.0018** | 321 | -20 | **1132** | 30% ↘ | **0.0010** | 176 |
| Plppr5 | 2 | 11 | **63%** ↘ | **0.0005** | 450 | **-46** | 13 | **90%** ↘ | **0.0002** | 187 |
| **Satb2** | 3 | **211** | 35% ↘ | 0.0443 | 327 | -22 | 221 | 46% ↘ | 0.0247 | 190 |
| **Mafb** | 1 | **271** | **54%** ↗ | 0.0213 | 45 | -22 | **245** | 43% ↗ | 0.0412 | 228 |
| **Id2** | 1 | **790** | 27% ↘ | 0.**0050** | 234 | -10 | **801** | 31% ↘ | **0.0039** | 232 |
| Xist *X, N | 2 | **2158** | **79%** ↘ | **0.0038** | **2** 3, 6 | **+73** | **1831** | 26% ↗ | 0.0403 | 237 |
| **Fezf2** | 1 | **1300** | 24% ↘ | 0.0219 | 255 | -7 | **1311** | 26% ↘ | 0.0180 | 269 |
| Mapt = Tau | 5 | **1031** | 13% ↘ | 0.0385 | 1745 | -31 | **5019** | 26% ↘ | **0.0082** | 306 |
| **Neurod6** | 1 | **1659** | 18% ↘ | 0.1649 | 791 | -17 | **1708** | 25% ↘ | 0.0894 | 317 |
| **Dab1** | 3 | 920 | 25% ↘ | 0.0166 | 287 | -4 | 925 | 26% ↘ | 0.0149 | 364 |
| Foxo1 | 1 | 183 | 48% ↗ | 0.0302 | 108 | -15 | 171 | 41% ↗ | 0.0470 | 380 |
| Tubb3 = β3-Tubulin | 1 | 10329 | 12% ↘ | 0.2584 | 933 | -12 | **10450** | 15% ↘ | 0.1848 | 537 |
| **Cdh11** | 1 | 184 | 28% ↘ | **0.0000** | 675 | -2 | 184 | 28% ↘ | **0.0000** | 885 |
| Erdr1 XY | 2 | **1625** | 22% ↘ | 0.2318 | 566 | +9 | **1596** | 17% ↘ | 0.3175 | 890 |
| Ddx3y Y | 1 | **313** | 47% ↗ | **0.0078** | 71 | **-34** | **263** | 26% ↗ | 0.0371 | 993 |
| Eif2s3y Y | 2 | **913** | 48% ↗ | **0.0087** | **19** 39, 40 | **-40** | **731** | 21% ↗ | 0.0692 | 995 |

**Table 4: Results of RNA-Seq — part 2: top 1000**

Selection of the 1000 highest-ranked transcripts (by sex-corrected rank as shown in last column). Continuation and legend and on page 60.

p=0.1730 before and -6%, p=0.1730 after sex-correction). Expression roundabout 1 (Robo1), which is strongly increased in newborn Neurod2/6 *double*-deficient but not in Neurod1/2/6 *triple*-deficient mice (Bormuth, 2016), was not significantly changed in the RNA-Seq data (+11%, p=0.1963 before and -3% p=0.6141 after sex-correction).

| Gene / Transcripts: | | Not corrected: | | | | Corrected for sex-dependent expression: | | | | |
|---|---|---|---|---|---|---|---|---|---|---|
| Symbol | # | Level | Change | p | Rank | Sex | Level | Change | p | Rank |
| **Bim** = Bcl2l11 | 5 | **216** | 22% ↗ | 0.0259 | 1155 | +2 | **217** | 22% ↗ | 0.0246 | 1542 |
| Kdm5d *Y | 1 | **309** | 43% ↗ | 0.0293 | 103 | **-33** | **262** | 22% ↗ | 0.1294 | 1843 |
| Neurod2 | 1 | **2270** | 11% ↘ | 0.1758 | 2086 | -16 | **2303** | 15% ↘ | 0.1072 | 1195 |
| Tsix *X, N | 1 | 100 | **80% ↘** | **0.0091** | 21 | **+73** | 85 | 26% ↗ | 0.0973 | 2315 |
| **Vldlr** | 3 | 128 | 13% ↘ | 0.1413 | 5891 | -23 | 133 | 22% ↘ | 0.0568 | 2365 |
| **Neurod1** | 1 | **231** | 16% ↗ | **0.0055** | 2188 | +9 | **234** | 18% ↗ | **0.0042** | 2391 |
| **Prox1** | 2 | 44 | 25% ↗ | 0.0322 | 2183 | -1 | 44 | 24% ↗ | 0.0338 | 3086 |
| **Bcl2** | 2 | **228** | 12% ↘ | 0.0469 | 4278 | -6 | **230** | 14% ↘ | 0.0368 | 4027 |
| Fancd2 | 2 | 238 | 8% ↗ | **0.0000** | 7609 | +14 | **244** | 12% ↗ | **0.0000** | 4816 |
| **Tbr2** = Eomes | 2 | **3238** | 6% ↗ | 0.0392 | 4221 | -4 | **3230** | 6% ↗ | 0.0442 | 5568 |
| Bok | 1 | **365** | 18% ↘ | 0.2834 | 2620 | +11 | **360** | 15% ↘ | 0.3737 | 6294 |
| Kdm6a *X | 2 | **342** | 12% ↘ | 0.0268 | 3624 | +11 | **338** | 9% ↘ | 0.0452 | 7076 |
| **Tbr1** | 1 | **2303** | 5% ↘ | 0.1730 | 9792 | -8 | **2314** | 6% ↘ | 0.1730 | 7118 |
| **Bcl-XL** = Bcl2l1 | 6 | **781** | 7% ↘ | 0.1302 | 7686 | -5 | **783** | 8% ↘ | 0.1138 | 7270 |
| **Pax6** | 8 | **1351** | 6% ↗ | 0.0326 | 7420 | +2 | **1353** | 6% ↗ | 0.0305 | 7659 |
| Flcn | 5 | **251** | 7% ↘ | **0.9948** | 9465 | +1 | **251** | 7% ↘ | **0.9947** | 10248 |
| **Bax** | 1 | **1264** | 8% ↘ | 0.5473 | 11905 | -2 | **1266** | 9% ↘ | 0.5294 | 11242 |
| Gnb4 | 4 | 91 | 5% ↘ | 0.9183 | 17999 | -11 | 91 | 8% ↘ | 0.9601 | 12367 |
| **Apoer2** = Lrp8 | 2 | 1321 | 5% ↗ | 0.0107 | 8656 | -11 | 1304 | 3% ↗ | 0.0283 | 15617 |
| Sla | 2 | **510** | **68% ↗** | 0.0935 | **12** 23, 25 | **-37** | **321** | 15% ↗ | 0.7152 | 15904 |
| Mid1 XY | 5 | **2169** | 3% ↘ | 0.6551 | 27209 | +23 | **2208** | 4% ↗ | 0.5172 | 18703 |
| **Neurod4** | 3 | 106 | 8% ↗ | 0.4767 | 19745 | -1 | 106 | 8% ↗ | 0.4895 | 20261 |
| **Etv5** | 2 | 111 | 5% ↗ | 0.0489 | 16614 | -7 | 110 | 3% ↗ | 0.1192 | 23625 |
| Bcl-W = Bcl2l2 | 1 | **284** | 2% ↘ | 0.3636 | 28153 | -5 | **285** | 3% ↘ | 0.2872 | 24552 |
| **Robo1** | 1 | **337** | 11% ↗ | 0.1963 | 6394 | **-28** | **319** | 4% ↘ | 0.6141 | 25321 |
| **Brn2** = Pou3f2 | 1 | 582 | 7% ↗ | 0.5737 | 13606 | -14 | 568 | 4% ↗ | 0.3226 | 27792 |
| Lis1 = Pafah1b1 | 2 | 1807 | 2% ↗ | 0.7113 | 31642 | -1 | 1805 | 2% ↗ | 0.7227 | 30662 |
| Casp3 | 2 | **1752** | 1% ↘ | 0.8471 | 37175 | -5 | **1757** | 2% ↘ | 0.7396 | 31928 |
| **Map2** | 3 | **3454** | 3% ↗ | 0.6715 | 27476 | -11 | **3399** | 0% ↗ | 0.9788 | 39789 |

**Table 4: Results of RNA-Seq — part 3: lower rank**

Selection of the remaining transcripts (lower ranked by sex-corrected rank as shown in last column). **Symbol:** Gene symbol (see list of abbreviations on page 119; *bold font:* expression verified by ISH or IHC; *X/Y:* gene is located on X and/or Y chromosome; *asterisk:* used as reference transcript for sex-correction; *M*: micro RNA; *R*: ribosomal RNA; *N*: non coding); **#:** Number of transcripts (splice variants); if #>1, the following columns represent mean values over all transcripts; **Level:** Estimated overall expression level (normalized reads per kbp in Neurod1/2/6-deficient or control pool, whatever is higher; *bold font:* values ≥200); **Change:** Difference of expression in % of *level*: up (↗) or down (↘) in Neurod1/2/6-deficient versus control mice (*bold font:* values ≥50 ≡ FC≥∓2 ≡ Log2FC≥∓1); **p:** p-value of paired two-tailed student's t-test over (n=3+3 pools; *bold font*: values <0.01); **Rank:** Position in a ranked list of all transcripts/genes sorted by a combination of *Level*, *Change* and *p* (*bold font:* values ≤20); individual transcripts that rank ≤100 are shown in small font; **Sex:** Prediction of sex-dependent expression (+100=female-specific, -100=male-specific, 0=equal; *bold font:* absolute values ≥25). The table is ordered by rank after sex-correction (last column).

Gene expression patterns of the most prominent candidates were validated by in situ hybridization and rescue experiments were performed using in-utero electroporation of cDNA or shRNA constructs.

## 2.7 Harakiri Triggers Neuronal Apoptosis

THE MOST INTERESTING AND UNEXPECTED finding of the RNA-Seq experiment was a nearly 4-fold transcriptional up-regulation of the Bcl2 interacting protein Harakiri (Hrk) in Neurod1/2/6-deficient mice (sex-corrected: 328 to 1239 total reads; 74%↗; p=0.1012; rank 31 in tab 4; fig 23a). Hrk, also known as death protein 5 (DP5), is a small (92 AA) BH3-only protein of the Bcl2-family (Imaizumi et al., 1997, 2004). It localizes to the outer mitochondrial membrane where it binds and thereby inhibits the strong inhibitors of apoptosis Bcl-XL and Bcl2.

Hrk expression was not detectable by ISH in the cortex of control mice[1] at E13-E19 (upper panel in fig 23b), which confirmed that the calculated expression level of 45 normalized reads per kbp in control tissue is indeed well below the detection threshold of conventional ISH (sect 2.6.2). In Neurod1/2/6-deficient mice, Hrk was weakly expressed by a subset of cells in the CP at E13 (lower panel in fig 23b; robust staining could only be obtained after developing the slides for 1–2 days[2]), which confirmed that the calculated expression level of 231 normalized reads per kbp is just above the ISH detection threshold.

The increase of Hrk-expression was more robust at E14 and E15 (fig 23b), the time when deeper layer neurons normally settle in the CP and when the massive activation of caspase 3 reaches its peak in the neocortex of Neurod1/2/6 *triple*-deficient mice. Hrk-expression was low at E16 and not detectable at E19 when upper layer neurons normally settle in the CP. The temporal correlation of Hrk-expression and caspase 3 activation suggests that Harakiri does directly trigger programmed cell death in the absence of Neurod1/2/6. Hrk was also expressed in the DG of the Neurod1/6 *double*-deficient control embryos (arrow in fig 23c), which suggests that the apoptotic loss of most hippocampal granule neurons in the absence of Neurod1 (sect 1.4.2.1; Liu et al. 2000; Schwab et al. 2000) may also be triggered by Hrk.

Unexpectedly, the transcriptional up-regulation of Hrk in the developing CP of Neurod1/2/6 *triple*-deficient mice was not confined to the caudomedial cortex (arrowhead in fig 23c). The expression domain of Hrk is thus broader than the domain of caspase 3 activation, which is confined to the hippocampus and caudomedial neocortex of Neurod1/2/6-deficient embryos (sect 2.1).

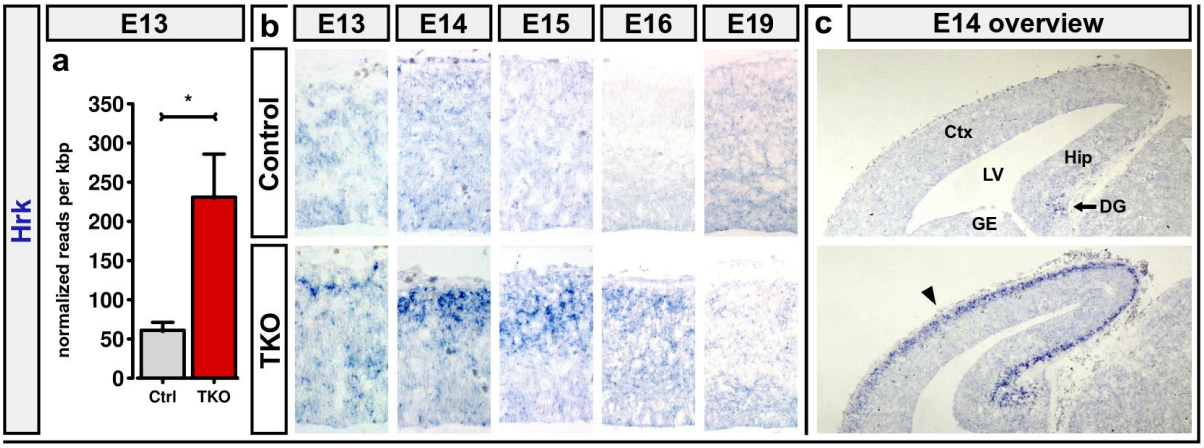


**Figure 23: Increase of Hrk-expression in the developing CP of Neurod1/2/6-deficient mice**

**(a)** Calculated expression in RNA-Seq at E13 (sex-corrected; normalized reads per kbp). **(b)** ISH in coronal sections of the central neocortex during embryonic cortex development. **(c)** Overview of ISH in coronal brain section at E14; the **arrow** identifies Hrk-positive cells in the DG of Neurod1/6 *double*-deficient control embryos; the **arrowhead** approximately points to the sharp border of strongly increased apoptosis in Neurod1/2/6 *triple*-deficient brains (compare fig 8a). **Abbreviations** on page 119.

### 2.7.1 Hrk Overexpression and Knockdown

To directly investigate the function of Hrk in the developing cortex, I cloned the complete coding region into a conditional bicistronic expression vector (pCAG-LoxP-mCherry-LoxP-Hrk-IRES-GFP; sect 4.8.1). IUE of this plasmid into the neocortex of Neurod6-positive mice at E13 resulted in rapid activation of caspase 3 and apoptotic cell death of most electroporated cells (fig 24a-c).

Neurod6-Cre mediated recombination of the plasmid DNA limits forced expression of Hrk and GFP to postmitotic pyramidal neurons in the SVZ, IZ, and CP. Stable expression can be considered approximately 24h after electroporation. IUE of an empty expression vector (containing GFP but no Hrk) at E13 and IHC for GFP at E15 confirmed that the method targets a large number of Cre-positive pyramidal neurons in the IZ and CP (fig 24a). Electroporation of the full Hrk-expressing vector at E13 resulted in only few cells that were positive for GFP or activated caspase 3 (fig 24b). The simplest explanation for the near absence of GFP-expression was that at E15 most Hrk-expressing cells had already undergone apoptosis and had been eliminated from the cortex. Visualization of mCherry (the gene being inactivated by Cre-mediated recombination) confirmed that the plasmid was robustly expressed before recombination (fig 24c).

[1] Genotype: Neurod1$^{flox/flox}$ × Neurod2$^{wt/null}$ × Neurod6$^{cre/cre}$

[2] The development of ISH-slides is based on an AP-based staining reaction (sect 4.5). ISH for stronger expressed transcripts (e. g. Sox5, which has a similar expression pattern but a calculated expression level of 726 normalized reads per kbp) usually results in robust staining after developing the slides for 1–2 hours. However, chromogenic ISH is a qualitative method and the staining intensity varies with probe properties (e. g. GC-content, length, position within the mRNA).

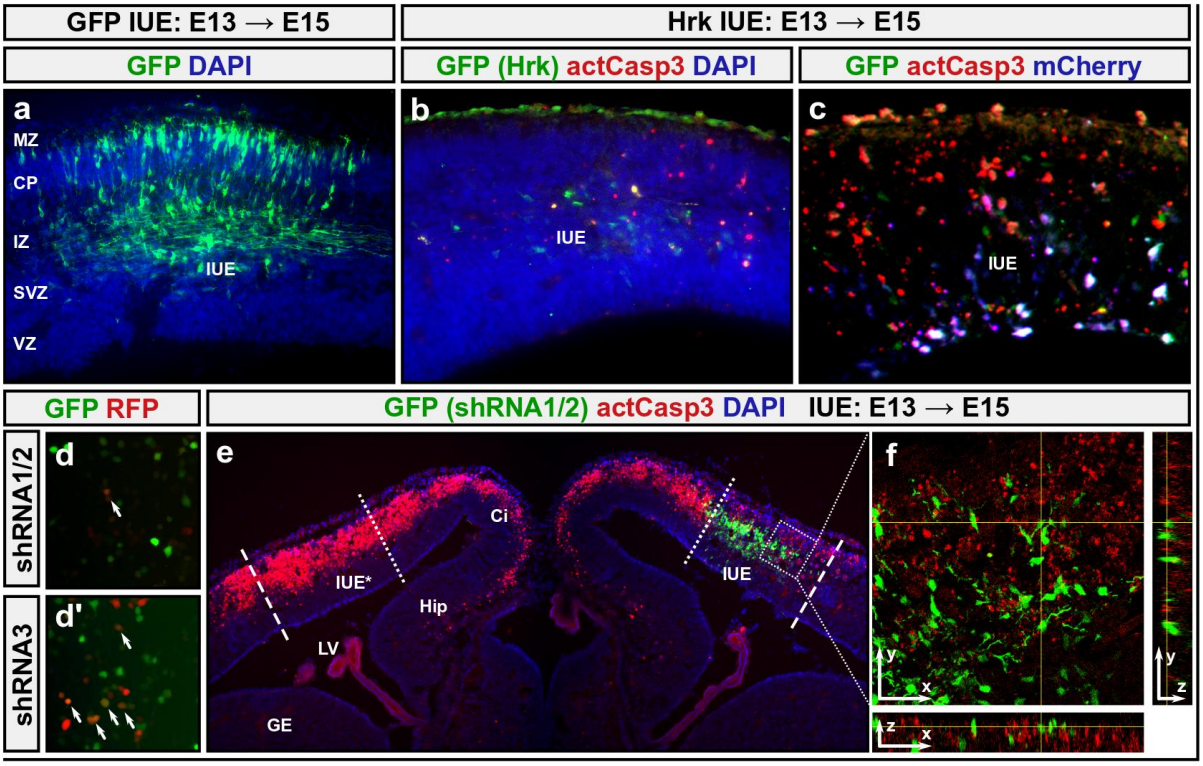


**Figure 24: Hrk drives apoptosis in the cerebral cortex**

**(a)** IUE of the empty (GFP only) conditional expression vector into the central neocortex of Neurod6-Cre positive mice at E13 and immunostaining for GFP (green) at E15; positive control for *b* and *c*. **(b)** Forced expression of Hrk resulted in the activation of caspase 3 (red) and the loss of electroporated (GFP-expressing; green) cells. **(c)** Visualization of electroporated cells that have not yet undergone cre-mediated recombination and hence express mCherry (blue) but not Hrk or GFP (green). **(d)** Overexpression of shRNA constructs targeting the 3'-UTR of Hrk (bicistronic GFP expression in green) and an RFP-based Hrk 3'-UTR reporter construct (red) in N2a cells. **(e)** IUE of shRNA targeting Hrk (shRNA1/2) into the central neocortex of Neurod1/2/6-deficient mice at E13 and IHC for GFP (green) and activated caspase 3 (red) at E15. **(f)** Orthogonal views of confocal image stack at approximately the boxed region in *e*. The **dotted** and **dashed lines** indicate the medial and lateral boundaries of the electroporation site in the ipsilateral cortex and the approximate projections into the contralateral cortex; **IUE** denotes the electroporation site; **IUE*** is an approximate projection of the electroporation site into the non-electroporated contralateral hemisphere. **Abbreviations** on page 119.

To silence the up-regulation of Hrk via RNA interference (RNAi) in the developing cortex of Neurod1/2/6-deficient mice, I cloned three bicistronic DNA constructs coding for GFP and Hrk-specific short hairpin RNA (shRNA). The interfering RNA sequences bind in different regions in the Hrk 3'-untranslated region (UTR), and they had previously been successfully used (Kalinec et al., 2005). DNA-sequencing confirmed that *shRNA1* and *shRNA2* were identical to the published constructs. However, *shRNA3* contained a mutation that prevents it from binding to the Hrk mRNA; *shRNA3* was subsequently used as negative control.

I tested the effectiveness of the shRNA vectors to silence Hrk-expression in vitro: Neuro2a (N2a) cells, which have many properties of neurons (LePage et al., 2005), were simultaneously transfected with the shRNA constructs and a reporter plasmid expressing red fluorescent protein (RFP) fused to the 3'-UTR of Hrk messenger RNA (mRNA). The Hrk-ORF was not expressed to prevent cell death in this assay. In

the case of shRNA1 and shRNA2, mutually exclusive expression of GFP and RFP indicated sufficient effectiveness of the shRNA vectors (the RFP-mRNA containing the shRNA target sequences was quickly eliminated from transfected cells). The strongest silencing effect was caused by co-expression *of shRNA1/2* (fig 24d). Expression of *the non-functional RNA3* resulted in many GFP/RFP double-positive cells (arrows in fig 24d').

I co-electroporated *shRNA1/2* into the developing neocortex of Neurod1/2/6-deficient mice at E13 and immunostained the fixed brain sections for GFP and activated caspase 3 at E15 (the time of strongest caspas 3 activation in Neurod1/2/6-deficient brains). Caspase 3 activation was strong in the *not* electroporated (contralateral) hemisphere (left side of fig 24e)., and it reached laterally beyond the center of the ventricle (dashed lines in fig 24e). Caspase 3 activation was comparable in the medial neocortex, cingulate cortex, and hippocampus of the electroporated (ipsilateral) hemisphere (right side of fig 24e). However, only relatively few cells in the central neocortex (where the shRNA constructs had been electroporated) were positive for activated caspase 3; strong activation of caspase 3 stopped abruptly at the level of the electroporation site (dotted lines in fig 24e). Three-dimensional image stacks obtained by confocal microscopy in the central neocortex (fig 24f) confirmed that the remaining activation of caspase 3 does not colocalize with the expression of GFP (Hrk-shRNA) on the cellular level.

I conclude that the transcriptional up-regulation of Hrk in the developing cerebral cortex of Neurod1/2/6-deficient mice does efficiently trigger caspase 3 dependent apoptotic cell death of deeper layer pyramidal neurons in the caudomedial cortex. However, this does not seem to be the case for upper layer neurons and the lateral neocortex. The next question was, how Hrk is regulated at the transcriptional level in the developing cortex.

## 2.8 Bhlhb5 and Prdm8 Prevent Neuronal Apoptosis

NEUROD-FAMILY TRANSCRIPTION FACTORS are usually considered transcriptional activators (Murre et al., 1994). Neurod1 has been called beta-cell E-box *transactivator* 2 (Beta2) in the field of diabetes research as it binds and transactivates the promoters of insulin and glucagon in the pancreas (Dumonteil et al., 1998). Neurod2 was identified in a transactivator-trap screen to mediate depolarization-induced transactivation of Gap43 in cultured cortical neurons (Ince-Dunn et al., 2006). Neurod6 was shown to directly promote the expression of Gap43 via two distinct transactivator domains (Uittenbogaard et al., 2003).

NeuroD-factors have occasionally been reported to inhibit the expression of other genes, but indirectly via the activation of transcriptional repressors or via competitive displacement of other transactivators from promoters. Neurod1 was shown to inhibit the expression of somatostatin by binding to E-box sequences and thereby displacing other transcription factors (Itkin-Ansari et al., 2005). Neurod2 was shown to indirectly repress RE1-silencing transcription factor (Rest) by transactivating its transcriptional repressor Zfhx1a (Ravanpay et al., 2010).

The transcriptional up-regulation of Harakiri in the developing cortex of Neurod1/2/6-deficient mice is thus most probably an indirect effect. A hypothetical mechanism could involve other transcription factors that act downstream of Neurod1/2/6 to repress Harakiri. The loss of Neurod1/2/6 should then result in the down-regulation of such repressors, and the loss of repression would result in the up-regulation of Harakiri.

Two transcription factors ranked particularly high in the comparable transcriptome analyses (tab 4): Bhlhb5 was the highest-ranked transcript after sex-correction; expression was robust in the central neocortex of control embryos (864 normalized reads per kbp) but very weak in Neurod1/2/6-deficient littermates (154 normalized reads per kbp; -81 %; p=0.0003; fig 25b). Prdm8 was the second-highest ranked transcription factor (#18 of all transcripts); expression was mild in the central neocortex of control embryos (256 normalized reads per kbp) and below ISH-detection threshold in Neurod1/2/6-deficient littermates (62 normalized reads per kbp; -75 %; p=0.0097; fig 26b). Both factors have previously been shown to act together in the same transcriptional repressor complex (Ross et al., 2012).

### 2.8.1 Bhlhb5 Expression

BHLH protein B5 (Bhlhb5), also called Bhlhe22 or Beta3, is an inhibitory bHLH transcription factor (Xu et al., 2002), that was shown to regulate the area identity of postmitotic pyramidal neurons in the developing cerebral cortex (Joshi et al., 2008).

Whole transcriptome expression analysis at E13 showed a highly significantly decrease of Bhlhb5-expression in the central neocortex of Neurod1/2/6-deficient mice (sex-corrected: 2772 to 495 total reads; 82 %↘; p=0.00032; rank 1 in tab 4; fig 25a). Independent of sex-correction, Bhlhb5 was the highest-ranked gene of the entire RNA-Seq study.

ISH in coronal brain section at E13–16 confirmed reduced Bhlhb5-expression, particularly in the lateral neocortex of Neurod1/2/6-deficient mice (fig 25c–f). In control mice, Bhlhb5 was already robustly expressed in the emerging CP at E13. In Neurod1/2/6-deficient littermates, Bhlhb5-mRNA was hardly detectable at E13. The levels increased quickly in the hippocampus and medial neocortex, but not in the lateral neocortex.

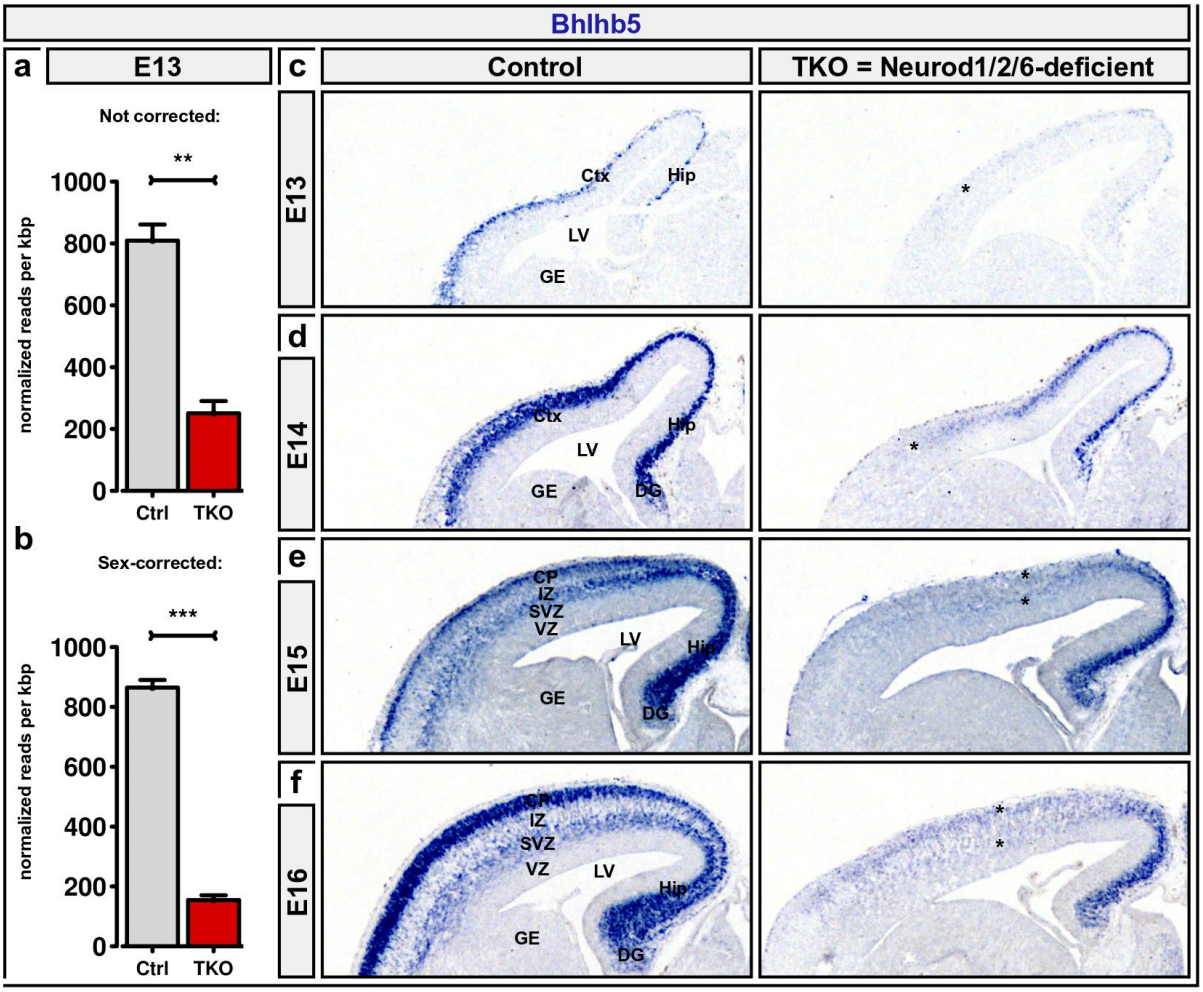


**Figure 25: Bhlhb5 expression during embryonic cortex development**

**(a, b)** Expression as calculated from RNA-Seq at E13 (normalized, before and after sex-correction in *a* and *b*, respectively). **(c-f)** ISH for Bhlhb5 in coronal sections of the central neocortex during embryonic cortex development E13, E14, E15, and E16. **Asterisks** denote strongly reduced expression in the cortex of Neurod1/2/6-deficient mice. **Abbreviations** on page 119.

This pattern was *not* in line with the proposed hypothesis. At E14/15, the rate of apoptosis was very high in the medial CP of Neurod1/2/6-deficient embryos (fig 5), but Bhlhb5-expression was relatively normal in this area. The lateral cortex, where Bhlhb5 expression was strongly decreased at all examined stages, was relatively unaffected by the loss of Neurod1/2/6 (sect 2.1; sect 2.2; Bormuth, 2016).

### 2.8.2 Prdm8 Expression

PR domain containing 8 (Prdm8) is a histone methyltransferase and an inhibitory transcription factor containing a double zinc-finger and a SET-domain (Xiao et al., 2003). In the cerebral cortex, Prdm8 is essential for the multipolar-to-bipolar transition of pyramidal neurons in the IZ (Inoue et al., 2014) and for the postnatal specification of layer 4 (Inoue et al., 2015).

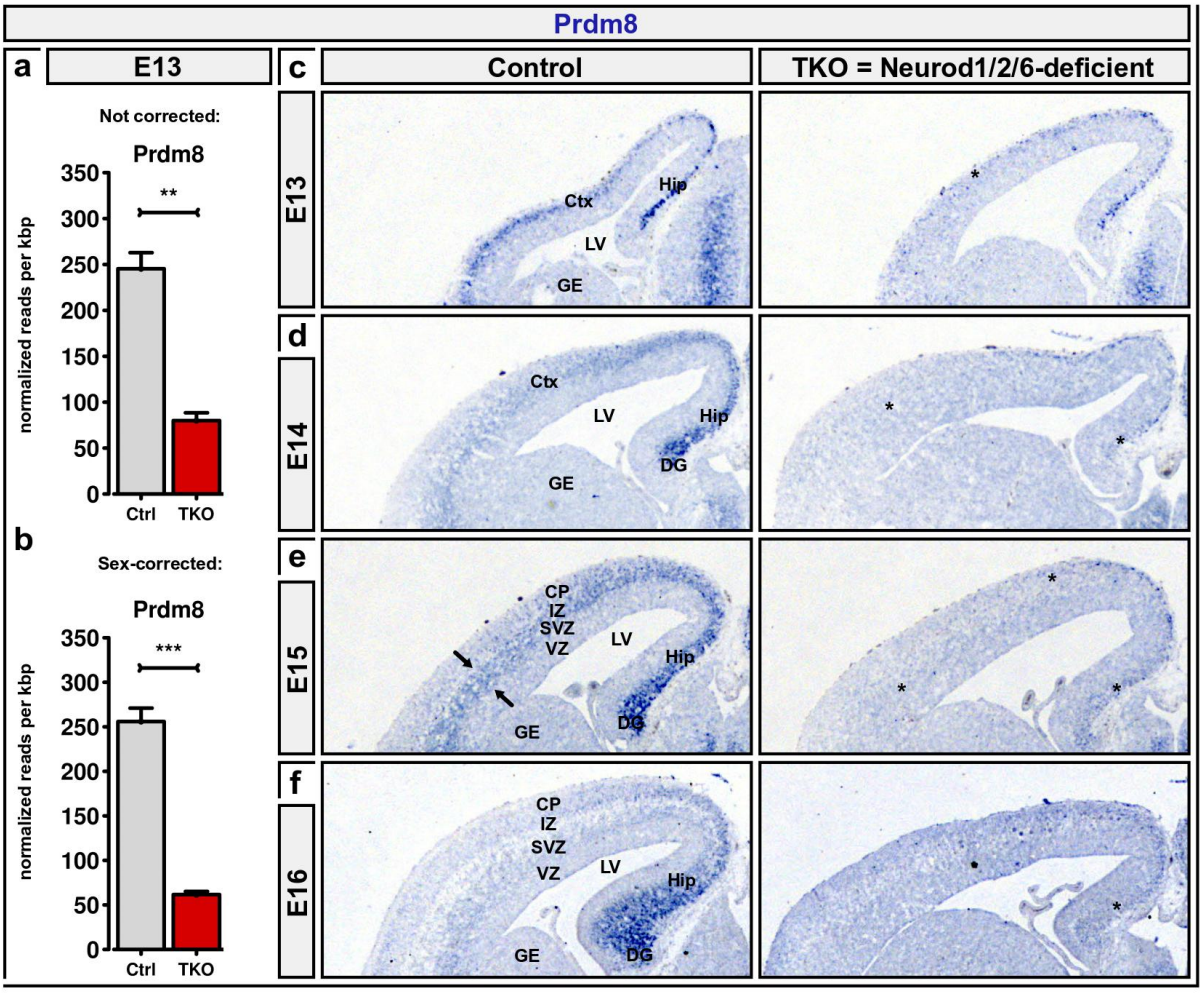


**Figure 26: Prdm8 expression during embryonic cortex development**

**(a, b)** Expression as calculated from RNA-Seq at E13 (normalized, before and after sex-correction in *a* and *b*, respectively). **(c-f)** ISH for Prdm8 in coronal sections of the central neocortex during embryonic cortex development at E13, E14, E15, and E16. **Arrows** indicate the Prdm8-positive SVZ/IZ in the lateral cortex at E15. **Asterisks** denote strongly reduced expression in the cortex of Neurod1/2/6-deficient mice. **Abbreviations** on page 119.

Whole transcriptome analysis at E13 showed significant decreased Prdm8-expression in the central neocortex of Neurod1/2/6-deficient mice (sex-corrected: 798 to 192 total reads; 76 %↘; p=0.0091; rank 17 in tab 4; fig 26a).

ISH at E13–16 confirmed strongly decreased expression of Prdm8 in the neocortex of Neurod1/2/6-deficient mice when compared to control littermates (fig 26c–f). In control mice, Prdm8 was already robustly expressed in the CP at E13. At later stages, expression was mostly confined to the medial neocortex and hippocampus. In the lateral cortex, Prdm8 was relatively weakly expressed and mostly confined to SVZ/IZ (arrows in fig 26e). In Neurod1/2/6-deficient mice, Prdm8-expression was weak at E13 and hardly detectable at E14–16.

The loss of Prdm8 in the medial neocortex and hippocampus of Neurod1/2/6-deficient mice was better compatible with the hypothesized role as a transcriptional repressor of Hrk and an indirect inhibitor of apoptosis. However, the expression pattern of

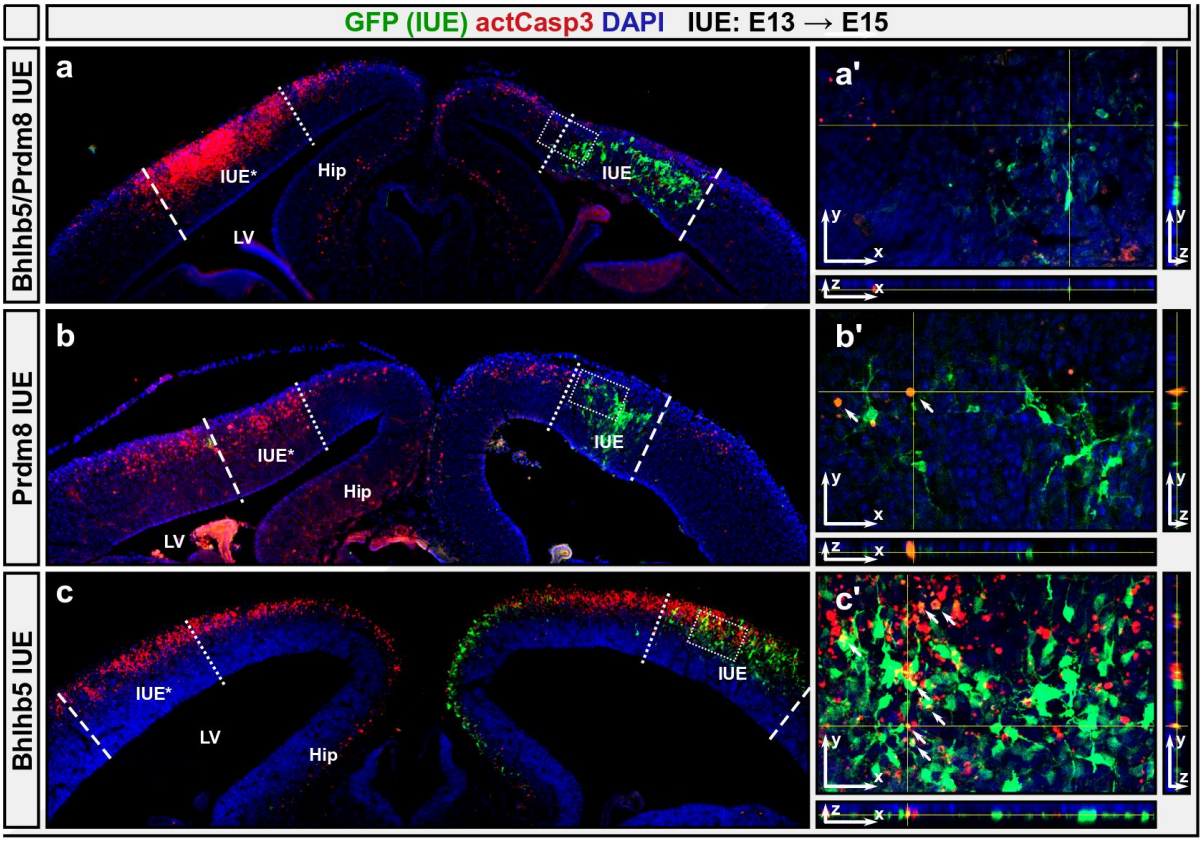


**Figure 27: Overexpression of Prdm8 and Bhlhb5**

**(a–c)** IUE of Bhlhb5 *(a)*, Prdm8 *(b)*, or both *(c)* into the central neocortex of Neurod1/2/6-deficient mice at E13 and IHC for GFP (green) and activated caspase 3 (red) at E15. **(a'-c')** Confocal image stacks at approximately the boxed region in *a–c*. The **dotted** and **dashed lines** indicate the medial and lateral boundaries of the electroporation site in the ipsilateral cortex and the approximate projections into the contralateral cortex; **IUE** denotes the electroporation site; **IUE*** is an approximate projection of the electroporation site into the non-electroporated contralateral hemisphere. **Abbreviations** on page 119.

Prdm8 in controls did not reproduce the abrupt border of apoptosis in the central neocortex of Neurod1/2/6-deficient embryos (fig 5) and loss of Prdm8-expression in the medial cortex cannot explain the increase of Hrk-expression in the lateral cortex of Neurod1/2/6-deficient mice at E14 (fig 23c).

### 2.8.3 Bhlhb5/Prdm8 Overexpression

Bhlhb5 and Prdm8 were shown to interact and function in the same repressor complex in the cerebral cortex (Ross et al., 2012). To directly investigate whether this complex can suppress cortical apoptosis, I cloned the complete coding region of both genes into the described bicistronic conditional expression vector. If Bhlhb5 and Prdm8 were indeed repressors of Hrk-expression or inhibitors of abnormal apoptosis in Neurod1/2/6-deficient mice, IUE of the expression vectors into the cortex of Neurod1/2/6-deficient mice at E13 would prevent the activation of caspase 3 in the electroporated hemisphere at E15.

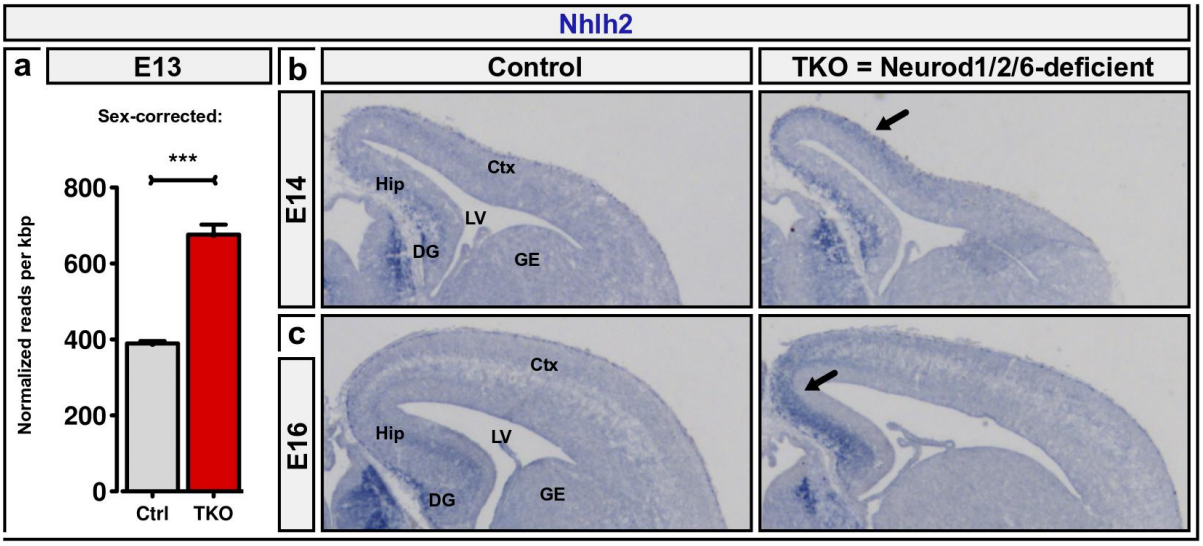


**Figure 28: Nhlh2 expression in embryonic cortex development**

**(a)** Expression as calculated from RNA-Seq at E13 (normalized, sex-corrected). **(b–c)** ISH in coronal sections of the central neocortex during embryonic cortex development at E14 and E16. **Arrows** point to increased expression in the medial neocortex and hippocampus of Neurod1/2/6-deficient mice. **Abbreviations** on page 119.

Co-electroporation of Bhlhb5 and Prdm8 indeed resulted in reliable suppression of cell death in the electroporated hemisphere (fig 27a). The GFP-positive electroporation site was nearly devoid of activated caspase 3 or pycnotic DAPI-positive nuclei. Even GFP-negative cells in the proximity of the electroporation site did not undergo apoptosis. These cells did most probably express Bhlhb5, Prdm8, and GFP at low levels, such that the visible GFP signal was below detection level.

Likewise, electroporation of only Prdm8 prevented apoptosis in the neocortex of Neurod1/2/6-deficient mice (fig 27b). The effect was arguably weaker in comparison to the co-electroporation, as few caspase 3 and GFP double-positive cells were detectable in the area of the electroporation site.

In contrast, electroporation of only Bhlhb5 had *no* comparable effect. The electroporation site was scattered with a large number of pycnotic nuclei and cells with strong caspase 3 activity (fig 27c). The extent of caspase 3 activation was comparable in the electroporated and not-electroporated hemispheres. Still, most clearly GFP-positive cells were negative for activated caspase 3. This suggests that Bhlhb5 might act as a *weak* inhibitor of apoptosis. Lower levels of Bhlhb5-expression might simply be insufficient to prevent the initiation of apoptosis.

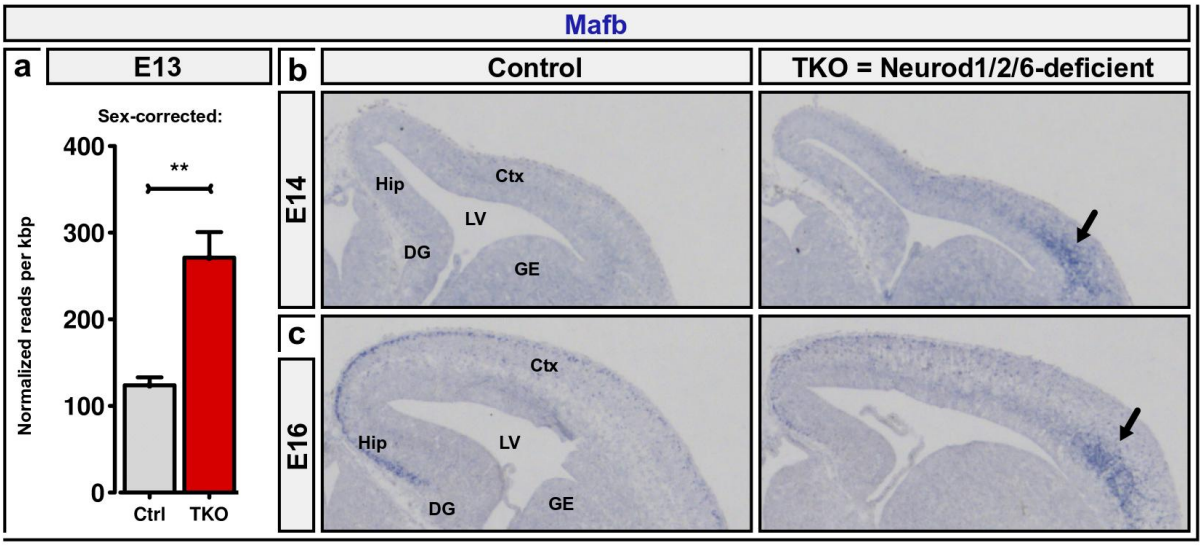


**Figure 29: Mafb expression in embryonic cortex development**

**(a)** Expression as calculated from RNA-Seq at E13 (normalized, sex-corrected). **(b–c)** ISH in coronal sections of the central neocortex during embryonic cortex development at E14 and E16. **Arrows** point to increased expression in the lateral neocortex of Neurod1/2/6-deficient mice. **Abbreviations** on page 119.

# 2.9 Other Candidate Genes

## 2.9.1 Nhlh2 is Increased in the Medial Cortex

Nescient helix loop helix 2 (Nhlh2), previously called Nscl2 or Hen2, is a neuron-specific bHLH transcription factor (Haire & Chiaramello, 1996). It is expressed during the differentiation of neuronal precursors in the cortex (Mattar et al., 2008). In the developing cerebellum, Nhlh1/2 were shown to be essential for neuronal migration and survival (Schmid et al., 2007).

Whole transcriptome analysis at E13 showed increased expression of Nhlh2 in the central neocortex of Neurod1/2/6-deficient embryos when compared to littermate controls (sex-corrected: 1305 to 2266 total reads; 42 %↗; p=0.0127; rank 80 in tab 4; fig 28a). Nhlh2 was the only transcription factor that was robustly up-regulated in Neurod1/2/6-deficient mice.

ISH in coronal brain sections at E14 confirmed a moderate increase of Nhlh2-expression in the central CP of Neurod1/2/6-deficient embryos (fig 28b). The level of Nhlh2 mRNA was particularly increased in the hippocampus and medial neocortex (fig 28b, c). Those are the areas particularly strong affected by apoptosis in the absence of Neurod1/2/6 (fig 5).

### 2.9.2 Mafb is Increased in the Lateral SVZ/IZ

V-maf musculoaponeurotic fibrosarcoma oncogene family protein B (Mafb) is a transcription factor of the basic leucine zipper (bZIP) family. It is involved in hindbrain and inner ear development (Cordes & Barsh, 1994). Naturally, Mafb-deficient (Kreisler) mice were described as hyperactive animals that toss their heads and run in circles (Kataoka et al., 1994; Sing et al., 2009).

Whole transcriptome analysis at E13 showed moderately increased Mafb-expression in the central neocortex of Neurod1/2/6-deficient mice (sex-corrected: 471 to 829 total reads; 245 reads per kbp; 43 %↗; p=0.0412; rank 228 in tab 4; fig 29a).

ISH confirmed increased Mafb-expression in Neurod1/2/6-deficient mice at E14 and E16 (fig 29). Particularly strong levels of Mafb-mRNA were detectable in the lateral cortex (arrows in fig 29b c).

The pattern of increased Mafb-expression is compatible with a potential anti-apoptotic or Hrk-repressing function in the lateral cortex of Neurod1/2/6-deficient mice. However, IUE-based gain of function experiments to rescue Hrk-expression and apoptotic cell death in the medial cortex of Neurod1/2/6-deficient mice were not yet performed.

### 2.9.3 Tiam2 is Lost in the CP

T cell lymphoma invasion and metastasis 2 (Tiam2) is a known guanine exchange factor (Chiu et al., 1999) and an activator of Rac1. It regulates neural development and is expressed in a region-specific and stage-specific manner in the developing and adult mouse brain (Yoshizawa et al., 2002). Tiam2-Rac1 signaling was shown to mediate trans-endocytosis of ephrin receptor EphB2 and thus is crucial for cellular repulsion (Gaitanos et al., 2016).

RNA-Seq at E13 showed significantly decreased Tiam2-expression in the central neocortex of Neurod1/2/6-deficient mice (sex-corrected: 3683 to 789 total reads; 79 %↘; p=0.0177; rank 3 in tab 4; fig 30a). Tiam2 was the second-highest ranked gene in this study (after Hrk; sex-corrected; excluding rRNA). ISH in coronal brain sections at E14 and E16 confirmed robustly reduced Tiam2-expression in the entire CP of Neurod1/2/6-deficient mice (fig 30b-c).

The loss of Tiam2-expression in the CP of Neurod1/2/6-deficient mice might be a secondary effect of failed or delayed terminal differentiation of cortical pyramidal neurons. IUE-based rescue experiments in the cortex of Neurod1/2/6-deficient mice have not yet been performed.

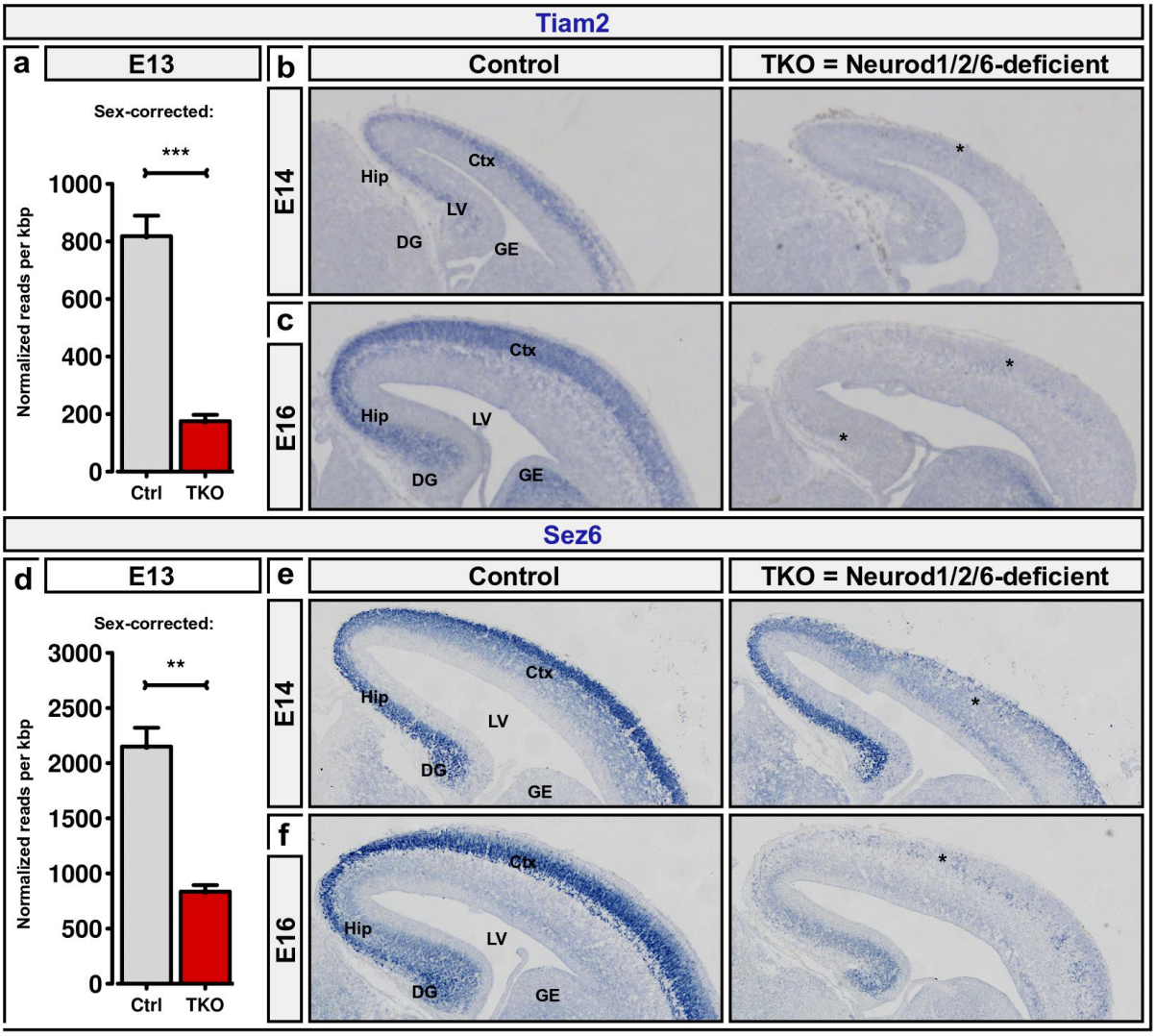


**Figure 30: Tiam2 and Sez6 expression in embryonic cortex development**

**(a, d)** Expression of Tiam2 (a) and Sez6 (d) as calculated from RNA-Seq at E13 (normalized, sex-corrected). **(b–c, d-f)** ISH for Tiam2 (a-c) and Sez6 (d-f) in coronal sections of the central neocortex during embryonic cortex development at E14 (b, e) and E16 (c, f). **Asterisks** denote strongly reduced expression in the cortex of Neurod1/2/6-deficient mice. **Abbreviations** on page 119.

## 2.9.4 Sez6 is Reduced in the Cortex

Seizure related gene 6 (Sez6) is a brain-specifically expressed membrane protein. Sez6-deficient mice show cognitive abnormalities, motor deficits, and reduced dendritic trees of cortical pyramidal neurons (Gunnersen et al., 2007).

Whole transcriptome analysis at E13 showed significantly decreased Sez6-expression in the central neocortex of Neurod1/2/6-deficient mice (sex-corrected: 9011 to 3500 total reads; 61 %↘; p=0.0239; rank 4 in tab 4; fig 30d). Sez6 was the third-highest ranked gene in this study (after Hrk and Tiam2; sec-corrected; excluding rRNA). ISH in coronal brain sections at E14 and E16 confirmed reduced Sez6-expression in the CP of Neurod1/2/6-deficient embryos (fig 30e-f).

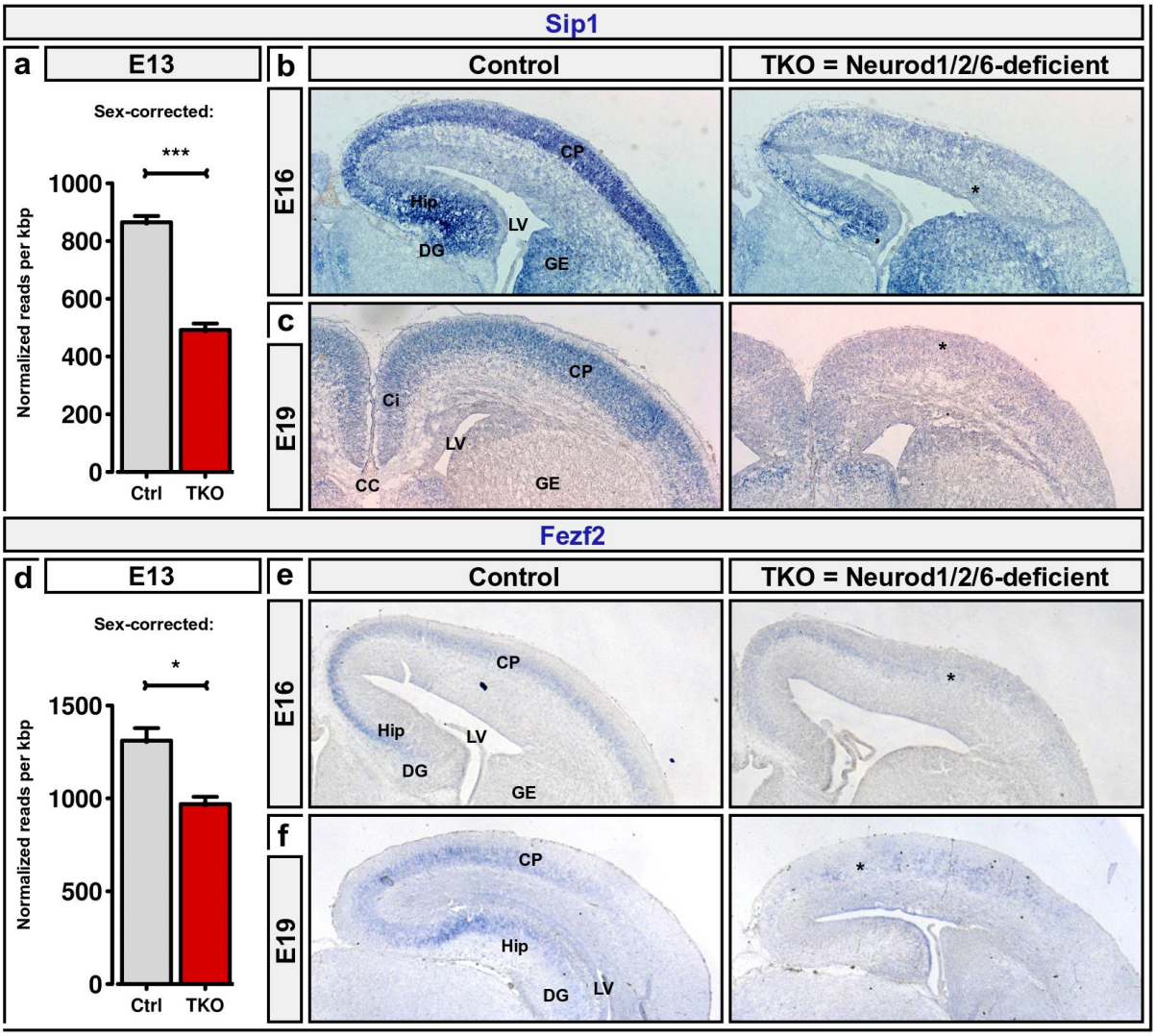


**Figure 31: Sip1and Fezf2 expression in embryonic cortex development**

**(a, d)** Expression of Sip1 (a) and Fezf2 (d) as calculated from RNA-Seq at E13 (normalized, sex-corrected). **(b–c, d-f)** ISH for Sip1 (a-c) and Fezf2(d-f) in coronal sections of the central neocortex during embryonic cortex development at E16 (b, e) and E19 (c, f). **Asterisks** denote strongly reduced expression in the cortex of Neurod1/2/6-deficient mice. **Abbreviations** on page 119.

## 2.9.5 Sip1 Reduced in the CP

Sip1 (Zeb2) is a zinc finger transcription factor interacting with SMAD proteins to mediate TGF-β signaling. Loss of Sip1 function results in Mowat–Wilson syndrome, a human developmental disorder characterized by microcephaly, intellectual disability, and craniofacial abnormalities (Epifanova et al., 2018). In the developing cerebral cortex of mice, Sip1 was shown to regulate the cell fate of neuronal progenitor cells in response to feedback signaling from the CP (Seuntjens et al., 2009). Specifically, Sip1 controls the switch from the production of Ctip2-positive deeper-layer neurons to Satb2-positive upper-layer neurons in response to increasing Ntf3-signaling from the increasingly populated CP (Parthasarathy et al., 2014).

Whole transcriptome analysis at E13 showed highly significantly decreased Sip1-expression in the central neocortex of Neurod1/2/6-deficient mice (sex-corrected: 6992 to 3976 total reads; 43 %↘; p=0.000007; rank 56 in tab 4; fig 31a). Independent of sex-correction, Sip1 was statistically the second-most significantly regulated transcript in the entire RNA-Seq experiment (only following Cdh11). ISH in coronal brain sections confirmed reduced Sip1-expression in the neocortex of Neurod1/2/6-deficient mice at E16 (fig 31b) and showed near loss of Sip1-expression at E19 (fig 31c).

Loss of Sip1 might cause disturbed pyramidal neuron identity and the presence of abnormal Ctip2/Satb2 double-positive neurons in the neocortex of Neurod1/2/6-deficient mice at E19 (sect 2.2). Gain of function experiments using IUE of Sip1 in Neurod1/2/6-deficient mice were beyond the scope of this work.

### 2.9.6 Fezf2 Reduced in the CP

Fezf2 (Zezl) is a zinc-finger transcription factor.

Whole transcriptome analysis at E13 showed moderately decreased Fezf2-expression in the central neocortex of Neurod1/2/6-deficient mice (sex-corrected: 3021 to 2234 total reads; 26 %↘; p=0.0180; rank 269 in tab 4; fig 31d). ISH in coronal brain sections confirmed reduced Fezf2-expression in the central neocortex of Neurod1/2/6-deficient mice at E16 and E19 (fig 31e-f).

# 3 Discussion

Transcription factors of the NeuroD-family are known to control important processes during embryonic cortex development, such as neuronal specification, differentiation, survival, migration, and connectivity (sect 1.4). I investigated those processes in Neurod1/2/6 *triple*-deficient mouse embryos, with a particular focus on the genetic control of apoptosis and cell survival in differentiating neocortical pyramidal neurons.

## 3.1 Pyramidal Neuron Specification

Detailed gene expression analysis and histochemical observations in the developing neocortex of Neurod2/6 *double*-deficient mice have shown a significant enlargement of the neocortical SVZ with a strong increase in the number of Tbr2-expressing cells at E17.5, E18.5, and P0 (Yan, 2016, 4.22; Li, 2017, 4.2). Tbr2 is a classical marker for IPCs, which are derived from RGCs and predominantly give rise to glutamatergic projection neurons in the upper cortical layers (Arnold et al., 2008; Hevner, 2019). Interestingly, IPCs in the SVZ express genes also expressed by mature upper-layer neurons, such as Brn2, Cux2, or Unc5d (Tarabykin et al., 2001; Zimmer et al., 2004). In humans, the evolutionary enlargement of the Tbr2-positive IPC-pool and the SVZ is thought to be a prerequisite for the strong expansion of upper layers and the extensive gyrification of the human neocortex (Hevner, 2019).

Most of the accumulating Tbr2-positive cells in the SVZ of Neurod2/6 *double*-deficient mice are born between E15.5 and E17.5, the time of normal upper-layer neuron generation (Yan, 2016, 4.23; Li, 2017, 4.3). The majority of those abnormal cells are postmitotic (Li, 2017, sect 4.4) and part of the Neurod6-lineage, as shown by co-expression of Cre from the endogenous Neurod6-promoter (Yan, 2016, 4.24). During prenatal cortex development, the expression domain of Neurod1, which is normally spatiotemporarily confined to a thin layer of IPCs in the SVZ, is extended into the outer SVZ and the CP of Neurod2/6 *double*-deficient mice (Yan, 2016, 4.19), suggesting a compensatory role of Neurod1 in the absence of Neurod2/6 (Yan, 2016, 5.3).

Using IUE to rescue the expression of either Neurod2 or Neurod6 in a subset of Cre-expressing (putative Neurod6-positive) cells in otherwise Neurod2/6 *double*-deficient mouse embryos was sufficient to overcome the cellular accumulation of electroporated cells in the SVZ. Rescued cells instead regained the abilities to down-regulate Tbr2 and Neurod1, to migrate into the CP, and to later express upper neuron marker Cux1 [1] (Yan, 2016, 4.25, 5.10).

We initially hypothesized that the compensatory up-regulation of Neurod1 in Neurod2/6 *double*-deficient pyramidal neurons might directly or indirectly lead to abnormal expression of Tbr2, and as a result, might lock accumulating IPCs in an immature multipolar stage (compare Bormuth 2016, 3.2; Yan 2016, 5.10; Li 2017, 5). To test this hypothesis, I analyzed Neurod1/2/6 *triple*-deficient mouse embryos lacking the compensatory up-regulation of Neurod1 in cortical pyramidal neurons of the Neurod6-linage (sect 2.1.1; sect 2.2). Unexpectedly, I observed similar accumulations of Tbr2-expressing cells and a similar expansion of the SVZ in the absence of Neurod1/2/6 ( fig 9i; fig 10a). The failure of Tbr2-positive putative IPCs in the Neurod2/6 *double*-deficient SVZ to differentiate neuronally and to migrate radially into the CP is thus not a result of compensatory Neurod1 up-regulation in those cells.

I rather suggest that Tbr2-expression and maintenance of the IPC-state might normally be actively inhibited by transcriptional repressors downstream of Neurod1/2/6. Possible candidates for this role include Bhlhb5 and Prdm8, both of which are robustly expressed in the SVZ of controls but not of Neurod1/2/6 *triple*-deficient embryos around E15 (fig 25d-f; fig 26d-f). Both factors are transcriptional repressors that can act together in the same protein complex (Ross et al., 2012).

Bhlhb5 (Beta3) was identified as a close homolog and functional antagonist of Neurod1 (Beta2) in pancreatic cells (Peyton et al., 1996) and was later shown to repress Pax6-expression in the brain (Xu et al., 2002). At E15.5 and E17.5, Bhlhb5 is predominantly expressed in the CP and at moderate levels the SVZ (Joshi et al., 2008, fig 1). Genetic inactivation of Bhlhb5 alone does not influence the morphology of the SVZ, as shown by ISH for Id2 and Lmo4 (Joshi et al., 2008, fig 3). Prdm8 was shown to regulate the multipolar-to-bipolar transition in the SVZ/IZ (Inoue et al., 2014) and to be essential for the normal generation of upper cortex layers and whisker barrels (Inoue et al., 2015). Genetic inactivation of Prdm8 alone does also not influence the morphology of the SVZ/IZ, as shown by IHC for Tbr2 and Unc5d (Inoue et al., 2015, fig 3c).

I electroporated Bhlhb5 and Prdm8 into the neocortex of Neurod1/2/6 *triple*-deficient mice at E13 to rescue the abnormal wave of apoptotic cell death during early cortex development (sect 2.8). Focussing on cellular survival, however, I assessed the tissue only at E15. The effect of Bhlhb5/Prdm8-electroporation on the morphology of the SVZ was ambiguous at that stage (fig 27), which might partially be due to

[1] Cux1 is expressed in the VZ and SVZ at earlier developmental stages but mostly confined to cortex layer II-IV at E18.5 (Nieto et al., 2004)

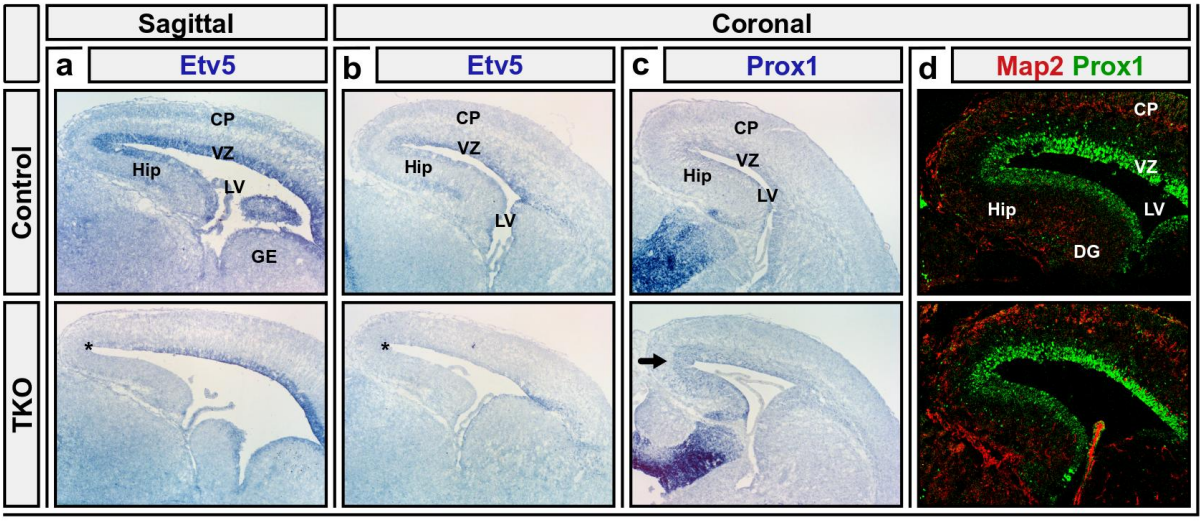


**Figure 32: Etv5 and Prox1 expression in embryonic cortex development**

**(a, b)** ISH for Etv5 in sagittal (a) and coronal (b) cortex sections at E16. **(b, c)** Expression of Prox1 in coronal cortex sections at E16 by ISH (c) and IHC (d). **Asterisks** denote strongly reduced expression in the cortex of Neurod1/2/6-deficient mice. **Abbreviations** on page 119.

artifacts from the electroporation itself. So far, I did not assess molecular effects of Bhlhb5/Prdm8-electroporation on the IPC-population in the SVZ/IZ. Co-staining for GFP (for electroporated cells) and layer-specific marker proteins (eg Tbr2, Sox5, Tbr1, Ctip2, Satb2, or Cux1) are still to be done in Bhlhb5/Prdm8-electroporated brains, ideally at later developmental stages.

## 3.2 Cell Fate, Cell Cycle, and Feedback Signaling

The establishment of neuronal fate and layer identity is severely disturbed in the developing cortex Neurod1/2/6-deficient mice (sect 2.2). Particularly in the dorsomedial cortex, the molecular phenotype is superimposed by a massive wave of apoptotic cell death (sect 2.1). Relative changes in the number of Tbr2-, Ctip2-, and Satb2-positive neurons might thus be due to stage-specific or cell type-specific cell death, rather than failure to establish neuronal fate and identity. In the rostrolateral cortex, however, cell death rates are comparably low (fig 5, fig 6), and the molecular phenotype is more likely to reflect changes in the establishment rather than selective survival of cellular identities. In the lateral cortex of Neurod1/2/6-deficient mice, dominate abnormal accumulations of Satb2/Ctip2 double-positive neurons in the IZ and CP at E17-19 (sect 2.2; dotted circles in fig 9i and in fig 10a). Cell fate switching from deeper to upper layer neuron identity is obviously disturbed or delayed in these cells.

The establishment of neuronal fate in the neocortex is regulated by an interacting network of transcription factors including Fezf2, Sox5, Tbr1, Ctip2, Satb2, and Bhlhb5 (Chen et al., 2008; Baranek et al., 2012; Srinivasan et al., 2012; Ku & Torii, 2020). Most of these factors are expressed in postmitotic pyramidal neurons of a certain identity to repress the differentiational programs of alternative identities. Fezf2 is already expressed in mitotic progenitor cells of the early developing neocortex (Chen et al., 2005) to specify Ctip2-positive subcerebral projection neurons of layer 5 (Molyneaux et al., 2005). In Neurod1/2/6-deficient mice, the progenitor pool is expanded (sect 3.1) and the relative proportion of Ctip2-positive neurons (layer 5) is increased at the expense of Sox5-positive (layer 6) and to a lesser extent Cux1- or Bhlhb5-positive (upper layer) neurons (sect 2.2; Bormuth, 2016, 2.5.4.3, 2.5.6.2). Despite expansion of the progenitor pool, Fezf2-expression was not increased but moderately decreased at E13 (26 %↘ in tab 4); ISH at E16 and E19 showed decreased expression in deeper layers of the CP (sect 2.9.6).

There has always been a big interest in Sip1-based feedback signaling in our research group (Seuntjens et al., 2009; Epifanova et al., 2018). Srinivas Parthasarathy found that differentiated pyramidal neurons in the CP secrete Ntf3 as a feedback signal towards RGCs and IPCs in the VZ/SVZ to influence fate switching from the production of Ctip2-positive deeper-layer to Satb2-positive upper-layer neurons and later to gliogenesis via Sip1 (Parthasarathy et al., 2014). In Neurod1/2/6-deficient mice, Sip1-expression in the developing CP is highly significantly decreased in the CP (sect 2.9.5). Ntf3-expression was barely detectable by RNA-Seq at E13 (1.5 total reads per kbp in controls and 0.0 reads in Neurod1/2/6-deficient mice) or by ISH at E16 and E1 (not shown). However, ISH was not extensively optimized, and I did not try to detect Ntf3 at the protein level.

Despite the massive wave of neuronal apoptosis at E14/15 (sect 2.1; fig 4b', c') and ongoing cell death at E16/17/19 (fig 4d', e'; fig 6e; Bormuth, 2016, 2.5.5), the total size of the cerebral cortex was only moderately decreased in Neurod1/2/6-deficient mice (fig 4e'; fig 6e; fig 10; Bormuth, 2016, 2.5.2). I hypothesized that neurogenesis in the VZ/SVZ might be increased in Neurod1/2/6-deficient mice to compensate for the massive loss of postmitotic neurons. Such a mechanism would necessarily rely on feedback signaling from the apoptotic IZ/CP to the neurogenic VZ/SZV. I quantified mitotic activity and cell cycle parameters at E13 and E15, but could not find significant differences in Neurod1/2/6-deficient mice (sect 2.4; fig 7a, b). Using ISH at E16, I assessed expression levels of various VZ-specific regulator genes in Neurod1/2/6-deficient mice at E16. I did not find obvious changes for eg Pax6, Ctnnb1 (β-Catenin), Notch1, Pcna, Gli1 (data not shown).

Expression of the ERM transcription factor Etv5 was reduced specifically in the Neurod1/2/6-deficient dorsomedial VZ (asterisks in fig 32a, b). Etv5-expression in the central neocortex was not significantly changed at E13 (sex-corrected: 463 to 479 total reads; 3%↗; p=0.1192; rank 23625 in tab 4). In human embryonic stem cells-derived

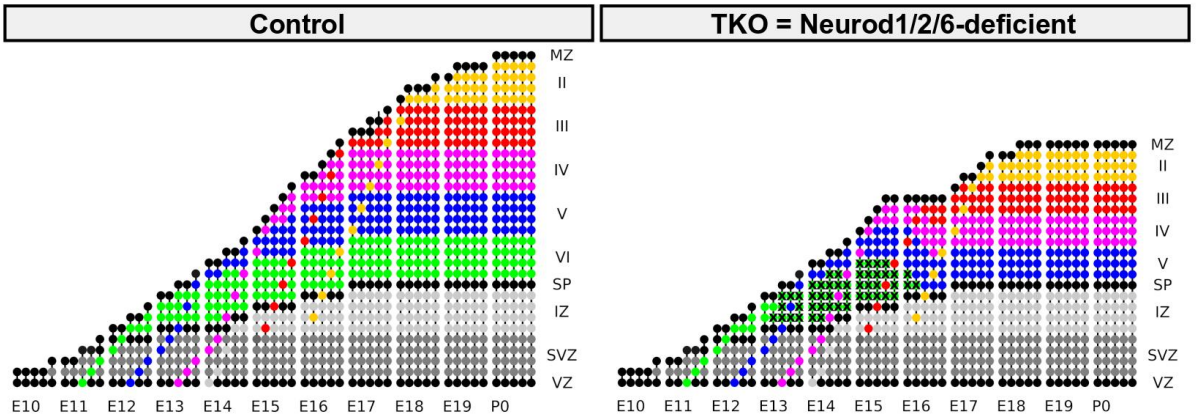


**Figure 33: Cell death and altered neuronal migration in the cortex of Neurod1/2/6 *triple*-deficient mice**
Abbreviations on page 119.

NPCs, Etv5 was shown to act as a repressor of Neurog2 that inhibits the glutamatergic and promotes the GABAergic fate (Liu & Zhang, 2019). In the cortical VZ of mice, Etv5-expression normally follows a MAPK-dependent rostrolateral (high) to caudomedial (low) gradient (Talley et al., 2021). It remains to be shown whether Etv5-expression in the VZ is reduced due to feedback signaling from the adjacent cortex, or whether the effect merely represents a shift in the naturally occurring gradient of Etv5-expression.

By ISH at E15, I also found a mild up-regulation of Prox1 in the dorsomedial neocortical SVZ of Neurod1/2/6-deficient mice (arrow in fig 32c). While not ranking high in the list of differentially expressed genes, RNA-Seq confirmed the mild up-regulation of Prox1 in the central neocortex at E13 (sex-corrected: 261 to 345 total reads; 24 %↗; p=0.0338; rank 3086 in tab 4). Unexpectedly, I could not reproduce the increase of Prox1 on the protein level (fig 32d). In adult neuronal stem cells, Prox1 promotes the identity of oligodendrocytes via Notch1 and Olig2 (Bunk et al., 2016). Interestingly, the number of Olig2-positive glial progenitor cells is increased in the neocortex of Neurod2/6-deficient mice at 16.5 and E18.5 (Yan, 2016, 4.26), and Neurod1 and Olig2 are not expressed by the same cells (Yan, 2016, 4.27). A potential role of Neurod1/2/6 to actively inhibit the oligodendroglial fate (potentially via cell-extrinsic signals) is open for further investigation.

## 3.3 Radial Migration into the Cortical Plate

Here I would like to address neuronal migration in the Neurod1/2/6-deficient developing cortex. I observed several typical features. 1. I see the accumulation of Tbr2-positive IPCs and thus an expansion of the SVZ. 2. Layer 5 Ctip2-positive cells as well as upper layer Satb2-positive cells fail to settle down in the correct layers, but

rather build rosette-like structures in the cortex. 3. Migration, as seen in the live imaging, could hardly be called radial, as the neurons do not follow a straight radial path, they turn and some even circle in the CP (fig 33).

The accumulation of Tbr2-positive basal progenitors in SVZ could be a result of failing cell migration into the CP in Neurod12/6-deficient brains. My colleagues in the group have shown that one of the downstream targets of NeuroD factors is Cntn2 (Tag-1), a cell surface molecule (Bormuth et al., 2013). With my experiments, I could confirm the direct regulation of Cntn2 by NeuroD factors. The depletion of Cntn2 expression in the developing mouse cortex leads to disruption of interkinetic nuclear migration (INM) and thus to overcrowded progenitor zone (Okamoto et al., 2013). This might explain the phenotype I see in Neurod1/2/6-deficient brains.

Studying the reelin-pathway in the brains of Neurod1/2/6-deficient mice, I was able to show significant down-regulation of Dab1, using RNA-Seq and ISH. It has been published that Dab1 is critical for stabilizing neuronal leading processes during radial migration. A mouse line, lacking Dab1 in early-born neurons, shows accumulations of neurons in SVZ. In late-born neurons, Dab1 is essential for their correct positioning in the cortex (Franco et al., 2011). Thus, down-regulation of Dab1 in the Neurod1/2/6-deficient cortex could explain both the expansion of SVZ and the mispositioning of neurons in layers 5 and 2-3.

Neurod1, Prdm8, and Unc5D were shown to be important for the cell transition from multipolar to bipolar phase during early neuron differentiation (Seo et al., 2007). Early B-cell factor 3 (Ebf3), a target gene of Prdm8 as well as Neurod1, have been identified as critical regulators of cell migration from the IZ to the CP (Iwai et al., 2018; Seo et al., 2007). Lack of Neurod1 can thus lead to then disturbed multipolar-to-bipolar transition that I observed in the Neurod1/2/6-deficient cortex. In mutant brains, I could detect and follow in live imaging multipolar cells, located not only in the IZ. Some multipolar cells have managed to enter the CP, indicating an affected migration in Neurod1/2/6-deficient brains.

## 3.4 Regionalization of the Neocortex

THE IMPACT of Neurod1/2/6-inactivation varied in different areas of the developing cortex. *Caudomedial* areas were particularly affected by apoptosis at E14/15 (actCasp3 in sect 2.1; fig 4b', c'; fig 5 fig 6c) and as a consequence loss of Satb2-positive upper-layer neurons at E19 (sect 2.2; asterisks in fig 10a). In *rostrolateral* areas, only relatively few cells died from apoptosis (arrowheads in fig 4b', c'; fig 5; fig 6c) and the number of Satb2-positive neurons was not substantially reduced at E19 (fig 10a). The lateral cortex, instead, was dominated by Satb2/Ctip2 double-positive neurons in the CP and patched accumulations of Satb2/Ctip2 double-positive cells below the

CP (circles in fig 9i and fig 10a). The latter correlated with maintained expression of Ntrk2 (TrkB) and Bcl2, expression of which was strongly reduced in the remaining Neurod1/2/6-deficient cortex (fig 16b'; fig 17b').

Comparative transcriptome analysis (sect 2.6) was based on tissue samples from the central neocortex (sect 2.6.1; fig 19a). Although the experiment was not designed to identify changes in neocortical arealization, I could identify several areal-specifically regulated genes: Expression of the strongest differentially expressed gene Bhlhb5 (tab 4) was predominantly reduced in the lateral neocortex of Neurod1/2/6-deficient mice by ISH at all tested stages (asterisks in fig 25). Expression of Mafb was moderately increased by RNA-Seq at E13 (fig 29a), but it was decreased in the MZ of the medial cortex and at the same time strongly increased in the SVZ of the lateral cortex of Neurod1/2/6-deficient mice by ISH at E16 (fig 29c).

## 3.5 Terminal Differentiation vs. Apoptosis

Most neuronal cells do permanently express pro-apoptotic and anti-apoptotic members of the cell death machinery. Balance fluctuations of these proteins are crucial for the regulation of apoptosis. Pre-existing apoptotic machinery is important to rapidly react to certain stress stimuli. However, strictly controlled developmental changes like simultaneous removal of many cells or remodeling processes rely on transcriptional control (Kumar & Cakouros, 2004). Examples of pro-apoptotic and anti-apoptotic proteins being regulated at the level of gene transcription are Bax (Grimes et al., 1996) and the BH3-only proteins Bim, Puma, Noxa, and Hrk (Puthalakath & Strasser, 2002).

Hrk is a possible target of c-Jun N-terminal kinases (JNKs) (Harris & Johnson, 2001; Bozyczko-Coyne et al., 2001). JNKs mainly react to stress stimuli, such as heat, radiation, osmotic changes, or inflammation signals (Ip & Davis, 1998). During cortex development, Hrk might be regulated by transcription factors that also control the establishment of neuronal fate or the elimination of neuronal cells. Here, I could show that the expression of Hrk (not other apoptotic proteins) is critical for neuronal cell death during cortex development. Neurod1/2/6 regulate Hrk expression levels and thus the extent of developmental cell death.

Hrk has been studied in adult brains as well. Hrk is one of the key molecules that control glioblastoma growth, a very aggressive brain tumor (Nakamura et al., 2005). Induction of Hrk expression leads to tumor cell apoptosis and increased survival in animal models. Hrk might thus be a therapeutic target in the field of brain oncology (Kaya-Aksoy et al., 2019). The interest in understanding the way Hrk is regulated in the brain is permanently growing.

NeuroD proteins are usually transcriptional activators and are thus unlikely to directly repress Hrk. I showed, that a complex of Bhlhb5/Prdm8 could play this role during cortex development. Bhlhb5 together with Olig1/2/3 belongs to the subfamily of bHLH transcription factors. In contrast to NeuroD and Neurogenin-family members, they function as transcriptional repressors (Xu et al., 2002; Zhou & Anderson, 2002). Previous studies showed that Bhlhb5 can mediate the inhibition of Neurod1 target-genes (Peyton et al., 1996). Bhlhb5 is almost exclusively expressed in post-mitotic neurons and thus can regulate through gene repression terminal differentiation of neurons (Joshi et al., 2008). Several studies associate the loss of Bhlhb5 with increased cell death. Amacrine and cone bipolar cells in the retina of Bhlhb5 mutant mice get apoptotically eliminated (Feng et al., 2006). Dysfunction of Bhlhb5 in the dorsal spinal cord results in apoptosis of inhibitory interneurons (Ross et al., 2010). Bhlhb5 alone is unable to repress target gene expression. Here comes Prdm8, which forms a repressor complex with Bhlhb5 (Ross et al., 2012). However, why some cell populations undergo apoptosis in the lack of Bhlhb5/Prdm8 was unclear.

I could show that down-regulation of Bhlhb5 and Prdm8 in the neocortex of Neurod1/2/6 *triple*-deficient mouse embryos is associated with Hrk induced neuronal cell death. Together, these observations argue for the possibility of the Bhlhb5/Prdm8 repressor complex to inhibit neuronal apoptosis. Interestingly, Bhlhb5 as well as Prdm8 mutant mice have relatively normal dorsal telencephalon development. Neurons differentiate and migrate, but are characterized by dramatic axonal mistargeting. Similar to Neurod2/6-*double* and Neurod1/2/6 *triple*-deficient mice, neuronal projections fail to find their targets, resulting in loss of corpus callosum, hippocampal and anterior commissure (Joshi et al., 2008; Ross et al., 2012). Nevertheless, cell survival in either Bhlhb5 or Prdm8 deficient cortex is not affected.

## 3.6 Conclusions and Outlook

In this study, I demonstrate that Neurod1/2/6 together control neuronal survival, specification, radial migration, and axonal guidance.

The survival of immature pyramidal neurons of the caudomedial cortex and hippocampus largely depends on Neurod1/2/6 transcriptional factors. Lack of these factors leads to severe and rash apoptotic cell death in embryonic *triple*-deficient mouse brains.

Neurod1/2/6 transcriptional factors play a crucial role in the specification of diverse pyramidal neuron subpopulations. Neurod1/2/6 *triple*-deficient animals lack correct arealization and laminarization of the neocortex.

The majority of cortical pyramidal neurons depend on Neurod1/2/6 to control radial migration. Cortical pyramidal neurons in *triple*-deficient mice often fail to initiate or terminate radial migration. Some cells even demonstrate a circular rather than a radial migration pattern.

Published work of my colleagues Ingo Bormuth and Kuo Yan demonstrates that Neurod1/2/6 factors are responsible for the axon growth of callosal pyramidal neurons (Bormuth et al., 2013; Bormuth, 2016; Yan, 2016). *Triple*-deficient animals fail to develop a corpus callosum, anterior commissure, and hippocampal commissure.

The main goal of my research was to identify the underlying mechanisms of these processes.

# 4 Material and Methods

## 4.1 Transgenic Mice

The following transgenic mice were used in this study: Neurod1-Flox (entire Neurod1 ORF flanked by LoxP sites; Goebbels et al., 2005), Neurod2-Null (entire Neurod2 ORF replaced by a neomycin resistance cassette; Bormuth et al., 2013), and Neurod6-Cre (also Nex-Cre; entire Neurod6 ORF replaced by Cre recombinase and a neomycin resistance selection cassette; Goebbels et al., 2006). To generate Neurod1/2/6 *triple*-deficient animals, I bread males and females with the genotype $Neurod1^{flox/flox} \times Neurod2^{\underline{wt/null}} \times Neurod6^{cre/cre}$. According to standard Mendelian inheritance for monohybrid crosses, 25 % of the offspring were Neurod1/2/6 *triple*-deficient with the genotype $Neurod1^{flox/flox} \times Neurod2^{\underline{null/null}} \times Neurod6^{cre/cre}$. Control animals were of the genotype $Neurod1^{flox/flox} \times Neurod2^{\underline{wt/wt}} \times Neurod6^{cre/cre}$ or $Neurod1^{flox/flox} \times Neurod2^{\underline{wt/null}} \times Neurod6^{cre/cre}$ (compare Bormuth, 2016). To avoid postnatal lethality, Neurod2-heterozygous breeders were generated by crossing $Neurod1^{flox/flox} \times Neurod2^{\underline{wt/null}} \times Neurod6^{cre/cre}$ males with $Neurod1^{flox/flox} \times Neurod2^{\underline{wt/wt}} \times Neurod6^{cre/cre}$ females. All animal experiments were performed according to German law and had been approved by the responsible authority (Landesamt für Gesundheit und Soziales of Berlin; G0079/11, G0003/14, G0206/16). In termed breedings, the day when the vaginal plug was observed was counted as E0; the gender of embryos was usually not considered (compare sect 2.6.3 and sect 4.10.6).

## 4.2 Genotyping

The genotype of transgenic mice was determined by polymerase chain reaction (PCR) on DNA extracts from small tissue samples that were obtained as a side product during ear tagging.

**a**

| Step | Temperature | Time | Loop |
|---|---|---|---|
| # 1 | 95 °C | 120 sec | |
| # 2 | 95 °C | 30 sec | ↰ |
| # 3 | mean primer TM | 30 sec | |
| # 4 | 72 °C | 75 sec per kbp | 39× to #2 |
| # 5 | 72 °C | 120 sec | |
| # 6 | 4 °C | ∞ | |

**b**

| Substance | Concentration | Amount |
|---|---|---|
| Template DNA | ~200 ng/µl | 1 µl |
| Primers (tab 6) | 10 pmol/µl | each 0.4 µl |
| 10 mM dNTPs (Invitrogen) | 20 pmol/ml | 0.4 µl |
| Polymerase buffer (GoTaq, Promega) | 5x | 4 µl |
| Taq polymerase (GoTaq, Promega) | 1 U/µl | 0.1 µl |
| $H_2O$ | | 13.3 µl |
| ∑ | | 20 µl |

**Table 5: Standard PCR reaction**
**(a)** Thermocycler program for genotyping PCR reactions. **(b)** Formulation of PCR reaction solution.

### 4.2.1 DNA Extraction

Tissue samples were lysed by vigorous shaking for 2–24 hours (h) in 0.3 ml lysis buffer (100 mM Tris-HCl pH 8.5, 200 mM NaCl, 5 mM EDTA, 0.2 % SDS, 0.1 mg/ml Proteinase K) at 55 °C until the tissue had dissolved. To remove remaining tissue debris, the lysates were centrifuged at 13,000 rotations per minute (rpm) in a benchtop centrifuge for 5 min and the supernatants were transferred to new tubes. To precipitate the DNA, an equal amount (0.3 ml) of isopropanol was added and the solution was mixed by inverting the tubes several times. The samples were centrifuged at 13,000 rpm for 15 min and the supernatants were discarded. To remove co-precipitated salts, DNA-containing pellets were washed in 80 % ethanol and centrifuged again for 1 min. After carefully removing the ethanol, the DNA pellets were air-dried at 45 °C and resuspended in 50 µl $H_2O$.

### 4.2.2 Polymerase Chain Reaction

PCR is a classic technique to sequence-specifically amplify DNA in vitro (Mullis et al., 1986). The protocol was adapted from Bormuth (2016). PCR reactions were performed in 0.2 ml reaction tubes (Thermo Scientific) in a T3 thermocycler (Biometra). The reaction volume was 20 µl. The lid of the thermocycler was heated to 102 °C to prevent condensation of the reaction solution in the top of the tube. The thermocycler program is described in table 5; the primer sequences are listed in table 6.

**a** **Neurod1-Flox genotyping PCR primers:**

| Primer | Sequence |
|---|---|
| Neurod1-fw | 5'-GTTTTTGTGAGTTGGGAGTG-3' |
| Neurod1-rv | 5'-TGACAGAGCCCAGATGTA-3' |

**b** **Neurod2-Null genotyping PCR primers:**

| Primer | Sequence |
|---|---|
| Neurod2-rv | 5'-CCCACAGGTAAGAGAGCACG-3' |
| Neurod2-fw | 5'-TTCTCGCTCAAGCAGGACTC-3' |
| Neo-rv (fw in allele) | 5'-AGTGACAACGTCGAGCACAG-3' |

**c** **Neurod6-Cre genotyping PCR primers:**

| Primer | Sequence |
|---|---|
| Neurod6-fw | 5'-GAGTCCTGGAATCAGTCTTTTTC-3' |
| Neurod6-rv | 5'-AGAATGTGGAGTAGGGTGAC-3' |
| Cre-rv | 5'-CCGCATAACCAGTGAAACAG-3' |

**Table 6: Genotyping PCR primers**
Primer sequences for Neurod1-Flox **(a)** Neurod2-Null **(b)** and Neurod6-Cre **(c)** genotyping PCRs.

### 4.2.3 Neurod2-Null PCR

In most cases, genotyping for Neurod2 was sufficient to identify Neurod1/2/6 *triple*-deficient mice because the breeders for experimental tissue were usually homozygous for Neurod1-Flox and Neurod6-Cre (sect 4.1). The Neurod2-Null PCR was redesigned to increase sensitivity for the wild-type allele and to allow amplification under standard conditions (compare Bormuth 2016).

The common reverse primer binds in the 3'-UTR of Neurod2, 138 base pairs (bp) after the stop codon. The forward primer for the wild-type allele binds in the ORF of Neurod2, 924 bp after the start codon. The forward primer for the transgenic allele is a reverse primer for the neomycin resistance cassette, which replaces the ORF of Neurod2 in reverse orientation; the primer binds 241 bp after the start codon of neomycin phosphotransferase. The genotyping of heterozygous tissue results in two bands: the smaller one (383 bp) identifies the wild-type allele, and the bigger one (598 bp) identifies the transgene allele.

### 4.2.4 Neurod1-Flox and Neurod6-Cre PCR

Genotyping for the Neurod1-Flox and Neurod6-Cre alleles were performed as previously described (Goebbels et al. 2005 and Goebbels et al. 2006, respectively).

**a**

| Substance | Amount | Final concentration |
|---|---|---|
| low melting agarose | 1.8 g | 1.5 % |
| Electrophoresis buffer (50×) | 2.4 ml | 2 % |
| Serva DNA stain G | 12 µl | 0.005 % |
| $H_2O$ | ad 120 ml | |

**b**

| Substance | Amount | Final concentration |
|---|---|---|
| Tris-HCl-Base | 242 g | 2 M |
| Glacial acetic acid | 57.1 ml | |
| 0,5 M EDTA, pH 8 | 100 ml | 1 mM |
| $H_2O$ | ad 1000 ml | |

**Table 7: DNA electrophoresis**
**(a)** Formulation for the preparation of agarose gels. **(b)** TAE electrophoresis buffer (50×).

### 4.2.5 Gel Electrophoresis

PCR products were separated by molecular weight using agarose gel electrophoresis (Sambrook & Russell, 2000) and visualized using the fluorescent dye Serva DNA stain G, which was added directly to the 1.5 % agarose gels (tab 7). The gels were imaged in a closed gel documentation system (INTAS), using UV light.

## 4.3 Tissue Processing

EMBRYOS were quickly dissected in ice-cold phosphate buffered saline (PBS) using a binocular. Before fixation, small tissue samples were put aside for genotyping (sect 4.2). Total brains were isolated and fixed in 4 % PFA. The fixation time varied depending on the embryonic stage: E11–13 = 5 h; E14–16 = 8 h; E17–P0 = overnight in PFA. Small brains (E11–13) were fixed inside the skull to avoid preparation artifacts.

Depending on the planned experiments, the fixed brain tissue was further processed for cryostat or paraffin sectioning. ISH and IHC with antibodies that only recognize native epitopes were generally performed on cryostat sections. IHC with all other antibodies and 3d-reconstructions were performed using paraffin section.

### 4.3.1 Cryostat Sectioning

Tissue used for cryostat sectioning was incubated in the sucrose solution to avoid crystal formation. After fixing in 4 % paraformaldehyde (PFA), brains were merged in 15 % sucrose 1xPBS solution till they sunk. Then they were incubated in 30 % sucrose in 1xPBS solution overnight at +4 °C. Brains were then washed in OCT (TissueTek) medium. If the tissue was prepared for coronal sections, brain stem and part of the

spinal cord, left after the preparation, were removed. In case of lateral sections brains were cut along the midline. Prepared samples were then placed in an embedding mold filled with fresh OCT to one-third of the volume. Using forceps brains were carefully positioned in OCT according to the cutting plane. Embedding molds were transported to a -80 °C freezer were they froze gradually and were left frozen till cutting.

Sectioning was performed using a cryostat (Leica). The temperature was set between -16 °C and -22 °C for the tissue sample and 3 °C lower for the cryostat chamber. Resulting sections with thickness from 14 µm to 25 µm were collected on adhesive Superfrost plus slides (Menzel-Gläser). Slides with collected brain sections were dried at RT 30 min to 1 h. Then they were transferred to the plastic box and stored at -80 °C. Before use, slides were dried for 30 min in a vacuum with silica granules.

### 4.3.2 Paraffin Sectioning

To prepare paraffin sections fixed brains were dehydrated using an ethanol series, starting from 30 %, then 50, 70, 80, 90 and 100 % twice. In each solution, tissue was incubated for 1 h. After ethanol brains were incubated in isopropanol for 2 h and in xylene twice for 2 h each time. After dehydration brains were transferred into 60 °C warm liquid paraffin solution and left overnight. Paraffin was changed once or twice to avoid traces of xylene in the tissue. The embedding was performed in liquid paraffin on the 65 °C platform of the embedding machine within the plastic box. The boxes with the brains were carefully moved to the ice-cold metal plate, where paraffin quickly solidified.

5–10 µm thick sections were made on the Microtome (Leica), merged with the brush into a water bath with 35–37 °C purified water and collected on the uncovered glass slides. The freshly cut tissue was dried at room temperature (RT), left overnight at 37 °C and then stored at RT till the moment of staining.

For further immunohistochemistry tissue was deparaffinized by incubation in xylene for 10 min twice, isopropanol for 5 min. Further re-hydration was performed in the ethanol raw with decreasing concentrations from 100 to 30 % for 2–3 min each, followed by dd$H_2O$

## 4.4 Immunohistochemistry

PARAFFIN SECTIONS were dehydrated to unmask protein epitopes. Prepared deparaffinized tissue was then boiled in already preheated unmasking solution (Vector Labs). The slides were then continuously boiled for 10 to 30 min. After boiling slides were left on ice to cool down to room temperature (RT). Then the slides were transferred into plastic boxes and washed with PBS 2-3 times.

Cryosections were dried in vacuum and transferred directly into the plastic boxes for further procedures. In case epitopes for antibodies were localized in the nucleus or cytoplasm, membrane permeabilization with 0.5 % Triton X-100 (TX-100) in PBS was performed.

After this preparations, the treatment of paraffin and cryosections was the same. Permeabilized by boiling or incubation with the TX-100 tissue was blocked in blocking solution containing 10 % Horse Serum (HS) and 0.1 % TX-100 diluted in 2 % Bovine Serum Albumin (BSA). Tissue sections were blocked for 1–2 h. Solution for Primary antibodies contained 5 % HS 0.05 % TX-100 diluted in 2 % BSA. 100 µl of this solution with antibodies (tab 8) were applied per each slide and were incubated in 4 °C overnight. To avoid evaporation and drying of the tissue, slides were covered with pieces of parafilm of appropriate size. On the following day, slides were extensively washed with PBS to prevent background staining of the tissue. Secondary antibodies conjugated to fluorophore (1:500, Molecular Probes) were then applied on the slides in 2 % BSA solution for 2 h to overnight. After antibody treatment, the slides were washed in PBS. To visualize cell nuclei tissue was stained with DAPI or Hoechst 1:500 dilution in PBS. then the tissue was again washed in PBS, rinsed in purified water and mounted in mounting media with fluorescence protection – DAKO Fluorescence Mounting Medium or DABCO media (Polyvinyl alcohol, Glycerol, 0.2 M TRIS pH 8.5 and DABCO).

Images of immunostained tissue (IHC) and cells (ICC) were taken on confocal microscopes Zeiss LSM Exciter and Leica TCS SL as well as fluorescence microscope Olympus BX51.

## 4.5 In Situ Hybridization

### 4.5.1 Cloning and Synthesis of Riboprobes

Fragments with sequence length from 400 to 1500 bp were chosen either in the coding region of the interested gene or in the 3'-UTR prime region of this gene. Forward and reverse primers were designed with the help of Primer3 program. The amplification of this region was performed on the mouse cDNA from E17 embryos. For PCR GoTaq Polymerase was used because it can provide 'A' overhangs on the amplified fragment. That is needed for T-cloning. The amplicon was extracted from the gel and ligated into the pGEMT vector (Promega) or pAL2T vector (Evrogen) through T-cloning. The plasmid including the insert was then transfected into the XL-10GOLD or DH5alfa line of the competent bacterial cells. 50 µl of competent cells were incubated for 20 min on ice with the ligated plasmid, then heat shock in 42 °C for 45 sec was

| Target | Class | Host | Tissue | Dilution | Supplier (TM) | Product-ID |
|---|---|---|---|---|---|---|
| BrdU | IgG2a | rat | C,P | 200 | Abcam | ab6326 |
| BrdU/IdU | IgG1 | mouse | C,P | 100 | Merck | MAB3424 |
| Brn2 = Pou3f2 | pc | goat | P | 200 | Santa Cruz | sc-6029 |
| Casp3 (activated, Asp175) | pc | rabbit | C,P | 300 | Cell Signaling | 9661 |
| Cre | pc | rabbit | V,C,P* | 2000 | Covance/Babco | PRB-106P |
| Ctip2 = Bcl11b | IgG2a | rat | P | 500 | Abcam | ab18465 |
| GFP | pc | goat | P | 1000 | Rockland | 600-101-215 |
| GFP | pc | chicken | P | 1000 | Abcam | ab13970 |
| Ki67 | IgG | rabbit | P | | Forschungszentrum Borstel | |
| Map2 (a+b) | IgG1 | mouse | V,C,P | 200 | Merck | MAB378 |
| Pax6 | pc | rabbit | C,P | 300 | Merck | AB2237 |
| Pcna | pc | rabbit | P | 200 | Abcam | - |
| Reelin | IgG | mouse | P | 500 | Chemicon | 553731 |
| RFP | pc | rabbit | P | | Abcam | ab62341 |
| Satb2 | pc | rabbit | C | 1000 | Tarabykin | |
| Satb2 | IgG1 | mouse | C,P | 200 | Abcam | ab51502 |
| Sox5 | pc | goat | P | 500 | R&D Systems | AF5286 |
| Tbr1 | pc | rabbit | P | 300 | Abcam | ab31940 |
| Tbr2 = Eomes | pc | rabbit | P | 300 | Abcam | ab23345 |
| Tbr2 | pc | chicken | P | 300 | Merck | AB15894 |
| Tubb3 = Tuj1 | IgG2b | mouse | T | | Sigma-Aldrich | T8660 |
| Vglut1 = Slc17a7 | pc | rabbit | P | 250 | Synaptic Systems | 135 303 |

**Table 8: Primary antibodies**

**Target:** Gene symbol of the detected protein; **Class:** Immunoglobulin isotype of monoclonal antibodies or 'pc' for polyclonal sera; **Host:** Species the antibody was raised in; **Tissue:** Antibody was successfully used in tissue processed for **V**: vibratome, **C**: cryostat, or **P**: paraffin sectioning (***** only successful after extensive antigen unmasking); **Dilution**: Supplied antibody solutions were diluted for final use.

performed. The bacteria were then cultured at 37 °C in LB medium for 40 to 60 min and plated on agarose with ampicillin for resistance selection and X-gal and IPTG (isopropyl beta-D-1-thiogalactopyranoside) for blue-white selection. Plates were kept in 37 °C overnight. Positive white clones were picked up next day and cultured in 6 ml LB medium with ampicillin for 10 h. Mini-prep kit (Qiagen) was used to extract the plasmid. The presence of insert and its orientation in the received plasmids was checked by sequencing with T7 sequencing primer. Part of the in situ probes used in this work were prepared by Dr. Kuo Yan (Institute of Cell- and Neurobiology, Charité Berlin).

| Substance | Amount |
|---|---|
| Plasmid | 75 µl |
| Restriction enzyme buffer | 10 µl |
| Restriction enzyme | 4 µl |
| Purified water | 11 µl |

**Table 9: Plasmid linearization**

### 4.5.2 Plasmid Linearization

Sequencing data showed the orientation of the insert - sense or antisense. According to this information the vector was cut either with NcoI or SphI restriction enzymes for sense orientation and NsiI or PstI for anti-sense (tab 9). The linearized plasmid was then loaded on the gel and after electrophoresis extracted in 40 µl DEPC-water. This is the template for the probe.

### 4.5.3 In Vitro Transcription

The insert was transcribe using SP6 (for sense probe) or T7 (for anti-sense probe) polymerase in 37 °C for 3 h. After 2.5 h DNase buffer and DNase 2.5 µl each were added to the reaction and kept another 30 to 45 min at 37 °C (tab 10). The reaction was stopped by transferring on ice.

### 4.5.4 RNA Precipitation

For further precipitation, 2 µl of 0.2 M EDTA pH 8.0, followed by 3 µl of 4 M LiCl and 90 µl 100 % Ethanol were added to the reaction. This mix was then left overnight in -20 °C. On the next day, probes were centrifuged for 20 min at 4 °C at 13.000 RPM in a benchtop centrifuge. After removing a supernatant one could see a white pellet. To wash the pellet 70 µl of 70 % Ethanol were added to the tube and centrifuged for 10 min as above. This step was repeated twice. To dry the pellet the tubes were left at 37 °C for 5 min. The pellet was dissolved in 33 µl DEPC-water. 3 µl were immediately loaded on the gel for electrophoresis to check the presence of the RNA. If the band was strong and had the correct size, 180 µl of hybridization buffer (tab 11) were added to 30 µl of the probe, mixed well and placed in -20 °C until use.

| Substance | Amount |
|---|---|
| Template | 1–2 µg |
| T7 or Sp6 polymerase | 2 µl |
| Transcriptional buffer 10x | 2 µl |
| Dig RNA-labelling mixture | 2 µl |
| RNase inhibitor | 0.5 µl |
| DEPC-water | up to 20 µl |

**Table 10: In vitro transcription**

### 4.5.5 Preparation of Sections and Probe Application

Embryos were isolated in PBS-DEPC and fixed overnight in 4 % PFA. Next day the fixing solution was changed to 15 % sucrose in PBS-DEPS and, after brains sank, to 30 % sucrose in PBS-DEPC. The brains were then embedded in Tissuetek and stored at -80 °C till cutting. On the day of cutting blocks with the embedded brains were quickly transferred into the cryostat were sections of 16 µm thickness were obtained. Cutting was usually complete in 40 min. Sections were then dried in vacuum for 30 min and fixed in 4 % PFA in DEPC-PBS for 15 min at room temperature. After fixation sections were washed twice in DEPC-PBS for 5 min. The sections then were digested with proteinase K in proteinase K buffer (20 mM Tris pH 7.5 and 1 mM EDTA pH 8.0). The buffer was heated in a microwave to 37 °C, 20 µg/ml proteinase K was added to the buffer. Sections were kept in this solution for 2-3 min at room temperature. Digested sections were merged to 0.2 % Glycine in PBS-DEPC for 5 min and then washed twice in PBS-DEPC. Postfixation was performed in 4 % PFA 0.2 % Glutaraldehyde in PBS-DEPC for 20 min at room temperature. The sections were washed again twice in PBS-DEPC for 5 min and prepared for prehybridization. In each compartment of incubation box, 20 ml of 50 % Formamide/5xSSC were applied, what would create humidity in the box. Slides were carefully placed into the boxes. 150 µl of hybridization buffer (tab 11) were applied on top of each slide. To avoid evaporation slides were covered with parafilm. Prehybridization was performed for 2 h in 65 °C. In this time 10 µl of probe RNA in 150 µl of hybridization mix were denatured at 90 °C for 5 min. Denatured probes were transferred on ice until application on sections. After 2 h of prehybridization, 160 µl of the denatured probe in hybridization mix were applied on slides. They were again covered with parafilm and kept overnight at 65 °C.

### 4.5.6 Antibody Application

Next day sections were treated with 2xSSC pH 4.5 for 5 min at room temperature. Then sections were transferred into preheated to 37 °C RNase buffer (15 ml 5 M NaCl and 1.5 ml 1 M Tris pH 7.5 in 150 ml of purified water) for 5 min. After this, step

| Substance | Amount |
|---|---|
| Formamide 50 % | 10 ml |
| 5x SSC | 5 ml 20x SSC, pH 4.5 or pH 7.0 |
| Boehringer block 1 % | 200 mg |
| DEPC water | 4.36 ml |
| EDTA 5 mM | 200 µl 0.5 M EDTA |
| Tween 0.1 % | 20 µl |
| CHAPS 0.1 % | 200 µl CHAPS 10 % |
| Heparin 0.1 mg/ml | 20 µl Heparin 100 mg/ml |
| Yeast RNA 100 µg/ml | 200 µl Yeast RNA 10 mg/ml |

**Table 11: Hybridization buffer**

20 µg/ml of RNase were added to the buffer and sections were incubated for another 30 min at 37 °C. Slides were then treated with Formamide 3 times in 65 °C and washed twice in KTBT solution. For blocking 20 % sheep serum in KTBT were used. Anti-DIG alkaline phosphatase antibody 1:1000 dilution were applied overnight.

### 4.5.7 Washing, Developing and Mounting

Sections were washed six times with KTBT (tab 12) and then three times with NTMT (tab 13) at room temperature. Staining development was performed in 1:50 NBT/BCIP solution in NTMT. When the signal was strong enough slides were washed three times in PBST (1xPBS, 0,1 % TX-100). Then sections were fixed for 10 min in 4 % PFA, rinsed in PBS and dehydrated in ethanol raw and mounted in *Entellan new rapid mounting medium* (Millipore).

### 4.5.8 Microscopy and Imaging

Bright field images were taken on a microscope Olympus BX60 and Axiovision software.

## 4.6 Cell Culture

### 4.6.1 Treatment of Glass Coverslips

In a rotating shaker, glass coverslips were washed overnight in 70 % ethanol, three times in purified water, rinsed twice with 100 % ethanol and once with 70 % ethanol in purified water and stored in 100 % ethanol at 4 °C until use. One day before the cell culture experiment, pretreated coverslips were coated with 0.1 mg/ml poly-L-lysine (Sigma Aldrich) in purified water overnight at 37 °C.

| Stock solution | Volume | Final concentration |
|---|---|---|
| 1 M Tris pH 7.5 | 50 ml | 50 mM |
| 5 M NaCl | 30 ml | 150 mM |
| 1 M KCl | 10 ml | 10 mM |
| TX-100 | 10 ml | 1 % |
| Purified water | 900 ml | |

**Table 12: KTBT solution**

### 4.6.2 Dissociation of Cortical and Hippocampal Neurons

Hippocampus or cortex from E15 – E17 mice were quickly prepared in a dish with an ice-cold 1xHBSS with Ca and Mg (GIBCO). Tissue was collected in 2 ml ice-cold 1xHBSS with Ca and Mg. Then the tissue was several times washed with 1xHBSS without the supplements. After last wash 3.5 ml 1xHBSS should be left in the tube. 0.5 ml of Trypsin 2.5 % (GIBCO) were added to the tube. Trypsinization was performed for 30 min in 37 °C. Every 10 min brain tissue in solution was gently mixed. To stop the trypsinization 2 ml FBS (Biochrom) were added to the tube. Then trypsinized tissue was gently washed 3 times in 1xHBSS with Ca and Mg. To prevent or reduce cell clumping 100 µl DNase I (Roche) were used followed by multiple washing in Neurobasal medium (GIBCO). After the last washing step, 2 ml of medium were left in the tube. The cells were dissociated with a pipette tip (1 ml) and centrifuged for 5 min at 1200 g at 4 °C. The supernatant was carefully removed and cells were dissociated in 1 ml of pre-warmed Neurobasal complete medium (tab 14). To count the cells 10 µl of trypan blue were added to 10 µl of cell suspension. 100,000 cells were plated in each well of a 24-well plate (BD Falcon). the cultures were incubated for 3 to 6 days at 37 °C, 5 % $CO_2$.

### 4.6.3 Mixed Coculture

To confirm that cell death in Neurod1/2/6 mutant mice is regulated cell intrinsically we cocultured mutant hippocampal neurons with GFP-positive wild-type neurons. Hippocampi from both mouse lines were prepared simultaneously. Trypsinization and cell dissociation were performed as described above.

### 4.6.4 Immunocytochemistry

After 3 or 6 days in vitro cells were fixed for 10 min in 4 % PFA in PBS. Coverslips were transferred into a staining box and 50 µl of 0.4 % TX-100 in PBS were applied on top of each coverslip for 20 min to permeabilize the cells. Cells then were blocked in blocking

| Stock solution | Volume | Final concentration |
|---|---|---|
| 1 M Tris pH 9.5 | 50 ml | 100 mM |
| 5 M NaCl | 10 ml | 100 mM |
| 1 M MgCl2 | 25 ml | 50 mM |
| Tween-20 | 0.5 ml | 0.1 % |
| Purified water | 415 ml | |

**Table 13: NTMT solution**

solution (10 % HS, 0.2 % TX-100 in 2 % BSA) for 1 h in room temperature. Primary antibody were applied in the blocking solution and left overnight at +4 °C. Next day coverslips were washed 3 times 15 min each in PBS. Cells then were covered by 50 µl of secondary antibody in the concentration 1:500 in 2 % BSA for 2 h. Coverslips were washed with PBS 3 times for 5 min with addition of DAPI in the first wash. Finally, the coverslips were mounted in the fluorescent mounting medium (DAKO).

## 4.7 Organotypic Slice Culture

### 4.7.1 Coating of Plates

Sterile cell culture inserts (Falcon) with a pore size of 1 µm were coated with Laminin (Sigma-Aldrich) and poly-L-lysine (Sigma-Aldrich) overnight at 37 °C. On the next day, the coating solution was collected from the inserts and frozen at -20 °C to be reused 2–3 times.

### 4.7.2 Slice Preparation

Electroporated at E14 brains were taken at E15 and cut on the vibratome 250 µm thick. Preparation of the brains and cutting was performed in Complete Hank's Balanced Salt Solution (tab 15a). Slices were cultured on the inserts in slice culture medium (tab 15b) as previously described (Polleux & Ghosh, 2002). If slices were prepared for live cell imaging a Millicell inserts (Merck Millipore) with 0.4 µm pore size were used.

### 4.7.3 Time-Lapse Microscopy

Live cell imaging was performed on a spinning disc confocal microscope (CXU-S1, Zeiss). Brain slices were placed in 37 °C and imaged for 60 hours every 20 minutes.

| Substance | Amount | Final concentration | Supplier |
|---|---|---|---|
| 1x Neurobasal medium | 50 ml | 1x | GIBCO |
| 50x B27 Supplement | 1 ml | 1x | GIBCO |
| 100x Glutamax | 0.5 ml | 1x | GIBCO |
| 100x Penicillin/Streptomycin | 0.5 ml | 1x | Sigma |
| ß-mercaptoethanol (142 mM) | 9 µl | 25 µM | GIBCO |
| | ~50 ml | | |

**Table 14: Formulation of neuronal cell culture medium**

## 4.8 In Utero Electroporation

A TIMED PREGNANT MOUSE was anesthetized using Isoflurane in a closed chamber or by intraperitoneal injection of ketamine and xylazine (100 µg and 10 g per gram body weight, respectively). For additional analgesia the opioid Buprenorphine (0.1 µg per gram of body weight) was injected subcutaneously. The mouse was placed on a warm platform and the uterine horns were surgically exposed. 1 µg/µl of DNA in a water based solution with the negatively charged dye fast green was injected into the lateral ventricle of embryos using a fine glass capillary that had been pulled using a HEKA-PIP6 capillary puller. Small gold electrodes (2 mm diameter) were applied to the uterine surface and positioned parietally (cathode) and fronto-temporararily over the injected ventricle (anode) of the embryo's head; electroporation was performed using a ECM 830 electroporator (BTX) (six pulses of 50 ms, 35 Volts direct current with 100 ms intervals). The uterine horns were carefully placed back into the abdomen and washed with PBS containing penicillin (100 U/ml) and streptomycin (0,1 mg/ml) for antibiotic prophylaxis. The wound was surgically closed and the mouse was carefully observed until complete recovery. Operated animals were closely monitored for any signs of pain, infection, or surgical complications. Suspicion of pain was met by additional administration of Buprenorphine; any other complication resulted in termination of the experiment. In principal, the procedure followed the protocols previously described in Saito (2006).

### 4.8.1 Overexpression

The full ORF of a given gene of interest (GOI) was conditionally and bicistronically expressed from the CAG promoter followed by the LoxP-flanced red-fluorescent protein mCherry, an internal ribosomal entry site (IRES), and the green fluorescent protein (GFP) for visualization. Expression vector: pCAG–LoxP–mCherry(stop)–LoxP–GOI–IRES–GFP.

**a**

| Stock solution | Volume | Final concentration |
|---|---|---|
| 10x HBSS | 50 ml | 1x |
| 1 M Hepes pH 7.4 | 1.25 ml | 2.5 mM |
| 1 M D-Glucose | 15 ml | 30 mM |
| 100 mM $CaCl_2$ | 5 ml | 1 mM |
| 100 mM $MgSo_4$ | 5 ml | 1 mM |
| 1 M $NaHCO_3$ | 2 ml | 4 mM |
| Purified water | to 500 ml | |

**b**

| Stock solution | Volume | Final concentration |
|---|---|---|
| Basal Medium Eagle | 35 ml | 70 % |
| Complete HBSS | 10.75 ml | ~10 % |
| 1 M D-glucose | 1 ml | 20 mM |
| 200 mM L-glutamine | 0.25 ml | 1 mM |
| Penicillin/Streptomycin | 0.5 ml | 1 % = 100 U/ml and 0.1 mg/ml, respectively |
| Heat-inactivated Horse Serum | 2.5 ml | 5 % |
| | 50 ml | |

**Table 15: Formulation of slice culture media**
**(a)** Complete Hank's balanced salt solution (HBSS). **(b)** Slice culture medium.

## 4.8.2 Knockdown

RNA-interference is a well established molecular technique, that allows precise gene suppression. To study Hrk function specific shRNAs were introduced.

### 4.8.2.1 Design of shRNA Expression Constructs

Forward and reverse oligonucleotides were designed in the way that they contain a unique sequence from the 3'-UTR of Harakiri (Hrk) mRNA. To inhibit Hrk expression 3 different shRNA were used (Kalinec et al., 2005). Sense and antisense orientation of the unique sequences was separated by a 9 nucleotide spacer sequence as described in pSUPER RNAi System Manual. Forward and reverse oligonucleotides contain on the 5' end BglII and on the 3' end HindIII restriction sites used for cloning into the pSUPER.retro vector (Oligoengine).

### 4.8.2.2 Annealing of Single Strand Oligonucleotides

To receive the working concentration of the oligonucleotides 3 mg/ml they were dissolved in water. 1 µl of forward and reverse oligonucleotides were mixed together and 48 µl annealing buffer (100 mM NaCl and 50 mM HEPES pH 7.4 were added to the mixture. Incubation was performed at 90 °C for 4 min followed by 70 °C for 10 min. The annealed oligonucleotides were slowly cooled down to 10 °C and stored at -20 °C.

Annealed oligonucleotides were then cloned into the linearized pSUPER.retro vector using BglII and HindIII restriction sites. The vector was transformed into competent bacteria cells according to the standard transformation protocol used in the laboratory.

#### 4.8.2.3 Cloning of Harakiri 3'-UTR

To visualize the efficiency of shRNAs Hrk 3'-UTR cloning into pCAG-RFP was used. Both vectors containing shRNA and RFP-Hrk 3'-UTR were co-transfected into the N2f cell line and fluorescence intensity was checked. As the control were used pCAGEN - empty vector and shRNA3 with deletion.

#### 4.8.2.4 In Utero Electroporation of shRNA

The most efficient shRNA constructs were used for in vivo Hrk inhibition with the help of in utero electroporation technique. shRNA mixture was injected into ventricles of E13 embryos of Neurod1/2/6 *triple*-deficient embryos. Brains were analyzed 2 days later at E15. Cell death was visualized by immunostaining for activated caspase 3.

## 4.9 Cellular Birth Dating

BrdU, IdU and EdU are synthetic thymidine analogs, which are incorporated into the DNA of replicating cells during the S-phase. Sequential intraperitoneal injection to timed pregnant female mice (100 µl per gram bodyweight ) were used to differentiate cells of different cell cycle stages in vivo(Nowakowski et al., 1989).

The number of cells that had left the cell cycle after a defined time (90 minutes) was used to quantify the total s-phase length ($T_S$) and the cell cycle legth ($T_C$). As described in Martynoga et al. (2005), IdU was injected first followed by BrdU. Cells going through S-phase at the beginning of the experiment incorporate IdU. After 1.5 h BrdU was injected, that in turn is incorporated in cells that are still in s-phase by the end of the experiment. After 30 min the pregnant mouse was sacrificed and the embryonic brains were analyzed by immunohistochemistry (Martynoga et al., 2005). A specific primary antibody that binds BrdU and an antibody that can recognize both BrdU and IdU were used for immunofluorescent staining (Shibui et al., 1989). Cortical and hippocampal areas were analyzed independently. The cell population that was only IdU-positive leaves s-phase (L-cells) by the time of BrdU injection. Cells that were double BrdU/IdU positive stay in s-phase (S-cells) by the end of the experiment. The number of cells in both cell populations could be used for Ts quantification: Ts = 1.5 h/(L-cells/S-cells). Ts can be further used in order to quantify Tc: Tc = Ts/(S-cells/P-cells). The total

| Substance / Stock solution | Amount | Note |
|---|---|---|
| Ammonium sulfate $(NH_4)_2SO_4$ | 70 g | solubility in water is 75 g / 100 ml at RT |
| EDTA (0.5 M, ph 8) | 4 ml | final concentration: 2 mM |
| Sodium citrate (1 M) | 2.5 ml | final concentration: 25 mM |
| Purified water | 93.5 ml | final volume: 100 ml |

Mix components, heat until completely dissolved, cool, and adjust pH to 5.2 using 1M $H_2So_4$.
Source: US patent US6204375B1 (Ambion Inc.)

**Table 16: RNA-stabilization buffer**

number of all actively proliferated cells (P-cells) was estimated by applying antibody against antigen identified by monoclonal antibody Ki 67 (Ki67). Cell cycle parameters were independently analyzed at two different embryonic stages, E13 and E15.

## 4.10 Transcriptome Analysis

### 4.10.1 Tissue Processing

Mice with the genotype *Neurod1*$^{flox/flox}$ × *Neurod2*$^{\underline{wt/null}}$ × *Neurod6*$^{cre/cre}$ were bred to generate Neurod1/2/6 *triple*-deficient embryos (genotype *Neurod1*$^{flox/flox}$ × *Neurod2*$^{\underline{null/null}}$ × *Neurod6*$^{cre/cre}$) and littermate controls (genotype *Neurod1*$^{flox/flox}$ × *Neurod2*$^{\underline{wt/null}}$ × *Neurod6*$^{cre/cre}$) — the genetic difference was only one allele of Neurod2. Embryos were collected 13 days following the observation of a vaginal plug (E13). Preparations were always performed at the same time (at 11 AM).

Embryonic tissue was immediately submerged in RNA-stabilizing solution (tab 16), brains were removed from the skull, the central neocortices of both hemispheres were manually dissected under a binocular microscope at RT, and the tissue was immediately snap frozen in liquid nitrogen and stored to a -80°C freezer.

### 4.10.2 RNA Extraction

Total RNA was separately extracted for every embryo; littermates were generally processed in parallel. The frozen tissue samples were submerged in 500 µl guanidinium thiocyanate (Trizol). The tissue was homogenized using a mechanical tissue homogenizer (Ultra Turrax); the device was cleaned with 3 % hydrogen peroxide and rinsed with water before each sample. The suspension was incubated for 5 min on ice to allow for the dissociation of nucleoprotein complexes. After adding 100 µl chloroform, the samples were mixed and kept on ice for another 2–3 min. After centrifugation at 12,000 g for 15 min at 4°C, the upper RNA-containing aqueous phase was transferred

| Pool no. | Genotype | | Litter no. | Concentration ng/µl | Quality 28s/18s | Quality RIN | Used µl | $H_2O$ µl | Final µl |
|---|---|---|---|---|---|---|---|---|---|
| **1** | Neurod1$^{flox/flox}$ | control | 1 | 308.14 | 1.5 | 9.8 | 3.25 | 11.67 | 20 |
| | Neurod2$^{\mathbf{wt/null}}$ | | 2 | 222.00 | 2.0 | 10.0 | 4.50 | | |
| | Neurod6$^{cre/cre}$ | | 3 | 254.89 | 2.0 | 10.0 | 3.92 | | |
| **2** | Neurod1$^{flox/flox}$ | TKO | 1 | 330.15 | 1.8 | 9.5 | 3.03 | 12.01 | 20 |
| | Neurod2$^{\mathbf{null/null}}$ | | 2 | 259.86 | 2.0 | 10.0 | 3.85 | | |
| | Neurod6$^{cre/cre}$ | | 3 | 195.00 | 1.9 | 10.0 | 5.13 | | |
| **3** | Neurod1$^{flox/flox}$ | control | 2 | 237.14 | 2.1 | 10.0 | 4.22 | 11.81 | 20 |
| | Neurod2$^{\mathbf{wt/null}}$ | | 4 | 293.23 | 2.0 | 10.0 | 3.41 | | |
| | Neurod6$^{cre/cre}$ | | 5 | 239.00 | 1.9 | 10.0 | 4.18 | | |
| **4** | Neurod1$^{flox/flox}$ | TKO | 2 | 233.00 | 1.9 | 10.0 | 4.29 | 17.86 | 20 |
| | Neurod2$^{\mathbf{null/null}}$ | | 4 | 242.11 | 1.9 | 10.0 | 4.13 | | |
| | Neurod6$^{cre/cre}$ | | 5 | 106.00 | 1.9 | 10.0 | 9.43 | | |
| **5** | Neurod1$^{flox/flox}$ | control | 4 | 372.75 | 2.0 | 10.0 | 2.68 | 8.89 | 20 |
| | Neurod2$^{\mathbf{wt/null}}$ | | 6 | 376.30 | 2.0 | 10.0 | 2.66 | | |
| | Neurod6$^{cre/cre}$ | | 7 | 282.00 | 1.9 | 10.0 | 3.55 | | |
| **6** | Neurod1$^{flox/flox}$ | TKO | 4 | 276.00 | 1.9 | 10.0 | 3.62 | 12.45 | 20 |
| | Neurod2$^{\mathbf{null/null}}$ | | 6 | 226.49 | 1.9 | 10.0 | 4.42 | | |
| | Neurod6$^{cre/cre}$ | | 7 | 226.49 | 2.0 | 10.0 | 4.42 | | |

**Table 17: RNA samples and pooling for sequencing**

**Pool:** Number of the RNA-pool; **Genotype:** Genotype of all embryos used for this pool; **Litter:** Number of the originating litter; pools were paired as #1/2, #3/4, #5/6; **Concentration:** RNA concentration as measured by capillary electrophoresis; **Quality:** Estimation of RNA-quality (28S/18S ribosomal RNA ratio; RNA integrity number); **Used**: Volume of RNA solution used from this embryo (equals 1 µg of RNA); **Water:** Volume of water added for dilution; **Final:** Final volume sent for sequencing (final concentration was 150 ng/µl).

to a new tube. For RNA precipitation, 250 µl isopropanol was added, the samples were inverted several times, were kept at -20°C for 2 h, were centrifuged at 12,000 g for 10 min at 4°C, and the supernatant was discarded. The RNA pellet was washed with 70 % ice-cold ethanol, centrifuged at 12,000 g for 10 min at 4°C, and the supernatant was removed. The RNA-containing pellets were dried for 10 min at RT and resuspended in 30 µl ultra-pure water. Small aliquots were removed for RNA quality control and quantification and the samples were immediately frozen at -80°C.

### 4.10.3 Quality Control and Pooling

For pre-analytic quality control, RNA extracts from every embryo were separately analyzed by capillary electrophoresis (Bioanalyzer, Agilent) by Ute Ungethüm at the *Labor für Funktionale Genomforschung* at Charité (LFGC). Based on these data, RNA samples were selected and pooled for sequencing at a final concentration of 150 ng/µl (tab 17).

### 4.10.4 RNA Sequencing

RNA sequencing was performed by Mirjam Feldkamp at the *Scientific Genomics Platform* (AG Chen) at the *Max-Delbrück-Center for Molecular Medicine* in Berlin. Pooled RNA samples were shipped on dry ice. PolyA-based mRNA enrichment and tagged library generation (TruSeq, Illumina) were performed using a fully automated pipetting device (epMotion, Eppendorf). The sample concentration was adjusted to 10 nM. All six samples were sequenced in a single lane of an *HiSeq sequencing device* (Illumina) with a read length of 101 bp plus tags. The sequencing depth was approximately 30 million reads per sample (tab 3). We received the raw reads as *fastq files* for data analysis.

### 4.10.5 Data Analysis

The raw sequencing data was analyzed by Ingo Bormuth using *Ocaml* and *R*. Raw reads were mapped to the mouse reference transcriptome as published by the National Center for Biotechnology Information (NCBI); the initial analysis was based on version 2015-01-12; the final re-analysis was based on version 2018-08-14. Base mismatches were not allowed. Predicted transcripts were not considered. Approximately 75 % of the reads could be fully mapped to the 41,514 annotated transcripts (tab 3). Read counts for genes with multiple annotated transcripts were considered proportionally.

Read counts were normalized using a variant of the *DESeq* algorithm (Dillies et al., 2013), which is based on the assumption that only a minority of transcripts is truly differentially expressed (DE) and that most inter-sample variations are due to technical error. The relative variance of raw reads over the six samples was calculated for every transcript. The average variance over all transcripts was considered the cutoff for differential expression, which resulted in 32,361 of the 49,451 annotated transcripts (65.5 %) being considered *not differentially expressed*. For each of the six samples, the average read count of those stably expressed transcripts (column *Stable* in tab 3) was used as a normalization factor for all raw reads (normalized reads = raw reads / average reads of all stable transcripts). This affected the average read count per sample (columns *Raw* vs *Norm* in tab 3) but not the mean values over all samples (both 1,309).

Absolute expression levels of any given transcript in Neurod1/2/6 *triple*-deficient ($Level_{TKO}$) or control tissue ($Level_{Ctrl}$) were estimated using the number of normalized reads per kbp transcript length (averaged over the three biological replicates for each genotype). The higher one of the two values was considered the genotype-independent overall expression level (column *Level* in tab 4). Relative changes in expression levels were calculated as $Change = \frac{Level_{TKO} - Level_{Ctrl}}{max(Level_{TKO}, Level_{Ctrl})} \times 100$. This representation is symmetric for up- and down-regulation; the smallest possible value is -100 % (maximum down-regulation, e.g. from any number to 0 reads); the largest possible value is +100 %

(maximum up-regulation, e.g. from 0 to any number of reads); the central value is 0 (no change of expression). The more commonly used *fold change* (FC) can be calculated from that value by $FC = \frac{100}{100 - Change}$.

The statistical significance of expression changes was calculated using two-tailed paired student's t-tests over the six paired sample pools (n=3+3). The resulting p-values were visualized as *** for p<0.001; ** for p<0.01; and * for p<0.05. Every transcript was rated using the formula $Rating = \sqrt{Level} \times Change^2 \times p^2$. The resulting values ranged from 0 to 2,720,584,839 (mean: 13,180,254; median: 1,670,434). This rating was used to generate ranked lists of all transcripts (column *Rank* in tab 4).

### 4.10.6 Sex-Correction

Sex-correction was based on six sex-chromosomal reference genes (asterisks in the first column of tab 4) that had previously been shown to be sex-specifically expressed in the cerebral cortex of newborn mice (Armoskus et al., 2014). The female-specific reference genes were Xist (2 transcripts with 17,918 and 12,250 kbp), Tsix (1 transcript with 4,306 kbp), and Kdm6a (2 transcripts with 5,918 and 6,935 kbp). The male-specific reference genes were Ddx3y (1 transcript with 4,640 kbp), Eif2s3y (2 transcripts with 1784 and 1689 kbp), and Kdm5d (1 transcript with 5471 kbp).

The normalized numbers of reads for the nine reference transcripts in each of the six RNA-pools were used to calculate a reference pattern for typical sex-specific expression (fig 21). For each of the 41,513 annotated transcripts, the relative pattern of normalized reads per RNA-pool was calculated and correlated to the sex-specific reference pattern individually for both genotypes. Hight correlation was interpreted as prediction of sexual dimorphic expression (+100: female-specific; -100: male-specific; 0: sex-independent in column *Sex* of tab 4ff).

For sex correction, the sex-specific reference pattern was subtracted from the normalized reads in proportion to the predicted degree of sexually dimorphic expression and to the average number of reads.

## 4.11 Manuscript Processing and Layout

THIS DOCUMENT was processed in *LyX-2.3* and typeset using *TeX* with *LaTeX* and *KOMA-Script* from the *TeX-Live* distribution. References were managed using *Zotero-5*. Images were edited using *GIMP-2.10* and *ImageJ-1.53*. Statistical visualizations were generated using *R-3.5*. Composite figures were created using *Scribus-1.5*. Workflow and layout templates were adopted from Bormuth (2016). Spelling and grammar were corrected using *LanguageTool*-5 the AI-based online service *Grammarly*.

# Bibliography


Acehan D, Jiang X, Morgan DG, Heuser JE, Wang X & Akey CW, *Three-dimensional structure of the apoptosome: implications for assembly, procaspase-9 binding, and activation*. Mol Cell (2002): 9 (2), 423–432. Cited on p 21.

Adams JM, *Ways of dying: multiple pathways to apoptosis*. Genes Dev (2003): 17 (20), 2481–2495. Cited on p 22 and 23.

Adams JM & Cory S, *The Bcl-2 protein family: arbiters of cell survival*. Science (1998): 281 (5381), 1322–1326. Cited on p 48.

Alberts B, Johnson A, Lewis J, Raff M, Roberts K & Walter P, *Molecular Biology of the Cell*. Garland Science 2002, 4th ed. Cited on p 19.

Alcamo EA, Chirivella L, Dautzenberg M, Dobreva G, Fariñas I, Grosschedl R & McConnell SK, *Satb2 regulates callosal projection neuron identity in the developing cerebral cortex*. Neuron (2008): 57 (3), 364–77. Cited on p 18.

Allen SJ & Dawbarn D, *Clinical relevance of the neurotrophins and their receptors*. Clinical Science (2006): 110 (2), 175–191. Cited on p 23.

Anthony TE, Klein C, Fishell G & Heintz N, *Radial glia serve as neuronal progenitors in all regions of the central nervous system*. Neuron (2004): 41 (6), 881–890. Cited on p 14.

Arlotta P, Molyneaux BJ, Chen J, Inoue J, Kominami R & Macklis JD, *Neuronal subtype-specific genes that control corticospinal motor neuron development in vivo*. Neuron (2005): 45 (2), 207–21. Cited on p 18.

Armoskus C, Moreira D, Bollinger K, Jimenez O, Taniguchi S & Tsai HW, *Identification of sexually dimorphic genes in the neonatal mouse cortex and hippocampus*. Brain Res (2014): 1562, 23–38. Cited on p 56 and 102.

Arnold HH & Winter B, *Muscle differentiation: more complexity to the network of myogenic regulators*. Curr Opin Genet Dev (1998): 8 (5), 539–544. Cited on p 28.

Arnold SJ, Huang GJ, Cheung AFP, Era T, Nishikawa SI, Bikoff EK, Molnár Z, Robertson EJ & Groszer M, *The T-box transcription factor Eomes/Tbr2 regulates neurogenesis in the cortical subventricular zone*. Genes Dev (2008): 22 (18), 2479–2484. Cited on p 75.

Assadi AH, Zhang G, Beffert U, McNeil RS, Renfro AL, Niu S, Quattrocchi CC, Antalffy BA, Sheldon M, Armstrong DD et al., *Interaction of reelin signaling and Lis1 in brain development*. Nat Genet (2003): 35 (3), 270–276. Cited on p 17.

Baranek C, Dittrich M, Parthasarathy S, Bonnon CG, Britanova O, Lanshakov D, Boukhtouche F, Sommer JE, Colmenares C, Tarabykin V et al., *Protooncogene Ski cooperates with the chromatin-remodeling factor Satb2 in specifying callosal neurons*. Proc Natl Acad Sci USA (2012): 109 (9), 3546–3551. Cited on p 37 and 78.

Bayer SA, Altman J, Russo RJ, Dai XF & Simmons JA, *Cell migration in the rat embryonic neocortex*. J Comp Neurol (1991): 307 (3), 499–516. Cited on p 17.

Bear MF, Connors BW & Paradiso MA, *Neuroscience: exploring the brain*. Williams & Wilkins, Baltimore 1996. Cited on p 14.

Bedogni F, Hodge RD, Elsen GE, Nelson BR, Daza RAM, Beyer RP, Bammler TK, Rubenstein JLR & Hevner RF, *Tbr1 regulates regional and laminar identity of postmitotic neurons in developing neocortex*. Proc Natl Acad Sci USA (2010): 107 (29), 13129–13134. Cited on p 37.

Benn SC & Woolf CJ, *Adult neuron survival strategies–slamming on the brakes*. Nat Rev Neurosci (2004): 5 (9), 686–700. Cited on p 21.

Bertrand N, Castro DS & Guillemot F, *Proneural genes and the specification of neural cell types*. Nat Rev Neurosci (2002): 3 (7), 517–530. Cited on p 25.

Blake JA, Bult CJ, Eppig JT, Kadin JA, Richardson JE & Mouse Genome Database Group, *The Mouse Genome Database: integration of and access to knowledge about the laboratory mouse*. Nucleic Acids Res (2014): 42 (Database issue), D810–817. Cited on p 120.

Blaschke AJ, Staley K & Chun J, *Widespread programmed cell death in proliferative and postmitotic regions of the fetal cerebral cortex*. Development (1996): 122 (4), 1165–1174. Cited on p 20 and 34.

Blatt NB & Glick GD, *Signaling pathways and effector mechanisms pre-programmed cell death*. Bioorg Med Chem (2001): 9 (6), 1371–1384. Cited on p 21.

Böhm I & Schild H, *Apoptosis: The Complex Scenario for a Silent Cell Death*. Molecular Imaging & Biology (2003): 5 (1), 2–14. Cited on p 21.

Borisov AY, Shtark OY, Zhukov VA, Nemankin TA, Naumkina TS, Pinaev AG, Akhtemova GA, Voroshilova VA, Ovchinnikova ES, Rychagova TS et al., *Interaction of legumes with beneficial soil microorganisms: From plant genes to varieties*. Agricultural Biology (2011): 2011 (3), 41–47. Cited on p 128.

Bormuth I, *Roles of bHLH Transcription Factors Neurod1, Neurod2 and Neurod6 in Cerebral Cortex Development and Commissure Formation*. Ph.D. thesis (2016). Cited on p 26, 27, 28, 29, 30, 31, 35, 36, 59, 66, 76, 78, 83, 84, 85, 86, and 102.

Bormuth I, Yan K, Yonemasu T, Gummert M, Zhang M, Wichert S, Grishina O, Pieper A, Zhang W, Goebbels S et al., *Neuronal basic helix-loop-helix proteins Neurod2/6 regulate cortical commissure formation before midline interactions*. J Neurosci (2013): 33 (2), 641–651. Cited on p 26, 27, 28, 46, 57, 80, 83, 84, and 128.

Bozyczko-Coyne D, O'Kane TM, Wu ZL, Dobrzanski P, Murthy S, Vaught JL & Scott RW, *CEP-1347/KT-7515, an inhibitor of SAPK/JNK pathway activation, promotes survival and blocks multiple events associated with Abeta-induced cortical neuron apoptosis*. J Neurochem (2001): 77 (3), 849–863. Cited on p 24 and 81.

Bradshaw RA, Blundell TL, Lapatto R, McDonald NQ & Murray-Rust J, *Nerve growth factor revisited*. Trends Biochem Sci (1993): 18 (2), 48–52. Cited on p 23.

Britanova O, de Juan Romero C, Cheung A, Kwan KY, Schwark M, Gyorgy A, Vogel T, Akopov S, Mitkovski M, Agoston D et al., *Satb2 is a postmitotic determinant for upper-layer neuron specification in the neocortex*. Neuron (2008): 57 (3), 378–92. Cited on p 18 and 37.

Bröhl D, Strehle M, Wende H, Hori K, Bormuth I, Nave KA, Müller T & Birchmeier C, *A transcriptional network coordinately determines transmitter and peptidergic fate in the dorsal spinal cord*. Dev Biol (2008): 322 (2), 381–393. Cited on p 28.

Bulfone A, Smiga SM, Shimamura K, Peterson A, Puelles L & Rubenstein JL, *T-brain-1: a homolog of Brachyury whose expression defines molecularly distinct domains within the cerebral cortex*. Neuron (1995): 15 (1), 63–78. Cited on p 18.

Bull SJ, *Mechanisms Promoting Myelin Formation and Maintenance Under Normal and Pathological Conditions*. Biol. Diss. Montreal, Canada, Montreal, Canada 2011. Cited on p 13.

Bunk EC, Ertaylan G, Ortega F, Pavlou MA, Gonzalez Cano L, Stergiopoulos A, Safaiyan S, Völs S, van Cann M, Politis PK et al., *Prox1 Is Required for Oligodendrocyte Cell Identity in Adult Neural Stem Cells of the Subventricular Zone*. Stem Cells (2016): 34 (8), 2115–2129. Cited on p 79.

Buss RR, Sun W & Oppenheim RW, *Adaptive roles of programmed cell death during nervous system development*. Annu Rev Neurosci (2006): 29, 1–35. Cited on p 20 and 44.

Cameron S, Clark SG, McDermott JB, Aamodt E & Horvitz HR, *PAG-3, a Zn-finger transcription factor, determines neuroblast fate in C. elegans*. Development (2002): 129 (7), 1763–1774. Cited on p 24.

Caviness VS & Takahashi T, *Proliferative events in the cerebral ventricular zone*. Brain Dev (1995): 17 (3), 159–163. Cited on p 15.

Cecconi F, Alvarez-Bolado G, Meyer BI, Roth KA & Gruss P, *Apaf1 (CED-4 homolog) regulates programmed cell death in mammalian development*. Cell (1998): 94 (6), 727–737. Cited on p 50.

Chautan M, Chazal G, Cecconi F, Gruss P & Golstein P, *Interdigital cell death can occur through a necrotic and caspase-independent pathway*. Curr Biol (1999): 9 (17), 967–970. Cited on p 20.

Chen B, Schaevitz LR & McConnell SK, *Fezl regulates the differentiation and axon targeting of layer 5 subcortical projection neurons in cerebral cortex*. Proc Natl Acad Sci USA (2005): 102 (47), 17184–9. Cited on p 78.

Chen B, Wang SS, Hattox AM, Rayburn H, Nelson SB & McConnell SK, *The Fezf2-Ctip2 genetic pathway regulates the fate choice of subcortical projection neurons in the developing cerebral cortex*. Proc Natl Acad Sci U S A (2008): 105 (32), 11382–7. Cited on p 78.

Chen G & Goeddel DV, *TNF-R1 signaling: a beautiful pathway*. Science (2002): 296 (5573), 1634–1635. Cited on p 21.

Cherry TJ, Wang S, Bormuth I, Schwab M, Olson J & Cepko CL, *NeuroD factors regulate cell fate and neurite stratification in the developing retina*. J Neurosci (2011): 31 (20), 7365–7379. Cited on p 28.

Chiaramello A, Neuman T, Peavy DR & Zuber MX, *The GAP-43 gene is a direct downstream target of the basic helix-loop-helix transcription factors*. J Biol Chem (1996): 271 (36), 22035–22043. Cited on p 57.

Chiu CY, Leng S, Martin KA, Kim E, Gorman S & Duhl DM, *Cloning and characterization of T-cell lymphoma invasion and metastasis 2 (TIAM2), a novel guanine nucleotide exchange factor related to TIAM1*. Genomics (1999): 61 (1), 66–73. Cited on p 71.

Clarke PG, *Developmental cell death: morphological diversity and multiple mechanisms*. Anat Embryol (1990): 181 (3), 195–213. Cited on p 19.

Cooper JA, *Molecules and mechanisms that regulate multipolar migration in the intermediate zone*. Front Cell Neurosci (2014): 8, 386. Cited on p 15.

Cordes SP & Barsh GS, *The mouse segmentation gene kr encodes a novel basic domain-leucine zipper transcription factor*. Cell (1994): 79 (6), 1025–1034. Cited on p 71.

Creutzfeldt OD, *Cortex Cerebri: Leistung, strukturelle und funktionelle Organisation der Hirnrinde*. Springer-Verlag, Berlin Heidelberg 1983. Cited on p 13.

Czabotar PE, Lessene G, Strasser A & Adams JM, *Control of apoptosis by the BCL-2 protein family: implications for physiology and therapy*. Nat Rev Mol Cell Biol (2014): 15 (1), 49–63. Cited on p 22 and 48.

De Juan Romero C & Borrell V, *Coevolution of radial glial cells and the cerebral cortex*. Glia (2015): 63 (8), 1303–1319. Cited on p 16.

Dekkers MP, Nikoletopoulou V & Barde YA, *Death of developing neurons: New insights and implications for connectivity*. J Cell Biol (2013): 203 (3), 385–393. Cited on p 20.

Dekkers MPJ & Barde YA, *Programmed Cell Death in Neuronal Development*. Science (2013): 340 (6128), 39–41. Cited on p 47.

Desai AR & McConnell SK, *Progressive restriction in fate potential by neural progenitors during cerebral cortical development*. Development (2000): 127 (13), 2863–2872. Cited on p 17.

Dijkers PF, Medema RH, Lammers JW, Koenderman L & Coffer PJ, *Expression of the pro-apoptotic Bcl-2 family member Bim is regulated by the forkhead transcription factor FKHR-L1*. Curr Biol (2000): 10 (19), 1201–1204. Cited on p 24.

Dillies MA, Rau A, Aubert J, Hennequet-Antier C, Jeanmougin M, Servant N, Keime C, Marot G, Castel D, Estelle J et al., *A comprehensive evaluation of normalization methods for Illumina high-throughput RNA sequencing data analysis*. Brief Bioinformatics (2013): 14 (6), 671–683. Cited on p 101.

Dumonteil E, Laser B, Constant I & Philippe J, *Differential regulation of the glucagon and insulin I gene promoters by the basic helix-loop-helix transcription factors E47 and BETA2*. J Biol Chem (1998): 273 (32), 19945–19954. Cited on p 64.

Eizenberg O, Faber-Elman A, Gottlieb E, Oren M, Rotter V & Schwartz M, *Direct involvement of p53 in programmed cell death of oligodendrocytes*. EMBO J (1995): 14 (6), 1136–1144. Cited on p 50.

Englund C, Fink A, Lau C, Pham D, Daza RAM, Bulfone A, Kowalczyk T & Hevner RF, *Pax6, Tbr2, and Tbr1 are expressed sequentially by radial glia, intermediate progenitor cells, and postmitotic neurons in developing neocortex*. J Neurosci (2005): 25 (1), 247–251. Cited on p 17 and 18.

Epifanova E, Babaev A, Newman AG & Tarabykin V, *Role of Zeb2/Sip1 in neuronal development*. Brain Res (2018): . Cited on p 73 and 78.

Epifanova E, Salina V, Lajkó D, Textoris-Taube K, Naumann T, Bormuth O, Bormuth I, Horan S, Schaub T, Borisova E et al., *Adhesion dynamics in the neocortex determine the start of migration and the post-migratory orientation of neurons*. Sci Adv (2021): 7 (27), eabf1973. Cited on p 128.

Feng L, Xie X, Joshi PS, Yang Z, Shibasaki K, Chow RL & Gan L, *Requirement for Bhlhb5 in the specification of amacrine and cone bipolar subtypes in mouse retina*. Development (2006): 133 (24), 4815–4825. Cited on p 82.

Finlay BL & Pallas SL, *Control of cell number in the developing mammalian visual system*. Progress in Neurobiology (1989): 32 (3), 207–234. Cited on p 20.

Fishell G & Hanashima C, *Pyramidal neurons grow up and change their mind*. Neuron (2008): 57 (3), 333–338. Cited on p 15.

Fishell G & Kriegstein AR, *Neurons from radial glia: the consequences of asymmetric inheritance*. Curr Opin Neurobiol (2003): 13 (1), 34–41. Cited on p 14.

Flora A, Garcia JJ, Thaller C & Zoghbi HY, *The E-protein Tcf4 interacts with Math1 to regulate differentiation of a specific subset of neuronal progenitors*. Proc Natl Acad Sci USA (2007): 104 (39), 15382–15387. Cited on p 24.

Franco SJ, Martinez-Garay I, Gil-Sanz C, Harkins-Perry SR & Müller U, *Reelin Regulates Cadherin Function via Dab1/Rap1 to Control Neuronal Migration and Lamination in the Neocortex*. Neuron (2011): 69 (3), 482–497. Cited on p 17, 41, and 80.

Franklin A, Kao A, Tapscott S & Unis A, *NeuroD homologue expression during cortical development in the human brain*. J Child Neurol (2001): 16 (11), 849–853. Cited on p 25.

Frantz GD & McConnell SK, *Restriction of late cerebral cortical progenitors to an upper-layer fate*. Neuron (1996): 17 (1), 55–61. Cited on p 17.

Fuchs Y & Steller H, *Programmed cell death in animal development and disease*. Cell (2011): 147 (4), 742–758. Cited on p 20.

Fünfschilling U & Reichardt LF, *Cre-mediated recombination in rhombic lip derivatives*. Genesis (2002): 33 (4), 160–169. Cited on p 53.

Gaitanos TN, Koerner J & Klein R, *Tiam-Rac signaling mediates trans-endocytosis of ephrin receptor EphB2 and is important for cell repulsion*. J Cell Biol (2016): 214 (6), 735–752. Cited on p 71.

Galluzzi L, Vitale I, Aaronson SA, Abrams JM, Adam D, Agostinis P, Alnemri ES, Altucci L, Amelio I, Andrews DW et al., *Molecular mechanisms of cell death: recommendations of the Nomenclature Committee on Cell Death 2018*. Cell Death Differ (2018): 25 (3), 486–541. Cited on p 19.

Gaspard N, Bouschet T, Hourez R, Dimidschstein J, Naeije G, van den Ameele J, Espuny-Camacho I, Herpoel A, Passante L, Schiffmann SN et al., *An intrinsic mechanism of corticogenesis from embryonic stem cells*. Nature (2008): 455 (7211), 351–357. Cited on p 44.

Gaspard N, Gaillard A & Vanderhaeghen P, *Making cortex in a dish: In vitro corticopoiesis from embryonic stem cells*. Cell Cycle (2009): 8 (16), 2491–2496. Cited on p 44.

Gavathiotis E, Suzuki M, Davis ML, Pitter K, Bird GH, Katz SG, Tu HC, Kim H, Cheng EHY, Tjandra N et al., *BAX activation is initiated at a novel interaction site*. Nature (2008): 455 (7216), 1076–1081. Cited on p 22.

Gibson L, Holmgreen SP, Huang DC, Bernard O, Copeland NG, Jenkins NA, Sutherland GR, Baker E, Adams JM & Cory S, *bcl-w, a novel member of the bcl-2 family, promotes cell survival*. Oncogene (1996): 13 (4), 665–675. Cited on p 48.

Giguère V, *Orphan nuclear receptors: from gene to function*. Endocr Rev (1999): 20 (5), 689–725. Cited on p 18.

Gilmore EC & Herrup K, *Cortical development: receiving reelin*. Curr Biol (2000): 10 (4), R162–166. Cited on p 17.

Goebbels S, *Zelltyp-spezifische Expression der Rekombinase Cre im Nervensystem der Maus*. Biol. Diss. Heidelberg 2002. Cited on p 26.

Goebbels S, Bode U, Pieper A, Funfschilling U, Schwab MH & Nave KA, *Cre/loxP-mediated inactivation of the bHLH transcription factor gene NeuroD/BETA2*. Genesis (2005): 42 (4), 247–52. Cited on p 27, 53, 84, and 86.

Goebbels S, Bormuth I, Bode U, Hermanson O, Schwab MH & Nave KA, *Genetic targeting of principal neurons in neocortex and hippocampus of NEX-Cre mice*. Genesis (2006): 44 (12), 611–621. Cited on p 26, 27, 36, 45, 53, 84, and 86.

Golstein P, *Cell Death in Us and Others*. Science (1998): 281 (5381), 1283–1283. Cited on p 19.

Goodsell DS, *The Molecular Perspective: Caspases*. The Oncologist (2000): 5 (5), 435–436. Cited on p 22.

Grabrucker S, Haderspeck JC, Sauer AK, Kittelberger N, Asoglu H, Abaei A, Rasche V, Schön M, Boeckers TM & Grabrucker AM, *Brain Lateralization in Mice Is Associated with Zinc Signaling and Altered in Prenatal Zinc Deficient Mice That Display Features of Autism Spectrum Disorder*. Front Mol Neurosci (2017): 10, 450. Cited on p 54.

Grimes HL, Gilks CB, Chan TO, Porter S & Tsichlis PN, *The Gfi-1 protooncoprotein represses Bax expression and inhibits T-cell death*. Proc Natl Acad Sci USA (1996): 93 (25), 14569–14573. Cited on p 81.

Gummert M, *Vergleichende Expressionsanalyse basischer Helix-Loop-Helix Proteine der NeuroD-Subfamilie im Zentralnervensystem der Maus*. Biol. Diss. Göttingen 2003. Cited on p 26.

Gunnersen JM, Kim MH, Fuller SJ, De Silva M, Britto JM, Hammond VE, Davies PJ, Petrou S, Faber ESL, Sah P et al., *Sez-6 proteins affect dendritic arborization patterns and excitability of cortical pyramidal neurons*. Neuron (2007): 56 (4), 621–639. Cited on p 72.

Haire MF & Chiaramello A, *Transient expression of the basic helix-loop-helix protein NSCL-2 in the mouse cerebellum during postnatal development*. Molecular Brain Research (1996): 36 (1), 174–178. Cited on p 70.

Han W, Kwan KY, Shim S, Lam MMS, Shin Y, Xu X, Zhu Y, Li M & Sestan N, *TBR1 directly represses Fezf2 to control the laminar origin and development of the corticospinal tract*. Proc Natl Acad Sci USA (2011): 108 (7), 3041–3046. Cited on p 37.

Happo L, Strasser A & Cory S, *BH3-only proteins in apoptosis at a glance*. J Cell Sci (2012): 125 (Pt 5), 1081–1087. Cited on p 22.

Harris CA & Johnson EM, *BH3-only Bcl-2 family members are coordinately regulated by the JNK pathway and require Bax to induce apoptosis in neurons*. The Journal of Biological Chemistry (2001): 276 (41), 37754–37760. Cited on p 24, 48, and 81.

Hayashi K, Kubo KI, Kitazawa A & Nakajima K, *Cellular dynamics of neuronal migration in the hippocampus*. Front Neurosci (2015): 9, 135. Cited on p 32.

Hempstead BL, *Dissecting the diverse actions of pro- and mature neurotrophins*. Curr Alzheimer Res (2006): 3 (1), 19–24. Cited on p 23.

Hengartner MO, *The biochemistry of apoptosis*. Nature (2000): 407 (6805), 770–776. Cited on p 22.

Hevner RF, *Intermediate progenitors and Tbr2 in cortical development*. J Anat (2019): 235 (3), 616–625. Cited on p 33 and 75.

Hevner RF, Shi L, Justice N, Hsueh Y, Sheng M, Smiga S, Bulfone A, Goffinet AM, Campagnoni AT & Rubenstein JL, *Tbr1 regulates differentiation of the preplate and layer 6*. Neuron (2001): 29 (2), 353–66. Cited on p 18.

Hiesberger T, Trommsdorff M, Howell BW, Goffinet A, Mumby MC, Cooper JA & Herz J, *Direct binding of Reelin to VLDL receptor and ApoE receptor 2 induces tyrosine phosphorylation of disabled-1 and modulates tau phosphorylation*. Neuron (1999): 24 (2), 481–489. Cited on p 17.

Hinds MG, Smits C, Fredericks-Short R, Risk JM, Bailey M, Huang DCS & Day CL, *Bim, Bad and Bmf: intrinsically unstructured BH3-only proteins that undergo a localized conformational change upon binding to prosurvival Bcl-2 targets*. Cell Death Differ (2007): 14 (1), 128–136. Cited on p 22.

Hirota Y & Nakajima K, *Control of Neuronal Migration and Aggregation by Reelin Signaling in the Developing Cerebral Cortex*. Front Cell Dev Biol (2017): 5, 40. Cited on p 18.

Hofer M, Pagliusi SR, Hohn A, Leibrock J & Barde YA, *Regional distribution of brain-derived neurotrophic factor mRNA in the adult mouse brain*. EMBO J (1990): 9 (8), 2459–2464. Cited on p 23.

Howell BW, Herrick TM & Cooper JA, *Reelin-induced tyrosine [corrected] phosphorylation of disabled 1 during neuronal positioning*. Genes Dev (1999): 13 (6), 643–648. Cited on p 17.

Hsieh AL & Dang CV, *MYC, Metabolic Synthetic Lethality, and Cancer*. Recent Results Cancer Res (2016): 207, 73–91. Cited on p 24.

Huang DC & Strasser A, *BH3-Only proteins-essential initiators of apoptotic cell death*. Cell (2000): 103 (6), 839–842. Cited on p 24.

Hutt KJ, *The role of BH3-only proteins in apoptosis within the ovary*. Reproduction (2015): 149 (2), R81–R89. Cited on p 22 and 48.

Imaizumi K, Tsuda M, Imai Y, Wanaka A, Takagi T & Tohyama M, *Molecular Cloning of a Novel Polypeptide, DP5, Induced during Programmed Neuronal Death*. J Biol Chem (1997): 272 (30), 18842–18848. Cited on p 24 and 61.

Imaizumi K, Benito A, Kiryu-Seo S, Gonzalez V, Inohara N, Leiberman AP, Kiyama H & Nuñez G, *Critical Role for DP5/Harakiri, a Bcl-2 Homology Domain 3-Only Bcl-2 Family Member, in Axotomy-Induced Neuronal Cell Death*. J Neurosci (2004): 24 (15), 3721–3725. Cited on p 61.

Ince-Dunn G, Hall BJ, Hu SC, Ripley B, Huganir RL, Olson JM, Tapscott SJ & Ghosh A, *Regulation of thalamocortical patterning and synaptic maturation by NeuroD2*. Neuron (2006): 49 (5), 683–95. Cited on p 26, 28, and 64.

Inoue M, Kuroda T, Honda A, Komabayashi-Suzuki M, Komai T, Shinkai Y & Mizutani Ki, *Prdm8 regulates the morphological transition at multipolar phase during neocortical development*. PLoS ONE (2014): 9 (1), e86356. Cited on p 17, 66, and 76.

Inoue M, Iwai R, Yamanishi E, Yamagata K, Komabayashi-Suzuki M, Honda A, Komai T, Miyachi H, Kitano S, Watanabe C et al., *Deletion of Prdm8 impairs development of upper-layer neocortical neurons*. Genes Cells (2015): 20 (9), 758–770. Cited on p 66 and 76.

Ip YT & Davis RJ, *Signal transduction by the c-Jun N-terminal kinase (JNK)–from inflammation to development*. Curr Opin Cell Biol (1998): 10 (2), 205–219. Cited on p 81.

Itkin-Ansari P, Marcora E, Geron I, Tyrberg B, Demeterco C, Hao E, Padilla C, Ratineau C, Leiter A, Lee JE et al., *NeuroD1 in the endocrine pancreas: localization and dual function as an activator and repressor*. Dev Dyn (2005): 233 (3), 946–953. Cited on p 65.

Iwai R, Tabata H, Inoue M, Nomura Ki, Okamoto T, Ichihashi M, Nagata Ki & Mizutani Ki, *A Prdm8 target gene Ebf3 regulates multipolar-to-bipolar transition in migrating neocortical cells*. Biochemical and Biophysical Research Communications (2018): 495 (1), 388–394. Cited on p 17 and 80.

Iwasaki K, Chung Eh, Egashira N, Hatip-Al-Khatib I, Mishima K, Egawa T, Irie K & Fujiwara M, *Non-NMDA mechanism in the inhibition of cellular apoptosis and memory impairment induced by repeated ischemia in rats*. Brain Research (2004): 995 (1), 131–139. Cited on p 20.

Jones EG, *Viewpoint: the core and matrix of thalamic organization*. Neuroscience (1998): 85 (2), 331–345. Cited on p 13.

Joshi PS, Molyneaux BJ, Feng L, Xie X, Macklis JD & Gan L, *Bhlhb5 regulates the postmitotic acquisition of area identities in layers II-V of the developing neocortex*. Neuron (2008): 60 (2), 258–272. Cited on p 25, 65, 76, and 82.

Kalinec GM, Fernandez-Zapico ME, Urrutia R, Esteban-Cruciani N, Chen S & Kalinec F, *Pivotal role of Harakiri in the induction and prevention of gentamicin-induced hearing loss*. Proc Natl Acad Sci U S A (2005): 102 (44), 16019–16024. Cited on p 63 and 97.

Kandel ER, Schwartz JH & Jessell TM, *Principles of Neural Science*. Mcgraw-Hill Professional 2000, 4th ed. Cited on p 12, 13, 14, and 23.

Karlebach G & Francks C, *Lateralization of gene expression in human language cortex*. Cortex (2015): 67, 30–36. Cited on p 54.

Kataoka K, Fujiwara KT, Noda M & Nishizawa M, *MafB, a new Maf family transcription activator that can associate with Maf and Fos but not with Jun*. Mol Cell Biol (1994): 14 (11), 7581–7591. Cited on p 71.

Kaya-Aksoy E, Cingoz A, Senbabaoglu F, Seker F, Sur-Erdem I, Kayabolen A, Lokumcu T, Sahin GN, Karahuseyinoglu S & Bagci-Onder T, *The pro-apoptotic Bcl-2 family member Harakiri (HRK) induces cell death in glioblastoma multiforme*. Cell Death Discov (2019): 5. Cited on p 81.

Kerr JF, Wyllie AH & Currie AR, *Apoptosis: a basic biological phenomenon with wide-ranging implications in tissue kinetics*. Br J Cancer (1972): 26 (4), 239–257. Cited on p 19.

Kim WY, *NeuroD1 is an upstream regulator of NSCL1*. Biochemical and Biophysical Research Communications (2012): 419 (1), 27–31. Cited on p 25.

Konishi Y, Aoki T, Ohkawa N, Matsu-ura T, Mikoshiba K & Tamura Ta, *Identification of the C-terminal activation domain of the NeuroD-related factor (NDRF)*. Nucleic Acids Res (2000): 28 (12), 2406–2412. Cited on p 26.

Ku RY & Torii M, *New Molecular Players in the Development of Callosal Projections*. Cells (2020): 10 (1), E29. Cited on p 78.

Kumar S & Cakouros D, *Transcriptional control of the core cell-death machinery*. Trends Biochem Sci (2004): 29 (4), 193–199. Cited on p 23 and 81.

Kume H, Maruyama K, Tomita T, Iwatsubo T, Saido TC & Obata K, *Molecular cloning of a novel basic helix-loop-helix protein from the rat brain*. Biochem Biophys Res Commun (1996): 219 (2), 526–30. Cited on p 25.

Kuwana T, Bouchier-Hayes L, Chipuk JE, Bonzon C, Sullivan BA, Green DR & Newmeyer DD, *BH3 Domains of BH3-Only Proteins Differentially Regulate Bax-Mediated Mitochondrial Membrane Permeabilization Both Directly and Indirectly*. Molecular Cell (2005): 17 (4), 525–535. Cited on p 22.

Kvansakul M, Yang H, Fairlie WD, Czabotar PE, Fischer SF, Perugini MA, Huang DCS & Colman PM, *Vaccinia virus anti-apoptotic F1l is a novel Bcl-2-like domain-swapped dimer that binds a highly selective subset of BH3-containing death ligands*. Cell Death Differ (2008): 15 (10), 1564–1571. Cited on p 22.

Lai T, Jabaudon D, Molyneaux BJ, Azim E, Arlotta P, Menezes JRL & Macklis JD, *SOX5 controls the sequential generation of distinct corticofugal neuron subtypes*. Neuron (2008): 57 (2), 232–47. Cited on p 18 and 37.

Lam YW & Sherman SM, *Functional Organization of the Somatosensory Cortical Layer 6 Feedback to the Thalamus*. Cereb Cortex (2010): 20 (1), 13–24. Cited on p 13.

Lancaster MA, Renner M, Martin CA, Wenzel D, Bicknell LS, Hurles ME, Homfray T, Penninger JM, Jackson AP & Knoblich JA, *Cerebral organoids model human brain development and microcephaly*. Nature (2013): 501 (7467), 373–379. Cited on p 44.

Lee JE, Hollenberg SM, Snider L, Turner DL, Lipnick N & Weintraub H, *Conversion of Xenopus ectoderm into neurons by NeuroD, a basic helix-loop-helix protein*. Science (1995): 268 (5212), 836–844. Cited on p 25.

Lee SK & Pfaff SL, *Synchronization of Neurogenesis and Motor Neuron Specification by Direct Coupling of bHLH and Homeodomain Transcription Factors*. Neuron (2003): 38 (5), 731–745. Cited on p 24.

LePage KT, Dickey RW, Gerwick WH, Jester EL & Murray TF, *On the use of neuro-2a neuroblastoma cells versus intact neurons in primary culture for neurotoxicity studies*. Crit Rev Neurobiol (2005): 17 (1), 27–50. Cited on p 63.

Li Y, *Functional analysis of NeuroD2 and NeuroD6 in neuronal differentiation during cerebral cortical development*. Ph.D. thesis, Charié - Berlin Medical University, Berlin (2017). Cited on p 29, 75, and 76.

Lin CH, Stoeck J, Ravanpay AC, Guillemot F, Tapscott SJ & Olson JM, *Regulation of NeuroD2 expression in mouse brain*. Dev Biol (2004): 265 (1), 234–45. Cited on p 26.

Lin CH, Hansen S, Wang Z, Storm DR, Tapscott SJ & Olson JM, *The dosage of the NeuroD2 transcription factor regulates amygdala development and emotional learning*. Proc Natl Acad Sci U S A (2005): 102 (41), 14877–82. Cited on p 26, 28, and 29.

Lindsten T & Thompson CB, *Cell death in the absence of Bax and Bak*. Cell Death Differ (2006): 13 (8), 1272–1276. Cited on p 20.

Liu M, Pleasure SJ, Collins AE, Noebels JL, Naya FJ, Tsai MJ & Lowenstein DH, *Loss of BETA2/NeuroD leads to malformation of the dentate gyrus and epilepsy*. Proc Natl Acad Sci U S A (2000): 97 (2), 865–70. Cited on p 28 and 61.

Liu Y & Zhang Y, *ETV5 is Essential for Neuronal Differentiation of Human Neural Progenitor Cells by Repressing NEUROG2 Expression*. Stem Cell Rev Rep (2019): 15 (5), 703–716. Cited on p 79.

Lockshin RA & Zakeri Z, *Caspase-independent cell deaths*. Curr Opin Cell Biol (2002): 14 (6), 727–733. Cited on p 20.

Longo A, Guanga GP & Rose RB, *Crystal structure of E47-NeuroD1/Beta2 bHLH domain-DNA complex: heterodimer selectivity and DNA recognition*. Biochemistry (2008): 47 (1), 218–229. Cited on p 24.

Lossi L & Merighi A, *In vivo cellular and molecular mechanisms of neuronal apoptosis in the mammalian CNS*. Progress in Neurobiology (2003): 69 (5), 287–312. Cited on p 19 and 20.

Ma Q, Kintner C & Anderson DJ, *Identification of Neurogenin, a vertebrate neuronal determination gene*. Cell (1996): 87 (1), 43–52. Cited on p 25.

Maino B, Ciotti MT, Calissano P & Cavallaro S, *Transcriptional Analysis of Apoptotic Cerebellar Granule Neurons Following Rescue by Gastric Inhibitory Polypeptide*. Int J Mol Sci (2014): 15 (4), 5596–5622. Cited on p 26.

Malatesta P, Hartfuss E & Götz M, *Isolation of radial glial cells by fluorescent-activated cell sorting reveals a neuronal lineage*. Development (2000): 127 (24), 5253–5263. Cited on p 15.

Marín O, *Cellular and molecular mechanisms controlling the migration of neocortical interneurons*. Eur J Neurosci (2013): 38 (1), 2019–2029. Cited on p 14.

Martynoga B, Morrison H, Price DJ & Mason JO, *Foxg1 is required for specification of ventral telencephalon and region-specific regulation of dorsal telencephalic precursor proliferation and apoptosis*. Dev Biol (2005): 283 (1), 113–127. Cited on p 32, 43, and 98.

Mattar P, Langevin LM, Markham K, Klenin N, Shivji S, Zinyk D & Schuurmans C, *Basic helix-loop-helix transcription factors cooperate to specify a cortical projection neuron identity*. Mol Cell Biol (2008): 28 (5), 1456–69. Cited on p 25 and 70.

McConnell SK, *Constructing the cerebral cortex: Neurogenesis and fate determination*. Neuron (1995): 15 (4), 761–768. Cited on p 14.

McEvilly RJ, de Diaz MO, Schonemann MD, Hooshmand F & Rosenfeld MG, *Transcriptional regulation of cortical neuron migration by POU domain factors*. Science (2002): 295 (5559), 1528–1532. Cited on p 18.

Metzstein MM & Horvitz HR, *The C. elegans cell death specification gene ces-1 encodes a snail family zinc finger protein*. Mol Cell (1999): 4 (3), 309–319. Cited on p 24.

Miller MW, *Relationship of the time of origin and death of neurons in rat somatosensory cortex: barrel versus septal cortex and projection versus local circuit neurons*. J Comp Neurol (1995): 355 (1), 6–14. Cited on p 23.

Miyama S, Takahashi T, Nowakowski RS & Caviness VS, *A gradient in the duration of the G1 phase in the murine neocortical proliferative epithelium*. Cereb Cortex (1997): 7 (7), 678–689. Cited on p 44.

Miyata T, Maeda T & Lee JE, *NeuroD is required for differentiation of the granule cells in the cerebellum and hippocampus*. Genes Dev (1999): 13 (13), 1647–52. Cited on p 25 and 28.

Mizushima N & Komatsu M, *Autophagy: Renovation of Cells and Tissues*. Cell (2011): 147 (4), 728–741. Cited on p 19.

Molyneaux BJ, Arlotta P, Hirata T, Hibi M & Macklis JD, *Fezl is required for the birth and specification of corticospinal motor neurons*. Neuron (2005): 47 (6), 817–831. Cited on p 78.

Molyneaux BJ, Arlotta P, Menezes JRL & Macklis JD, *Neuronal subtype specification in the cerebral cortex*. Nat Rev Neurosci (2007): 8 (6), 427–37. Cited on p 17.

Muchmore SW, Sattler M, Liang H, Meadows RP, Harlan JE, Yoon HS, Nettesheim D, Chang BS, Thompson CB, Wong SL et al., *X-ray and NMR structure of human Bcl-xL, an inhibitor of programmed cell death*. Nature (1996): 381 (6580), 335–341. Cited on p 22.

Mullis K, Faloona F, Scharf S, Saiki R, Horn G & Erlich H, *Specific enzymatic amplification of DNA in vitro: the polymerase chain reaction*. Cold Spring Harb Symp Quant Biol (1986): 51 Pt 1, 263–73. Cited on p 85.

Murre C, Bain G, van Dijk MA, Engel I, Furnari BA, Massari ME, Matthews JR, Quong MW, Rivera RR & Stuiver MH, *Structure and function of helix-loop-helix proteins*. Biochim Biophys Acta (1994): 1218 (2), 129–135. Cited on p 24 and 64.

Nakamura M, Ishida E, Shimada K, Nakase H, Sakaki T & Konishi N, *Frequent HRK inactivation associated with low apoptotic index in secondary glioblastomas*. Acta Neuropathol (2005): 110 (4), 402–410. Cited on p 81.

Nakano K & Vousden KH, *PUMA, a novel proapoptotic gene, is induced by p53*. Mol Cell (2001): 7 (3), 683–694. Cited on p 24.

Naya FJ, Stellrecht CM & Tsai MJ, *Tissue-specific regulation of the insulin gene by a novel basic helix-loop-helix transcription factor*. Genes Dev (1995): 9 (8), 1009–1019. Cited on p 25.

Naya FJ, Huang HP, Qiu Y, Mutoh H, DeMayo FJ, Leiter AB & Tsai MJ, *Diabetes, defective pancreatic morphogenesis, and abnormal enteroendocrine differentiation in BETA2/NeuroD-deficient mice*. Genes Dev (1997): 11 (18), 2323–2334. Cited on p 25.

Nieto M, Monuki ES, Tang H, Imitola J, Haubst N, Khoury SJ, Cunningham J, Gotz M & Walsh CA, *Expression of Cux-1 and Cux-2 in the subventricular zone and upper layers II-IV of the cerebral cortex*. J Comp Neurol (2004): 479 (2), 168–180. Cited on p 18, 39, and 76.

Nishihara H, Kobayashi N, Kimura-Yoshida C, Yan K, Bormuth O, Ding Q, Nakanishi A, Sasaki T, Hirakawa M, Sumiyama K et al., *Coordinately Co-opted Multiple Transposable Elements Constitute an Enhancer for wnt5a Expression in the Mammalian Secondary Palate*. PLoS Genet (2016): 12 (10), e1006380. Cited on p 128.

Noctor SC, Flint AC, Weissman TA, Wong WS, Clinton BK & Kriegstein AR, *Dividing precursor cells of the embryonic cortical ventricular zone have morphological and molecular characteristics of radial glia*. J Neurosci (2002): 22 (8), 3161–3173. Cited on p 14.

Noctor SC, Martínez-Cerdeño V, Ivic L & Kriegstein AR, *Cortical neurons arise in symmetric and asymmetric division zones and migrate through specific phases*. Nat Neurosci (2004): 7 (2), 136–144. Cited on p 14 and 17.

Noma T, Yoon YS & Nakazawa A, *Overexpression of NeuroD in PC12 cells alters morphology and enhances expression of the adenylate kinase isozyme 1 gene*. Brain Res Mol Brain Res (1999): 67 (1), 53–63. Cited on p 25.

Nonomura K, Yamaguchi Y, Hamachi M, Koike M, Uchiyama Y, Nakazato K, Mochizuki A, Sakaue-Sawano A, Miyawaki A, Yoshida H et al., *Local apoptosis modulates early mammalian brain development through the elimination of morphogen-producing cells*. Dev Cell (2013): 27 (6), 621–634. Cited on p 20.

Nowakowski RS, Lewin SB & Miller MW, *Bromodeoxyuridine immunohistochemical determination of the lengths of the cell cycle and the DNA-synthetic phase for an anatomically defined population*. J Neurocytol (1989): 18 (3), 311–318. Cited on p 98.

Oda E, Ohki R, Murasawa H, Nemoto J, Shibue T, Yamashita T, Tokino T, Taniguchi T & Tanaka N, *Noxa, a BH3-only member of the Bcl-2 family and candidate mediator of p53-induced apoptosis*. Science (2000): 288 (5468), 1053–1058. Cited on p 24.

Ogawa M, Miyata T, Nakajima K, Yagyu K, Seike M, Ikenaka K, Yamamoto H & Mikoshiba K, *The reeler gene-associated antigen on Cajal-Retzius neurons is a crucial molecule for laminar organization of cortical neurons*. Neuron (1995): 14 (5), 899–912. Cited on p 17.

Okamoto M, Namba T, Shinoda T, Kondo T, Watanabe T, Inoue Y, Takeuchi K, Enomoto Y, Ota K, Oda K et al., *TAG-1-assisted progenitor elongation streamlines nuclear migration to optimize subapical crowding*. Nat Neurosci (2013): 16 (11), 1556–1566. Cited on p 80.

O'Leary DD & Sahara S, *Genetic regulation of arealization of the neocortex*. Curr Opin Neurobiol (2008): 18 (1), 90–100. Cited on p 44.

Olson JM, Asakura A, Snider L, Hawkes R, Strand A, Stoeck J, Hallahan A, Pritchard J & Tapscott SJ, *NeuroD2 is necessary for development and survival of central nervous system neurons*. Dev Biol (2001): 234 (1), 174–87. Cited on p 26 and 28.

Oppenheim RW, *Cell death during development of the nervous system*. Annu Rev Neurosci (1991): 14, 453–501. Cited on p 23.

Oppenheim RW, Blomgren K, Ethell DW, Koike M, Komatsu M, Prevette D, Roth KA, Uchiyama Y, Vinsant S & Zhu C, *Developing postmitotic mammalian neurons in vivo lacking Apaf-1 undergo programmed cell death by a caspase-independent, nonapoptotic pathway involving autophagy*. J Neurosci (2008): 28 (6), 1490–1497. Cited on p 20.

Parthasarathy S, Srivatsa S, Nityanandam A & Tarabykin V, *Ntf3 acts downstream of Sip1 in cortical postmitotic neurons to control progenitor cell fate through feedback signaling*. Development (2014): 141 (17), 3324–3330. Cited on p 73 and 78.

Peyton M, Stellrecht CM, Naya FJ, Huang HP, Samora PJ & Tsai MJ, *BETA3, a novel helix-loop-helix protein, can act as a negative regulator of BETA2 and MyoD-responsive genes*. Mol Cell Biol (1996): 16 (2), 626–633. Cited on p 76 and 82.

Pleasure SJ, Collins AE & Lowenstein DH, *Unique Expression Patterns of Cell Fate Molecules Delineate Sequential Stages of Dentate Gyrus Development*. J Neurosci (2000): 20 (16), 6095–6105. Cited on p 25.

Polleux F & Ghosh A, *The slice overlay assay: a versatile tool to study the influence of extracellular signals on neuronal development*. Sci STKE (2002): 2002 (136), pl9. Cited on p 95.

Puehringer D, Orel N, Lüningschrör P, Subramanian N, Herrmann T, Chao MV & Sendtner M, *EGF transactivation of Trk receptors regulates the migration of newborn cortical neurons*. Nat Neurosci (2013): 16 (4), 407–415. Cited on p 47.

Puthalakath H & Strasser A, *Keeping killers on a tight leash: transcriptional and post-translational control of the pro-apoptotic activity of BH3-only proteins*. Cell Death Differ (2002): 9 (5), 505–512. Cited on p 23 and 81.

Rakic P, *Mode of cell migration to the superficial layers of fetal monkey neocortex*. J Comp Neurol (1972): 145 (1), 61–83. Cited on p 17.

Rakic P, *Evolution of the neocortex: Perspective from developmental biology*. Nat Rev Neurosci (2009): 10 (10), 724–735. Cited on p 13.

Raoul C, Pettmann B & Henderson CE, *Active killing of neurons during development and following stress: a role for p75(NTR) and Fas?* Curr Opin Neurobiol (2000): 10 (1), 111–117. Cited on p 21.

Ravanpay AC & Olson JM, *E protein dosage influences brain development more than family member identity*. J Neurosci Res (2008): 86 (7), 1472–1481. Cited on p 24.

Ravanpay AC, Hansen SJ & Olson JM, *Transcriptional inhibition of REST by NeuroD2 during neuronal differentiation*. Mol Cell Neurosci (2010): 44 (2), 178–189. Cited on p 65.

Reichardt LF, *Neurotrophin-regulated signalling pathways*. Philosophical Transactions of the Royal Society of London B: Biological Sciences (2006): 361 (1473), 1545–1564. Cited on p 23.

Rice DS & Curran T, *Role of the reelin signaling pathway in central nervous system development*. Annu Rev Neurosci (2001): 24, 1005–1039. Cited on p 17.

Rolls ET, *The mechanisms for pattern completion and pattern separation in the hippocampus*. Front Syst Neurosci (2013): 7, 74. Cited on p 12.

de la Rosa EJ & de Pablo F, *Cell death in early neural development: beyond the neurotrophic theory*. Trends Neurosci (2000): 23 (10), 454–458. Cited on p 23.

Ross SE, Mardinly AR, McCord AE, Zurawski J, Cohen S, Jung C, Hu L, Mok SI, Shah A, Savner E et al., *Loss of inhibitory interneurons in the dorsal spinal cord and elevated itch in Bhlhb5 mutant mice*. Neuron (2010): 65 (6), 886–898. Cited on p 82.

Ross SE, McCord AE, Jung C, Atan D, Mok SI, Hemberg M, Kim TK, Salogiannis J, Hu L, Cohen S et al., *Bhlhb5 and Prdm8 form a repressor complex involved in neuronal circuit assembly*. Neuron (2012): 73 (2), 292–303. Cited on p 65, 68, 76, and 82.

Roztocil T, Matter-Sadzinski L, Alliod C, Ballivet M & Matter JM, *NeuroM, a neural helix-loop-helix transcription factor, defines a new transition stage in neurogenesis*. Development (1997): 124 (17), 3263–72. Cited on p 25.

Rubin RD, Watson PD, Duff MC & Cohen NJ, *The role of the hippocampus in flexible cognition and social behavior*. Front Hum Neurosci (2014): 8. Cited on p 13.

Saba R, Johnson JE & Saito T, *Commissural neuron identity is specified by a homeodomain protein, Mbh1, that is directly downstream of Math1*. Development (2005): 132 (9), 2147–2155. Cited on p 24.

Saito T, *In vivo electroporation in the embryonic mouse central nervous system*. Nat Protocols (2006): 1 (3), 1552–1558. Cited on p 96.

Sambrook J & Russell DW, *Molecular Cloning: A Laboratory Manual, 3 Vol.* Cold Spring Harbor Laboratory 2000, 0003rd ed. Cited on p 87.

Sanes DH, Reh TA & Harris WA, *Development of the Nervous System*. Academic Press 2000, google-Books-ID: T2_oPdo3hAIC. Cited on p 23 and 47.

Sastry PS & Rao KS, *Apoptosis and the nervous system*. J Neurochem (2000): 74 (1), 1–20. Cited on p 21.

Satoh Ji, Yamamoto Y, Asahina N, Kitano S & Kino Y, *RNA-Seq Data Mining: Downregulation of NeuroD6 Serves as a Possible Biomarker for Alzheimer's Disease Brains*. Dis Markers (2014): 2014. Cited on p 27.

Schiffmann SN, Bernier B & Goffinet AM, *Reelin mRNA expression during mouse brain development*. Eur J Neurosci (1997): 9 (5), 1055–1071. Cited on p 17.

Schiller D, Eichenbaum H, Buffalo EA, Davachi L, Foster DJ, Leutgeb S & Ranganath C, *Memory and Space: Towards an Understanding of the Cognitive Map*. J Neurosci (2015): 35 (41), 13904–13911. Cited on p 13.

Schmid T, Krüger M & Braun T, *NSCL-1 and -2 control the formation of precerebellar nuclei by orchestrating the migration of neuronal precursor cells*. J Neurochem (2007): 102 (6), 2061–2072. Cited on p 70.

Schore AN, *Affect Regulation and the Origin of the Self: The Neurobiology of Emotional Development*. Psychology Press 1994, google-Books-ID: 6H4xnJ46V18C. Cited on p 12.

Schwab MH, Druffel-Augustin S, Gass P, Jung M, Klugmann M, Bartholomae A, Rossner MJ & Nave KA, *Neuronal basic helix-loop-helix proteins (NEX, NeuroD, NDRF): spatiotemporal expression and targeted disruption of the NEX gene in transgenic mice*. J Neurosci (1998): 18 (4), 1408–18. Cited on p 26 and 36.

Schwab MH, Bartholomae A, Heimrich B, Feldmeyer D, Druffel-Augustin S, Goebbels S, Naya FJ, Zhao S, Frotscher M, Tsai MJ et al., *Neuronal basic helix-loop-helix proteins (NEX and BETA2/NeuroD) regulate terminal granule cell differentiation in the hippocampus*. J Neurosci (2000): 20 (10), 3714–24. Cited on p 25, 26, 27, 28, 29, and 61.

Schweichel JU & Merker HJ, *The morphology of various types of cell death in prenatal tissues*. Teratology (1973): 7 (3), 253–266. Cited on p 19.

Seo S, Lim JW, Yellajoshyula D, Chang LW & Kroll KL, *Neurogenin and NeuroD direct transcriptional targets and their regulatory enhancers*. EMBO J (2007): 26 (24), 5093–5108. Cited on p 17 and 80.

Sessa A, Mao CA, Hadjantonakis AK, Klein WH & Broccoli V, *Tbr2 directs conversion of radial glia into basal precursors and guides neuronal amplification by indirect neurogenesis in the developing neocortex*. Neuron (2008): 60 (1), 56–69. Cited on p 17.

Seuntjens E, Nityanandam A, Miquelajauregui A, Debruyn J, Stryjewska A, Goebbels S, Nave KA, Huylebroeck D & Tarabykin V, *Sip1 regulates sequential fate decisions by feedback signaling from postmitotic neurons to progenitors*. Nat Neurosci (2009): 12 (11), 1373–1380. Cited on p 44, 73, and 78.

Shalini S, Dorstyn L, Dawar S & Kumar S, *Old, new and emerging functions of caspases*. Cell Death Differ (2015): 22 (4), 526–539. Cited on p 22.

Shibui S, Hoshino T, Vanderlaan M & Gray JW, *Double labeling with iodo- and bromodeoxyuridine for cell kinetics studies*. J Histochem Cytochem (1989): 37 (7), 1007–1011. Cited on p 98.

Shoukimas GM & Hinds JW, *The development of the cerebral cortex in the embryonic mouse: an electron microscopic serial section analysis*. J Comp Neurol (1978): 179 (4), 795–830. Cited on p 17.

Sing A, Pannell D, Karaiskakis A, Sturgeon K, Djabali M, Ellis J, Lipshitz HD & Cordes SP, *A vertebrate Polycomb response element governs segmentation of the posterior hindbrain*. Cell (2009): 138 (5), 885–897. Cited on p 71.

Skinner MK, Rawls A, Wilson-Rawls J & Roalson EH, *Basic Helix-Loop-Helix Transcription Factor Gene Family Phylogenetics and Nomenclature*. Differentiation (2010): 80 (1), 1–8. Cited on p 24.

Slomianka L, Amrein I, Knuesel I, Sørensen JC & Wolfer DP, *Hippocampal pyramidal cells: the reemergence of cortical lamination*. Brain Struct Funct (2011): 216 (4), 301–317. Cited on p 12.

Song J, Park KA, Lee WT & Lee JE, *Apoptosis signal regulating kinase 1 (ASK1): potential as a therapeutic target for Alzheimer's disease*. Int J Mol Sci (2014): 15 (2), 2119–2129. Cited on p 20.

Southwell DG, Paredes MF, Galvao RP, Jones DL, Froemke RC, Sebe JY, Alfaro-Cervello C, Tang Y, Garcia-Verdugo JM, Rubenstein JL et al., *Intrinsically determined cell death of developing cortical interneurons*. Nature (2012): 491 (7422), 109–113. Cited on p 23 and 44.

Squire LR, *Memory and the hippocampus: a synthesis from findings with rats, monkeys, and humans*. Psychol Rev (1992): 99 (2), 195–231. Cited on p 13.

Squire LR, Berg D, Bloom FE, Lac SD, Ghosh A & Spitzer NC, *Fundamental Neuroscience: Fourth Edition*. Elsevier Inc. 2012. Cited on p 23.

Srinivasan K, Leone DP, Bateson RK, Dobreva G, Kohwi Y, Kohwi-Shigematsu T, Grosschedl R & McConnell SK, *A network of genetic repression and derepression specifies projection fates in the developing neocortex*. Proc Natl Acad Sci USA (2012): 109 (47), 19071–19078. Cited on p 37 and 78.

Talley MJ, Nardini D, Qin S, Prada CE, Ehrman LA & Waclaw RR, *A role for sustained MAPK activity in the mouse ventral telencephalon*. Dev Biol (2021): 476, 137–147. Cited on p 79.

Tarabykin V, Stoykova A, Usman N & Gruss P, *Cortical upper layer neurons derive from the subventricular zone as indicated by Svet1 gene expression*. Development (2001): 128 (11), 1983–1993. Cited on p 17 and 75.

Tau GZ & Peterson BS, *Normal Development of Brain Circuits*. Neuropsychopharmacology (2010): 35 (1), 147–168. Cited on p 20.

Teng KK, Felice S, Kim T & Hempstead BL, *Understanding Proneurotrophin Actions: Recent Advances and Challenges*. Dev Neurobiol (2010): 70 (5), 350–359. Cited on p 23.

Thellmann M, Hatzold J & Conradt B, *The Snail-like CES-1 protein of C. elegans can block the expression of the BH3-only cell-death activator gene egl-1 by antagonizing the function of bHLH proteins*. Development (2003): 130 (17), 4057–4071. Cited on p 24.

Tsujimoto Y & Shimizu S, *Bcl-2 family: life-or-death switch*. FEBS Lett (2000): 466 (1), 6–10. Cited on p 22.

Uittenbogaard M & Chiaramello A, *Constitutive overexpression of the basic helix-loop-helix Nex1/MATH-2 transcription factor promotes neuronal differentiation of PC12 cells and neurite regeneration*. Journal of Neuroscience Research (2002): 67 (2), 235–245. Cited on p 49.

Uittenbogaard M & Chiaramello A, *Expression profiling upon Nex1/MATH-2-mediated neuritogenesis in PC12 cells and its implication in regeneration*. Journal of Neurochemistry (2004): 91 (6), 1332–1343. Cited on p 43.

Uittenbogaard M & Chiaramello A, *The basic helix-loop-helix transcription factor Nex-1/Math-2 promotes neuronal survival of PC12 cells by modulating the dynamic expression of anti-apoptotic and cell cycle regulators*. Journal of Neurochemistry (2005): 92 (3), 585–596. Cited on p 26, 28, 49, and 50.

Uittenbogaard M, Martinka DL & Chiaramello A, *The basic helix-loop-helix differentiation factor Nex1/MATH-2 functions as a key activator of the GAP-43 gene*. J Neurochem (2003): 84 (4), 678–688. Cited on p 64.

Uittenbogaard M, Baxter KK & Chiaramello A, *Cloning and characterization of the 5'UTR of the rat anti-apoptotic Bcl-w gene*. Biochemical and Biophysical Research Communications (2009): 389 (4), 657–662. Cited on p 28.

Uittenbogaard M, Baxter KK & Chiaramello A, *NeuroD6 genomic signature bridging neuronal differentiation to survival via the molecular chaperone network*. Journal of Neuroscience Research (2010): 88 (1), 33–54. Cited on p 26, 49, and 50.

Vaux DL, Haecker G & Strasser A, *An evolutionary perspective on apoptosis*. Cell (1994): 76 (5), 777–779. Cited on p 19.

Wajant H, *The Fas Signaling Pathway: More Than a Paradigm*. Science (2002): 296 (5573), 1635–1636. Cited on p 21.

Weltman JK, *The 1986 Nobel Prize for Physiology or Medicine Awarded for Discovery of Growth Factors: Rita Levi-Montalcini, M.D., and Stanley Cohen, Ph.D.* Allergy and Asthma Proceedings (1987): 8 (1), 47–48. Cited on p 23.

Whitfield J, Neame SJ, Paquet L, Bernard O & Ham J, *Dominant-negative c-Jun promotes neuronal survival by reducing BIM expression and inhibiting mitochondrial cytochrome c release*. Neuron (2001): 29 (3), 629–643. Cited on p 24.

Whitton L, Apostolova G, Rieder D, Dechant G, Rea S, Donohoe G & Morris DW, *Genes regulated by SATB2 during neurodevelopment contribute to schizophrenia and educational attainment*. PLoS Genet (2018): 14 (7), e1007515. Cited on p 37.

Willis SN & Adams JM, *Life in the balance: how BH3-only proteins induce apoptosis*. Curr Opin Cell Biol (2005): 17 (6), 617–625. Cited on p 22.

Xiao B, Wilson JR & Gamblin SJ, *SET domains and histone methylation*. Curr Opin Struct Biol (2003): 13 (6), 699–705. Cited on p 66.

Xu ZP, Dutra A, Stellrecht CM, Wu C, Piatigorsky J & Saunders GF, *Functional and structural characterization of the human gene BHLHB5, encoding a basic helix-loop-helix transcription factor*. Genomics (2002): 80 (3), 311–318. Cited on p 65, 76, and 82.

Yaginuma H, Shiraiwa N, Shimada T, Nishiyama K, Hong J, Wang S, Momoi T, Uchiyama Y & Oppenheim RW, *Caspase activity is involved in, but is dispensable for, early motoneuron death in the chick embryo cervical spinal cord*. Mol Cell Neurosci (2001): 18 (2), 168–182. Cited on p 20.

Yamada M, Shida Y, Takahashi K, Tanioka T, Nakano Y, Tobe T & Yamada M, *Prg1 is regulated by the basic helix-loop-helix transcription factor Math2*. Journal of Neurochemistry (2008): 106 (6), 2375–2384. Cited on p 27.

Yamaguchi Y & Miura M, *Programmed Cell Death in Neurodevelopment*. Developmental Cell (2015): 32 (4), 478–490. Cited on p 20.

Yan K, *NeuroD family transcription factors regulate corpus callosum formation and cell differentiation during cerebral cortical development*. Ph.D. thesis, Freie Universität Berlin, Freie Universität Berlin, Germany (2016). Cited on p 27, 28, 29, 36, 43, 75, 76, 79, and 83.

Yan K, Bormuth I, Bormuth O, Tutukova S, Renner A, Bessa P, Schaub T, Rosário M & Tarabykin V, *TrkB-dependent EphrinA reverse signaling regulates callosal axon fasciculate growth downstream of Neurod2/6*. Cereb Cortex (2022): bhac170. Cited on p 128.

Yasunami M, Suzuki K, Maruyama H, Kawakami H, Nagai Y, Hagiwara M & Ohkubo H, *Molecular cloning and characterization of a cDNA encoding a novel basic helix-loop-helix protein structurally related to Neuro-D/BHF1*. Biochem Biophys Res Commun (1996): 220 (3), 754–8. Cited on p 25.

Yeo W & Gautier J, *Early neural cell death: dying to become neurons*. Dev Biol (2004): 274 (2), 233–244. Cited on p 20.

Yoshida H, Kong YY, Yoshida R, Elia AJ, Hakem A, Hakem R, Penninger JM & Mak TW, *Apaf1 is required for mitochondrial pathways of apoptosis and brain development*. Cell (1998): 94 (6), 739–750. Cited on p 50.

Yoshizawa M, Hoshino M, Sone M & Nabeshima Yi, *Expression of stef, an activator of Rac1, correlates with the stages of neuronal morphological development in the mouse brain*. Mech Dev (2002): 113 (1), 65–68. Cited on p 71.

Yuan J & Kroemer G, *Alternative cell death mechanisms in development and beyond*. Genes Dev (2010): 24 (23), 2592–2602. Cited on p 19.

Yuan J, Shaham S, Ledoux S, Ellis HM & Horvitz HR, *The C. elegans cell death gene ced-3 encodes a protein similar to mammalian interleukin-1 beta-converting enzyme*. Cell (1993): 75 (4), 641–652. Cited on p 22.

Yuan S, Yu X, Topf M, Ludtke SJ, Wang X & Akey CW, *Structure of an Apoptosome-Procaspase-9 CARD Complex*. Structure (2010): 18 (5), 571–583. Cited on p 21.

Zhang G, Assadi AH, McNeil RS, Beffert U, Wynshaw-Boris A, Herz J, Clark GD & D'Arcangelo G, *The Pafah1b Complex Interacts with the Reelin Receptor VLDLR*. PLoS ONE (2007): 2 (2). Cited on p 17.

Zhou Q & Anderson DJ, *The bHLH transcription factors OLIG2 and OLIG1 couple neuronal and glial subtype specification*. Cell (2002): 109 (1), 61–73. Cited on p 82.

Zhukov VA, Nemankin TA, Ovchinnikova ES, Kuznetsova EV, Zhernakov AI, Titov VS, Grishina OA, Sulima AS, Borisov YG, Borisov AY et al., *Creating a series of gene-specific molecular markers for comparative mapping of the genome of pea (Pisum sativum L.) and diploid alfalfa (Medicago truncatula Gaertn.)*. Factors of Experimental Evo (2010): 9 (2), 30–34. Cited on p 128.

Zimmer C, Tiveron MC, Bodmer R & Cremer H, *Dynamics of Cux2 expression suggests that an early pool of SVZ precursors is fated to become upper cortical layer neurons*. Cereb Cortex (2004): 14 (12), 1408–1420. Cited on p 75.

Zimmermann KC, Bonzon C & Green DR, *The machinery of programmed cell death*. Pharmacol Ther (2001): 92 (1), 57–70. Cited on p 21.

Zou H, Henzel WJ, Liu X, Lutschg A & Wang X, *Apaf-1, a Human Protein Homologous to C. elegans CED-4, Participates in Cytochrome c–Dependent Activation of Caspase-3*. Cell (1997): 90 (3), 405–413. Cited on p 48.

# Appendix

# Abbreviations

Gene symbols mostly follow the standard nomenclature of the mouse genome informatics database (MGI). Exceptions were made where the official naming is rarely used in the current literature of the field. Those cases are indicated by additionally providing the MGI symbol in underlined text. For better readability and to avoid conflicts with other abbreviations, protein symbols were not converted to all upper-case.

**AA** amino acid – *also amino acids*
**aIPC** apical intermediate precursor cell – *previously SNPC*
**AP** alkaline phosphatase
**Apaf1** apoptotic peptidase activating factor 1 *gene id: 11783*
**APC** Apical precursor cell = *RGC*
**Apoer2** apolipoprotein receptor related 8 = *Lrp8* *gene id: 16975*
**aRGC** apical radial glia cell
**Bad** Bcl2-associated agonist of cell death *gene id: 12015*
**Bak** Bcl2-antagonist/killer 1 *gene id: 12018*
**Bax** Bcl2-associated protein X *gene id: 12028*
**Bcl-W** BCL2-like 2 = *Bcl2l2* *gene id: 12050*
**Bcl-XL** BCL2-like 1 = *Bcl2l1* *gene id: 12048*
**Bcl2** B cell leukemia/lymphoma 2 *gene id: 12043*
**Bcl2a1a** Bcl2-related protein A1a *gene id: 12044*
**Bdnf** brain derived neurotrophic factor *gene id: 12064*
**bHLH** basic helix-loop-helix
**Bhlhb5** bHLH protein B5 = *Bhlhe22* *gene id: 59058*
**Bid** BH3 interacting domain death agonist *gene id: 12122*
**Bik** Bcl2-interacting killer *gene id: 12124*
**Bim** BCL2-like 11 = *Bcl2l11* *gene id: 12125*
**bIPC** basal intermediate precursor cell
**Bmf** Bcl2 modifying factor *gene id: 171543*
**Bok** Bcl2-related ovarian killer *gene id: 51800*
**bp** base pair – *also base pairs*
**BPC** Basal precursor cell = *IPC*
**BrdU** bromodeoxyuridine – *thymidine analog*
**bRGC** basal radial glia cell – *also oRGC*
**Brn2** brain 2 = *Pou3f2* *gene id: 18992*
**c** caudal
**CA** cornu ammonis
**CAG** synthetic chicken beta actin based *promoter*
**Calb2** calbindin 2 = *calretinin* *gene id: 12308*
**CAM** cell adhesion molecule
**Camk2b** calcium/calmodulin-dependent protein kinase II, beta = *CaMKII* *gene id: 12323*
**Casp3** caspase 3 *gene id: 12367*
**CC** corpus callosum
**Cdh11** cadherin 11 *gene id: 12552*
**CDK** cyclin-dependent kinase
**ces-1** cell death specification *(C. elegans)* *gene id: 185718*
**Ci** cingulate cortex
**Clmp** CXADR-like membrane protein *gene id: 71566*
**CNS** central nervous system
**Cntn2** contactin 2 *CAM = Tag-1* *gene id: 21367*
**CP** cortical plate
**CR** coronal radiation
**Cre** Cre recombinase
**Crym** $\mu$-crystallin *(thyroid hormone-binding)* *gene id: 12971*
**Ctip2** COUP-TF interacting 2 = *Bcl11b* *gene id: 58208*
**Ctx** cortex
**Cux1** cut-like homeobox 1 *gene id: 13047*
**Cux2** cut-like homeobox 2 *gene id: 13048*
**d** dorsal
**Dab1** disabled homolog 1 = *scrambler* *gene id: 13131*
**Dact1** dishevelled-binding antagonist of beta-catenin 1 *gene id: 59036*
**DAPI** 4',6-diamidino-2-phenylindole
**Ddx3y** Y-linked DEAD box polypeptide 3 = *Dby* *gene id: 26900*
**DEPC** diethyl pyrocarbonate
**DG** dentate gyrus
**E** embryonic day
**EdU** ethynyl desoxyuridine – *thymidine analog*
**egl-1** programmed cell death activator *(C. elegans)* *gene id: 179943*
**Eif2s3y** Y-linked eukaryotic translation initiation factor 2, subunit 3 *gene id: 26908*
**Erdr1** erythroid differentiation regulator 1 *gene id: 170942*
**Etv5** ets variant 5 *gene id: 104156*
**Fancd2** Fanconi anemia complementation group D2 *gene id: 211651*
**Fasl** first apoptosis signal ligand = *Fas ligand* *gene id: 14103*
**Fezf2** Fez family zinc finger 2 = *Fezl* = *Zfp312* *gene id: 54713*
**fig** figure – *also figures*
**Flcn** folliculin *gene id: 216805*
**Foxp2** forkhead box P2 *gene id: 114142*
**Gap43** growth associated protein 43 = *B-50* = *Basp2* *gene id: 14432*
**GE** ganglionic eminence
**GFP** green fluorescent protein

**Gnb4** guanine nucleotide binding protein beta 4 *gene id: 14696*
**h** hour – *also hours*
**Hip** hippocampus
**Hpca** hippocalcin *gene id: 15444*
**Hrk** Harakiri = *DP5* = *Bid3* *gene id: 12123* – *also BCL2-interacting BH3-only protein*
**Id2** inhibitor of DNA binding 2 = *bHLHb26* *gene id: 15902*
**IdU** idoxuridine – *thymidine analog*
**IHC** immunohistochemistry
**IPC** intermediate precursor cell
**IRES** internal ribosomal entry site
**ISH** in-situ hybridization
**IUE** in utero electroporation
**IZ** intermediate zone
**JNK** c-Jun N-terminal kinase = *Mapk8* *gene id: 26419*
**kbp** kilo base pair – *also kilo base pairs*
**Kcnq3** potassium voltage-gated channel, subfamily Q, member 3 <*110862:wq*>
**Kdm5d** lysine specific demethylase 5D = *Smcy* = *HY* *gene id: 20592*
**Kdm6a** lysine specific demethylase 6A *gene id: 22289*
**Ki67** antigen identified by monoclonal antibody Ki 67 = *Mki67* *gene id: 17345*
**l** lateral
**LFC** log2 fold change
**Lis1** lissencephaly 1 = *Pafah1b1* *gene id: 18472*
**Lmo1** LIM domain only 1 *gene id: 109594*
**Lmo4** lim domain only 4 *gene id: 16911*
**LoxP** locus of X-over P1 *(cre recognitions sequence)*
**Lppr4** phospholipid phosphatase related 4 *gene id: 229791*
**LV** lateral ventricle
**m** medial
**Mafb** v-maf musculoaponeurotic fibrosarcoma oncogene family protein B = *Kreisler* *gene id: 16658*
**Map2** microtubule associated protein 2 = *Mtap2* *gene id: 17756*
**MAPK** mitogen-activated protein kinase
**Mapt** microtubule associated protein $\tau$ = *Tau* *gene id: 17762*
**Mc4r** melanocortin 4 receptor *gene id: 17202*
**Mcl1** myeloid cell leukemia sequence 1 *gene id: 17210*
**MGI** mouse genome informatics database[1]
**Mid1** midline 1 *gene id: 17318*
**min** minute – *also minutes*
**mRNA** messenger RNA
**MZ** marginal zone
**N2a** Neuro2a *neuroblastoma cell line*
**NCBI** National Center for Biotechnology Information *(USA)*
**Ndrg1** N-myc downstream regulated 1 *gene id: 17988*
**Necab3** N-terminal EF-hand calcium binding protein 3 *gene id: 56846*
**NeoR** neomycin resistance
**NeuN** neuronal nuclear antigen = *Rbfox3* = *Fox-3* *gene id: 52897*
**Neurod1** neuronal differentiation factor 1 = *NeuroD* = *Beta2* = *BHF-1* = *bHLHa3* *gene id: 18012*
**Neurod1/2/6** Neurod1, Neurod2 and/or Neurod6
**Neurod2** neuronal differentiation factor 2 = *NDRF* = *KW8* = *bHLHa1* *gene id: 18013*
**Neurod2/6** Neurod2 and/or Neurod6
**Neurod4** neuronal differentiation factor 4 = *NeuroM* = *Math3* = *bHLHa4* *gene id: 11923*
**Neurod6** neuronal differentiation factor 6 = *NEX* = *Math2* = *bHLHa2* *gene id: 11922*
**Neurog2** neurogenin 2 = *Ngn2* = *Atoh4* = *Math4a* = *bHLHa8* *gene id: 11924*
**Ngf** nerve growth factor *gene id: 18049*
**Ngfr** nerve growth factor receptor = *p75*, = *p75NTR* *gene id: 18053*
**Nhlh2** nescient helix loop helix 2 = *Hen2* = *Nscl2* = *bHLHa34* *gene id: 18072*
**Notch1** notch homolog 1 *gene id: 18128*
**Noxa** phorbol-12-myristate-13-acetate-induced = *Pmaip1* *gene id: 58801*
**NPC** neural progenitor cell
**Nr4a3** nuclear receptor subfamily 4, group A, member 3 = *Nor1* *gene id: 18124*
**Ntf3** neurotrophin 3 = *NT3* *gene id: 18205*
**Ntf5** neurotrophin 5 = *NT4, NT5* *gene id: 78405*
**Ntrk1** neurotrophic tyrosine kinase 1 *gene id: 18211*
**Ntrk2** neurotrophic tyrosine kinase 2 *gene id: 18212*
**OB** olfactory bulb
**Olig2** oligodendrocyte transcription factor 2 = *Bhlhb1* = *bHLHe19* *gene id: 50913*
**ORF** open reading frame
**oRGC** outer radial glia cell – *also bRGC*
**P** postnatal day
**p** page – *also pages*
**Pax6** paired box gene 6 = *Sey* = *Dey* *gene id: 18508*
**PBS** phosphate buffered saline
**PCD** programmed cell death
**Pcna** proliferating cell nuclear antigen *gene id: 18538*
**PCR** polymerase chain reaction
**PFA** paraformaldehyde
**Plppr5** phospholipid phosphatase related 5 = *Prg5* = *Lppr5* *gene id: 75769*
**Plxna4** plexin A4 *gene id: 243743*
**PP** preplate
**Prdm8** PR domain containing 8 *gene id: 77630*
**Prokr2** prokineticin receptor 2 *gene id: 246313*
**Prox1** prospero homeobox 1 *gene id: 19130*
**Ptpro** protein tyrosine phosphatase receptor O *gene id: 19277*
**Puma** Bcl2 binding component 3 = *Bbc3* *gene id: 170770*
**r** rostral
**Reln** Reelin *gene id: 19699*
**Rest** RE1-silencing transcription factor = *Neuron-Restrictive silencer factor (NRSF)* *gene id: 19712*

[1] Blake et al. 2014; `http://informatics.jax.org/mgihome/nomen/`

**RFP** red fluorescent protein
**RGC** radial glia cell
**Rn18s** 18S ribosomal RNA *gene id: 19791*
**Rn28s1** 28S ribosomal RNA *gene id: 236598*
**Rn45s** 45S pre-ribosomal RNA *gene id: 100861531*
**RNA** ribonucleic acid
**RNA-Seq** RNA deep sequencing *(here mRNA enriched)*
**RNAi** RNA interference
**Robo1** roundabout 1 *gene id: 19876*
**Rorb** RAR-related orphan receptor beta = *Nr1f2* *gene id: 225998*
**ROS** reactive oxygen species
**rpm** rotations per minute
**Rs5-8s1** 5.8S ribosomal RNA *gene id: 790956*
**RT** room temperature
**Rtn4rl2** reticulon 4 receptor-like 2 *gene id: 269295*
**saRGC** subapical radial glia cell
**Satb2** special AT-rich sequence binding protein 2 *gene id: 212712*
**sec** second – *also seconds*
**sect** section – *also sections*
**SEM** standard error of the mean
**Sez6** seizure related gene 6 *gene id: 20370*
**Sh3gl2** SH3-domain GRB2-like 2 *gene id: 20404*
**shRNA** short hairpin RNA
**Sip1** Smad interacting protein 1 * *Zeb2 zinc finger E-box binding homeobox 2* *gene id: 9839*
**Sla** src-like adaptor *gene id: 20491*
**Snord22** small nucleolar RNA C/D box 22 = *Rnu22* *gene id: 100127111*
**SNPC** short neuronal precursor cell – *now aIPC*
**Sox2** sex determining region Y box 2 *gene id: 20674*
**Sox5** SRY-box 5 *gene id: 20678*
**SP** subplate
**SSC** saline-sodium citrate buffer
**SVZ** subventricular zone
**Syn2** synapsin II *gene id: 20965*
**Syt4** synaptotagmin IV *gene id: 20983*
**tab** table
**Tbr1** T-box brain 1 *gene id: 21375*
**Tbr2** T-box brain 2 = *Eomes* *gene id: 13813*
**$T_C$** cell cycle legth
**Tiam2** T cell lymphoma invasion and metastasis 2 *gene id: 24001*
**TKO** triple-deficient mice *('triple knockout')*
**TM** melting temperature
**TNFR** tumor necrosis factor receptor *(gene/protein family)*
**Trp53** transformation related protein 53 = *p53* *gene id: 22059*
**$T_S$** s-phase length
**Tsix** opposite strand of X inactive-specific transcript *gene id: 22097*
**Tubb3** tubulin beta 3 class III *gene id: 22152* – *target of Tuj1 antibody*
**TUNEL** terminal deoxynucleotidyl transferase dUTP nick end labeling *apoptose assay*
**TX-100** Triton X-100 = $C_{14}H_{22}O(C_2H_4O)_n$
**Unc5d** unc-5 netrin receptor D *gene id: 210801*
**UTR** untranslated region *(of gene)*
**v** ventral
**Vglut1** vesicular glutamate transporter 1 = *Slc17a7* *gene id: 72961*
**Vldlr** very low density lipoprotein receptor *gene id: 22359*
**vs** compared with *(versus, latin)*
**VZ** ventricular zone
**Xist** X inactive-specific transcripts *gene id: 213742*

# List of Figures

# List of Tables

# Index

# Publications

### Peer-reviewed articles:

- Yan K, Bormuth I, Bormuth O, Tutukova S, Renner A, Bessa P, Schaub T, Rosário M, Tarabykin V (2022):
  **TrkB-dependent EphrinA reverse signaling regulates callosal axon fasciculate growth downstream of Neurod2/6**
  *Cereb Cortex 2022 Apr 23 (online ahead of print)*
- Epifanova E, Salina V, Lajkó D, Textoris-Taube K, Naumann T, Bormuth O, Bormuth I, Horan S, Schaub T, Borisova E, Ambrozkiewicz MC, Tarabykin V, Rosário M (2021):
  **Adhesion dynamics in the neocortex determine the start of migration and the post-migratory orientation of neurons.**
  *Sci Adv 7 (27)*
- Nishihara H, Kobayashi N, Kimura-Yoshida C, Yan K, Bormuth O, Ding Q, Nakanishi A, Sasaki T, Hirakawa M, Sumiyama K, Furuta Y, Tarabykin V, Matsuo I, Okada N (2016):
  **Coordinately Co-opted Multiple Transposable Elements Constitute an Enhancer for wnt5a Expression in the Mammalian Secondary Palate.**
  *PLoS Genet 12 (10), e1006380*
- Bormuth I, Yan K, Yonemasu T, Gummert M, Zhang M, Wichert S, Grishina O, Pieper A, Zhang W, Goebbels S, Tarabykin V, Nave KA, Schwab MH (2013):
  **Neuronal basic helix-loop-helix proteins Neurod2/6 regulate cortical commissure formation before midline interactions.**
  *J Neurosci 33 (2), 641–651*
- Borisov AYu, Shtark OYu, Zhukov VA, Nemankin TA, Naumkina TS, Pinaev AG, Akhtemova GA, Voroshilova VA, Ovchinnikova ES, Rychagova TS, Tsyganov VE, Zhernakov AI, Kuznetsova EV, Grishina OA, Sulima AS, Fedorina YaV, Chebotar VK, Bisseling T, Lemanceau P, Gianinazzi-Pearson V, Ratet P, Sanjuan J, Stougaard J, Berg G, McPhee K, Ellis N, Tikhonovich IA (2011):
  **Interaction of legumes with beneficial soil microorganisms: From plant genes to varieties.**
  *Agricultural Biology 3, 41–47 (Russian).*
- Zhukov VA, Nemankin TA, Ovchinnikova ES, Kuznetsova EV, Zhernakov AI, Titov VS, Grishina OA, Sulima AS, Borisov YG, Borisov AY, Tikhonovich IA (2010):
  **Creating a series of gene-specific molecular markers for comparative mapping of the genome of pea (Pisum sativum L.) and diploid alfalfa (Medicago truncatula Gaertn.).**
  *Factors of Experimental Evo 9 (2), 30–34 (Russian)*

## Conference Posters:

- Grishina O, Bormuth I, Yan K, Yonemasu T, Goebbels S, Nave KA, Schwab MH, Tarabykin V (2014):
  **Neurod1/2/6 regulate pyramidal neuron differentiation and survival.**
  9th FENS (Federation of European Neuroscience Societies) Forum of Neuroscience, Milan, Italy.
- Grishina O, Bormuth I, Yan K, Yonemasu T, Goebbels S, Nave KA, Schwab MH, Tarabykin V (2013):
  **Neurod1/2/6 regulate hippocampal pyramidal neuron differentiation and survival.**
  Annual Meeting of the Society for Neuroscience, San Diego, California, USA.
- Bormuth I, Yan K, Yonemasu T, Gummert M, Zhang W, Wichert S, Grishina O, Pieper A, Goebbels S, Tarabykin V, Schwab MH (2013):
  **Neuronal basic helix-loop-helix proteins Neurod2/6 regulate cortical commissure formation before midline interactions.**
  Annual Meeting of the Society for Neuroscience, San Diego, California, USA.
- Grishina O, Bormuth I, Yan K, Yonemasu T, Goebbels S, Nave KA, Tarabykin V, Schwab MH (2013):
  **Role of NeuroD transcription factors in pyramidal neuron differentiation.**
  10th Meeting of the German Neuroscience Society, Göttingen, Germany.
- Bormuth I, Yan K, Yonemasu T, Gummert M, Zhang M, Wichert S, Grishina O, Pieper A, Zhang W, Goebbels S, Tarabykin V, Nave KA, Schwab M (2013):
  **Neuronal bHLH proteins Neurod2/6 regulate cortical commissure formation prior to midline interactions.**
  10th Meeting of the German Neuroscience Society, Göttingen, Germany.
- Zhukov VA, Nemankin TA, Ovchinnikova ES, Zhernakov AI, Titov VS, Grishina OA, Sulima AS, Rychagova TS, Kuznetsova EV, Borisov AY, Tikhonovich IA (2010):
  **Genetic mapping of pea (Pisum sativum L.) symbiotic genes using of gene-specific molecular markers. Strategy of interaction between microorganisms and plants with environment.**
  5th International conference of young scientists, Saratov, Russia, Abstract page 114.
- Borisov A, Nemankin T, Ovchinnikova E, Grishina O, Sulima A, Titov VS, Rychagova T, Zhukov V, Shtark O, Naumkina T, Vasilchikov A, Pinaev A, Chebotar V, Tikhonovich I (2010):
  **Multipartite symbiotic system of pea (Pisum sativum L.): plant - arbuscular mycorrhizal fungi - nodule and rhizosphere bacteria.**
  9th European Nitrogen Fixation Conference, Geneva, Switzerland, Abstract page 37.
- Grishina OA, Akhtemova GA, Zhukov VA, Shtark OY, Borisov AY, Tikhonovich IA (2010):
  **Analysis of the development and functioning of nitrogen-fixing pea nodules using transformed strains of Rhizobium leguminosarum bv viciae.**
  Joint 5th Postgraduate Course and Minisymposium of ABRMS “Adaptation to Climate Change in the Baltic Sea Region: Contributions from Plant and Microbial Biotechnology”, Mikkeli, Finland.

- Grishina OA, Akhtemova GA, Zhukov VA, Shtark OY, Borisov AY, Tikhonovich IA (2010):
  **Creation of Rhizobium leguminosarum bv viciae strains, carrying reported gene encoding beta-galactosidase (gusA) and using them for analysis of development and functioning of nitrogen-fixing pea nodules.**
  International Science Conference "Present condition and prospects of Microbiology and Biotechnology development", Minsk, Belarus, Abstract page 106–108.
- Borisov A, Ovchinnikova E, Nemankin T, Grishina O, Shtark O, Akhtemova G, Krasheninnikova A, Moloshonok A, Zhukov V, Kazakov A, Naumkina T, Vasilchikov A, Chebotar V, Gianinazzi-Pearson V, Tikhonovich I (2008):
  **New insight in legume breeding: plant genetics of beneficial plant-microbe systems, evolution and applications in sustainable agriculture.**
  2nd GL-TTP Workshop, Novi Sad, Serbia.
- Grishina OA, Kuznetsova EV, Zhukov VA, Borisov AY, Tikhonovich IA (2008):
  **Creation of molecular markers in 3rd chromosome of pea (Pisum sativum L.) for genetic mapping.**
  12th international School – Conference of Young Scientists "Biology – Science of XXI century". Moscow, Puschino, Abstract page 16.
- Borisov AY, Danilova TN, Grishina OA, Shtark OY, Akhtemova GA, Krasheninnikova AA, Moloshionok A, Kazakov AE, Naumkina TS, Vasilchikov AG, Chebotar VK, Gianinazzi-Pearson V, Tikhonovich IA (2008):
  **Genetic system of legumes controlling interactions with beneficial soil microflora: from fundamental to applications.**
  8th European Nitrogen Fixation Conference, Gent, Belgium, Abstract page 285.